

UNIVERSITÀ DEGLI STUDI DI UDINE

DOTTORATO IN TECNOLOGIE CHIMICHE ED ENERGETICHE
XXVI CICLO

Tesi di Dottorato

**PALLADIUM-BASED CATALYSTS AND
RELATED MATERIALS
FOR ENVIRONMENTALLY SUSTAINABLE
APPLICATIONS**

COMMISSION

Prof. Paolo Fornasiero	REVIEWER
Dr. Gianluca Landi	REVIEWER
Prof. Carla de Leitenburg	REFEREE
Dr. Frederic Meunier	REFEREE
Dr. Fabio Tatano	REFEREE
Prof. Alessandro Trovarelli	SUPERVISOR
Dr. Sara Colussi	SUPERVISOR
Prof. Alfredo Soldati	DIRECTOR OF PH.D. PROGRAM

I would like to thank all the catalysis group of the Department of Chemistry, Physics and Environment of the University of Udine and, in particular, **Prof. Alessandro Trovarelli** for giving me the opportunity to perform my PhD in such an intriguing research field and **Dr. Sara Colussi** for the precious help and the active support in the organization and in the development of my thesis project. A special thanks goes also to all the colleagues for the nice time spent together in these three years.

SUMMARY

Introduction:		<i>pag 1</i>
PART 1:	Supported palladium for environmentally friendly cross – coupling reactions	<i>pag 6</i>
	Chapter 1 : An efficient and reusable catalyst based on Pd/CeO ₂ for the room temperature aerobic Suzuki–Miyaura reaction in water/ethanol.	<i>pag 12</i>
	Chapter 2: Room-temperature Suzuki–Miyaura reaction catalyzed by Pd supported on rare earth oxides: influence of the point of zero charge on the catalytic activity	<i>pag 36</i>
PART 2:	Palladium-based catalysts for fuel processing for fuel cells applications.	<i>pag 54</i>
	Chapter 3: Ceria-based palladium-zinc catalysts as promising materials for water gas shift reaction.	<i>pag 60</i>
PART 3:	Methane catalytic combustion as a key technology for energy production and emissions abatement	<i>pag 73</i>
	Chapter 4: The effect of Ceria on the dynamics of CuO-Cu ₂ O redox transformation: CuO-Cu ₂ O hysteresis on Ceria	<i>pag 80</i>

Introduction

Nowadays sustainability and minimum environmental impact are key parameters for the improvement of existing processes and the development of new ones. Catalysis has a paramount importance when dealing with energy production, emissions abatement and green chemistry. Within these fields palladium-based catalysts are very interesting and efficient materials that are exploited in several applications due to their peculiar chemical properties.

Palladium is a chemical element with the symbol Pd and atomic number 46. It belongs to group 10 in the periodic table together with nickel (28) and platinum (78). It is a silvery-white metal that resembles platinum, soft and ductile when annealed and more hard and strong when it is treated at low temperature. Palladium dissolves slowly in concentrated nitric acid, in hot, concentrated, sulfuric acid, and, if finely divided, also in hydrochloric acid ^[1].

Its discovery (July 1802) is due to William Hyde Wollaston, a british chemist and physician who gave many contributions to science. Wollaston initially named his discovery “ceresium” after the newly-discovered asteroid Ceres; but he soon changed it to palladium after a different new asteroid discovery: Pallas, which, in turn, was named after the Greek Goddess of wisdom.

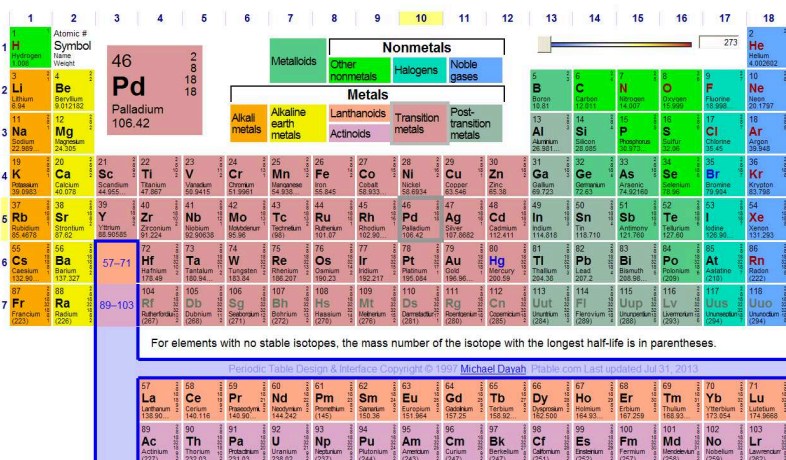


Figure 1: Periodic table of the Elements

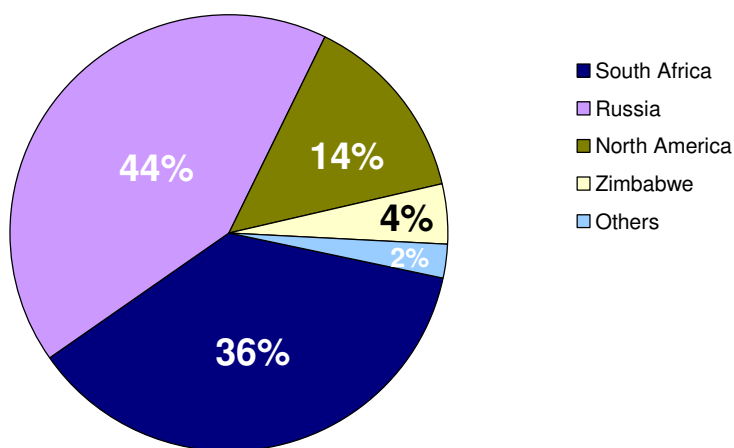


Figure 2: Metallic Palladium

Palladium has a very atypical configuration in its outermost electron shell compared to the other members of group 10, having fewer filled electron shells than the elements directly preceding it (a phenomenon unique to palladium). Common oxidation states of palladium are 0, +1, +2 and +4. No experimental evidence of the existence of +3 oxidation state has been found although it was previously reputed as one of the fundamental oxidation states of palladium. Palladium(VI) was discovered in 2002 for the first time via X-Ray Diffraction spectroscopy ^[2, 3]. Palladium, platinum, rhodium, ruthenium, iridium and osmium form a group of elements referred to as the platinum group metals (PGMs).

Due to their peculiar properties, palladium and its derivatives find application in many fields that range from electronics (as a substitute of gold for plating electronic components) to dentistry, jewelry, medicine (where palladium-103 radioactive isotope is showing promising results in the treatment of prostate and breast cancer ^[4]) and catalysis. In Figure 3 the global data for the usage of palladium-based materials are shown ^[5].

Palladium supply by region 2012



Palladium demand by application 2012

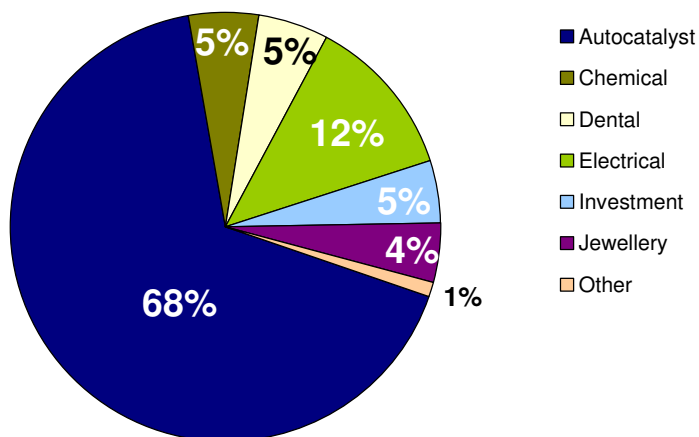


Figure 3: Worldwide usage and supply of Palladium

As it can be observed, palladium largest application is by far in the field of autocatalysts, i.e. for automotive catalytic converters. Today the number of vehicles is estimated around 450 millions of units and some forecasts suggest that this value is going to double in the next 30 years requiring a growing demand of palladium.

Autocatalysts convert over 90 percent of hydrocarbons, carbon monoxide and nitrogen oxides produced in the exhaust from gasoline engines into carbon dioxide, nitrogen and water vapour. The most common converter is the so-called “three way catalyst”. The term ‘three-way’ underlines the catalytic activity with respect to three different reactions: oxidation of CO into CO₂, oxidation of unburned hydrocarbons into CO₂ and H₂O, reduction of NO_x into N₂. In detail, the three reactions are:

1. $2\text{CO} + \text{O}_2 \rightarrow 2\text{CO}_2$
2. $\text{C}_x\text{H}_{2x+2} + [(3x+1)/2]\text{O}_2 \rightarrow x\text{CO}_2 + (x+1)\text{H}_2\text{O}$.
3. $2\text{NO}_x \rightarrow x\text{O}_2 + \text{N}_2$

Autocatalysts are not the only application of palladium-based compounds in catalysis. They are also employed in several industrial processes (as for example petroleum refining, production of nitric acid and synthesis of ethanol through the “Wacker Process”), and in many “green” and environmentally sustainable processes such as the production of energy avoiding the simultaneous emission of noxious by-products and the synthesis of fine chemicals without the use of toxic organic solvents.

Aim of this PhD thesis is to investigate the behavior of Pd-based materials for significant sustainable applications. In particular, the first object of study is the water gas shift reaction (WGSR) for the purification of hydrogen rich streams in order to lower the content of CO in the feed of PEM (Proton Exchange Membrane) fuel cells. The second application considered is the Suzuki-Miyaura reaction for the synthesis of carbon-carbon bonds at room temperature and in the presence of environmentally friendly solvents. The last chapter presents an investigation of the redox properties of copper-based materials for the catalytic combustion of methane in comparison with the well known behavior of Pd-based catalysts for the same reaction. Each chapter is based on papers published or submitted during this PhD. For each application considered, an overview that describes the topic and its implications is presented.

References

- [1]. Hammond, C. R. (2004). *The Elements, in Handbook of Chemistry and Physics 81st edition*. CRC press.
- [2]. Chen, W. (2002). "Synthesis and Structure of Formally Hexavalent Palladium Complexes". *Science* **295** (5553): 308.
- [3]. Crabtree, R. H. (2002). "CHEMISTRY: A New Oxidation State for Pd?". *Science* **295** (5553): 288.
- [4]. Tan, Robert S. (2005-04-15). *Aging men's health: a case-based approach*. Thieme. 136.
- [5]. www.platinum.matthey.com/publications/market-data-charts/palladium

PART 1:

Supported palladium for environmentally friendly cross – coupling reactions

Palladium-based catalysts find wide application also in the field of organic chemistry. In particular, they are employed for the synthesis of natural products, polymers, agrochemicals and pharmaceuticals. Almost every area of organic synthesis has been influenced by this transition metal due to versatility and ability of palladium to participate in catalytic transformations as well as its high functional group tolerance. In addition to this, palladium also enables hydrogenation; hydrogenolysis, carbonylation, formation of C–C, C–O, C–N, and C–S bonds, cycloisomerization and even pericyclic reactions ^[1, 2].

In the evolution of organic chemistry, carbon-carbon bond-forming reactions, such as Grignard, Diels-Alder and Wittig reactions, play an important role and constitute one of the bigger request for the synthesis of organic molecules. In the last five decades, a new family of carbon-carbon bond-forming reactions, catalyzed by transition-metal-based compounds, is gaining increasing importance. Since the first construction of a carbon-carbon bond made in 1845 by Kolbe in the synthesis of acetic acid, coupling reactions have played a decisive role in the chemical synthesis.

In organic chemistry, the term “**coupling reaction**” includes a variety of reactions where two hydrocarbon fragments are joined with the aid of a catalyst that, normally, is constituted by a metal or a metallic compound. This reaction forms a new carbon-carbon bond between the two starting fragments. In one important reaction type, an organometallic compound of the type RM (R = organic fragment, M = metallic centre) reacts with an organic halide of the type R'X (R' = organic fragment, X = halogen) with the formation of the R-R' product ^[3].

Broadly speaking, two types of coupling reactions are recognized:

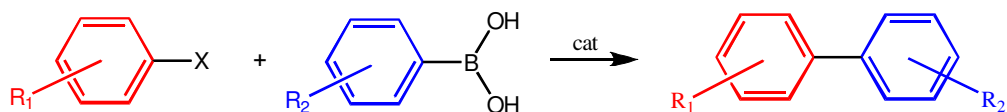
- **cross coupling reactions:** involve reactions between two different partners, for example bromobenzene (PhBr) and vinyl chloride to give styrene (PhCH=CH₂).

- **homocoupling reactions:** couple two identical partners, for example, the conversion of iodobenzene (PhI) to biphenyl (Ph-Ph).

The reaction mechanism usually involves three phases:

1. Oxidative addition of the organic halide to the catalyst.
2. Transmetalation of the second partner; in this step, both coupling partners are placed on the same metal centre.
3. Reductive elimination of the two coupling fragments to regenerate the catalyst and give the organic product.

A lot of coupling reactions, catalyzed by palladium compounds, were developed with the aim to obtain a huge variety of organic molecules; examples are constituted by “Kumada-Corriu coupling” (between a Grignard reagent and an organic halide), “Sonogashira coupling” (between a terminal alkyne and an aryl/vinyl halide), “Stille coupling” (between an organotin compound and an organic halide), “Fukuyama coupling” (between a thioester and an organozinc halide to produce ketones). Among all these, very important contributions to coupling reactions were given by Ei-ichi Negishi and Akira Suzuki who were awarded in 2010 with the Nobel Prize in Chemistry, together with Richard F. Heck ^[4]. The Pd-catalyzed cross coupling reaction developed by professor Akira Suzuki in cooperation with professor Norio Miyaura (the reaction is also known as Suzuki-Miyaura **SM** coupling) represents one of the most powerful methods for the construction of carbon-carbon bonds. Published for the first time in 1979, the **SM reaction** is the organic synthesis that couples an aryl/vinyl-boronic acid with an aryl/vinyl-halide, simple or containing an organic substituent; the process is catalyzed by a palladium(0) complex ^[5-7]. The reaction is commonly used to produce poly-olefins, styrene-based derivatives, or variously substituted biphenyls.



Scheme 1: The SM reaction

The reaction usually relies on a homogeneous palladium catalyst (more strictly a pre-catalyst) to effect part of the transformation. The palladium catalyst is 4-

coordinated, and normally involves phosphine supporting groups. The ligands used to obtain catalytically active systems for the less reactive substrates are generally air- and/or water-sensitive, expensive, toxic and often commercially not available. Furthermore, formation of insoluble non-catalytic palladium black from small aggregates is often observed as an undesired effect.

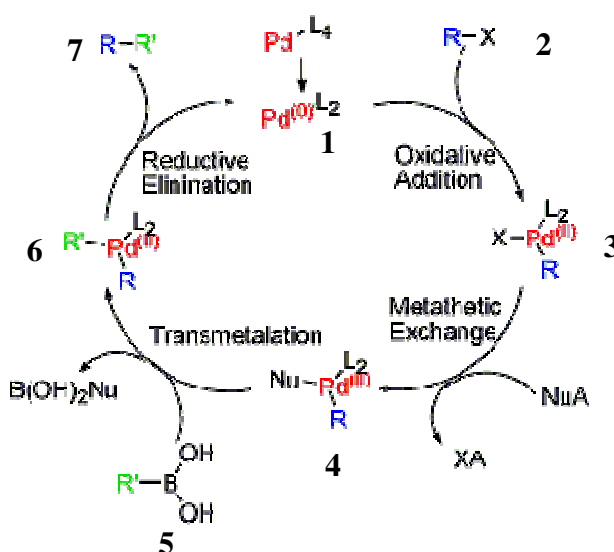
Although many other methods, like Stille, Kumada, Negishi etc couplings are available for the same purpose, the SM coupling, which produces biaryls, has recently proven to be the most suitable for this application. The preferences towards SM coupling are due to some economical and practical key features. First of all, the synthesis is run under mild reaction conditions (low temperatures and pH values close to neutrality). The boronic acids are commercially available and are environmentally safer with respect to other organometallic reactants ^[8-15]. Furthermore, the handling and removal of byproducts containing boron is easier compared to other organometallic reagents, especially in a large-scale application. The cross-coupling reactions based on Grignard precursors have several drawbacks like the ability of the Grignard reagents to attack the reactive functional groups present in the starting materials whereas the SM cross-coupling process tolerates a wide variety of functional groups in the starting partners. The disadvantage exposed by Grignard reagents can be minimized by employing tin compounds but the toxicity and the difficulties associated with the purification of certain tin-based products make them a less attractive choice. The usage of other accessible methods is restrained, as the availability of the corresponding organometallic reagents is somewhat, limited. Since biaryl-core-based molecules and their homologues are found in several molecular frameworks (e.g. drugs, polymers, liquid crystalline materials and ligands for organometallic chemistry) there is a urgent need for their development. The SM reaction has gained importance in the last few years because the conditions developed for the cross-coupling reaction have many desirable features for a large-scale employment and are amenable to the industrial synthesis of pharmaceuticals and fine chemicals.

Aim of this work was to synthesize a series of heterogeneous Pd-based compounds with the purpose of individuating a clean and long-lasting catalyst. For this reason, Pd was supported onto some Rare Earth Oxides (REO) and tested in the SM reaction. Catalytic activity, recyclability and the residual metal

in the reaction products were correlated to surface charge properties of the heterogeneous precatalysts.

Reaction mechanism:

The mechanism of the Suzuki reaction is best viewed from the perspective of the palladium catalyst. The first step is the **oxidative addition** of palladium (**1**) to the halide (**2**) to form the organopalladium species (**3**). Reaction with base gives intermediate (**4**) which, via transmetalation ^[16] with the boronate complex (**5**), forms the organopalladium species (**6**). Reductive elimination of the desired product (**7**) restores the original palladium catalyst (**1**).



Scheme 2: Mechanism of SM reaction

References:

- [1]. (a) Beccalli, E. M.; Brogini, G.; Martinelli, M.; Sottocornola, S. *Chem. Rev.* **2007**, 107, 5318–5365. (b) Muzart, J. *J. Mol. Catal. A: Chem.* **2007**, 276, 62–72. (c) Zeni, G.; Larock, R. C. *Chem. Rev.* **2006**, 106, 4644–4680.

(d) Buchwald, S. L.; Mauger, C.; Mignani, G.; Scholz, U. *Adv. Synth. Catal.* **2006**, *348*, 23–39. (e) Cacchi, S.; Fabrizi, G. *Chem. Rev.* **2005**, *105*, 2873–2920. (f) Zeni, G.; Larock, R. C. *Chem. Rev.* **2004**, *104*, 2285–2309. (g) Muzart, J. *Tetrahedron* **2005**, *61*, 5955–6008. (h) Muzart, J. *Tetrahedron* **2005**, *61*, 9423–9463. (i) Stahl, S. S. *Angew. Chem., Int. Ed.* **2004**, *43*, 3400–3420. (j) Sigman, M. S.; Schultz, M. J. *Org. Biomol. Chem.* **2004**, *2*, 2551–2554. (k) Stoltz, B. M. *Chem. Lett.* **2004**, *33*, 362–367. (l) Tietze, L. F.; Ila, H.; Bell, H. P. *Chem. Rev.* **2004**, *104*, 3453–3516. (m) Nishimura, T.; Uemura, S. *Synlett* **2004**, 201–216. (n) Dounay, A. B.; Overman, L. E. *Chem. Rev.* **2003**, *103*, 2945–2963. (o) Agrofoglio, L. A.; Gillaizeau, I.; Saito, Y. *Chem. Rev.* **2003**, *103*, 1875–1916. (p) Negishi, E.-I.; Anastasia, L. *Chem. Rev.* **2003**, *103*, 1979–2017. (q) Kiss, G. *Chem. Rev.* **2001**, *101*, 3435–3456. (r) Beletskaya, I. P.; Cheprakov, A. V. *Chem. Rev.* **2000**, *100*, 3009–3066. (s) Zimmer, R.; Dinesh, C. U.; Nandan, E.; Khan, F. A. *Chem. Rev.* **2000**, *100*, 3067–3125. (t) Amatore, C.; Jutand, A. *Acc. Chem. Res.* **2000**, *33*, 314–321. (u) Poli, G.; Giambastiani, G.; Heumann, A. *Tetrahedron* **2000**, *56*, 5959–5989. (v) Miyaura, N.; Suzuki, A. *Chem. Rev.* **1995**, *95*, 2457–2483. (w) Tsuji, J. *Synthesis* **1990**, 739–749.

[2]. (a) *Handbook of Organopalladium Chemistry for Organic Synthesis*; Negishi, E., Ed.; Wiley-Interscience: New York, 2002. (b) Tsuji, J. *Palladium Reagents and Catalysts: Innovations in Organic Synthesis*; Wiley and Sons: New York, 1995. (c) Tsuji, J. *Palladium Reagents and Catalysts: New Perspectives for the 21st Century*; Wiley and Sons: New York, 2003. (d) *Palladium in Organic Synthesis*; Tsuji, J., Ed.; Springer: Berlin, 2005. (e) Heck, R. F. *Palladium Reagents in Organic Synthesis*; Academic Press: New York, 1985. (f) Li, J. J.; Gribble, G. W. *Palladium in Heterocyclic Chemistry*; Pergamon: New York, 2000. (g) Heumann, A.; Jens, K.-J.; Reglier, M. *Progress in Inorganic Chemistry*; Karlin, K. D., Ed.; Wiley and Sons: New York, 1994; Vol. 42, pp. 483–576.

[3]. Organic Synthesis using Transition Metals Rod Bates

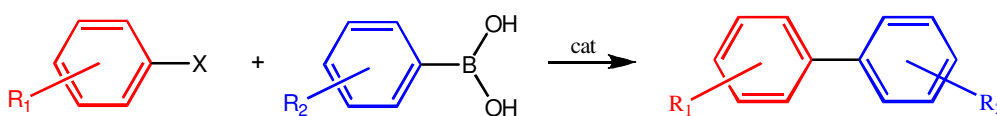
[4]. The Nobel Prize in Chemistry 2010 – Richard F. Heck, Ei-ichi Negishi, Akira Suzuki Nobel Prize.org. 2010-10-06. Retrieved 2010-10-06.

- [5]. Miyaura, Norio; Yamada, Kinji; Suzuki, Akira (1979). *Tetrahedron Letters* **20** (36): 3437–3440.
- [6]. Miyaura, Norio; Suzuki, Akira (1979). *Chem. Comm.* (19): 866–867.
- [7]. Miyaura, Norio; Suzuki, Akira (1995). *Chemical Reviews* **95** (7): 2457–2483.
- [8]. Suzuki, A. *Pure Appl. Chem.* 1985, *57*, 1749. Suzuki, A. *Pure Appl. Chem.* 1991, *63*, 419.
- [9]. Martin, A. R.; Yang, Y. *Acta Chem. Scand.* 1993, *47*, 221.
- [10]. Suzuki, A. *Pure Appl. Chem.* 1994, *66*, 213.
- [11]. Miyaura, N.; Suzuki, A. *Chem. Rev.* 1995, *95*, 2457.
- [12]. Stanforth, S. P. *Tetrahedron* 1998, *54*, 263.
- [13]. Miyaura, N. *Advances in Metal-organic Chemistry*; Libeskind, L. S., Ed.; Jai: London, 1998; Vol. 6, pp 187–243.
- [14]. Suzuki, A. *J. Organomet. Chem.* 1999, *576*, 147.
- [15]. Suzuki, A. In *Organoboranes for Syntheses*. ACS Symposium Series 783; Ramachandran, P. V., Brown, H. C., Eds.; American Chemical Society: Washington, DC, 2001; pp 80–93.
- [16]. Suzuki, A. *J. Organometallic Chem.* **1999**, *576*, 147–168. (Review)

CHAPTER 1 :

An efficient and reusable catalyst based on Pd/CeO₂ for the room temperature aerobic Suzuki–Miyaura reaction in water/ethanol.

The Suzuki–Miyaura (SM) reaction, based on the use of arylboronic acids or esters, is recognized as one of the most important synthetic methods for the construction of asymmetric biaryls (Scheme 1) ^[1–11]. It finds application in the production of agrochemical and pharmaceutical drugs and in material science.



Scheme 1: The Suzuki-Miyaura reaction.

The recent explosive growth of studies in this area is mainly due to air and moisture stability of organoboranes as well as to their low toxicity. Furthermore, the reaction tolerates a wide range of functional groups and can be performed under relatively mild experimental conditions. Usually, the SM coupling is homogeneously catalyzed by palladium compounds generally in organic solvents or biphasic systems. Recent investigations have confirmed the formation of soluble colloidal nanoparticles which can act as the catalyst or, more likely, as the precursor of the true catalyst ^[12–18]. The difficult removal of the catalyst and its decomposition products from the mixture containing the biaryl constitutes the main drawback of the reaction. For the practical and economical reasons already evidenced, as well as for environmental considerations, the use of simple heterogeneous catalysts for the SM coupling is therefore highly desirable. In this context, one of the fundamental aims is the production of fine chemicals (especially pharmaceuticals) which must be free of residual metal (<5 ppm). While a variety of heterogeneous catalysts, such as Pd/C, Pd/zeolites, Pd/sepiolites, Pd/LDH, Pd/hydroxyapatites and Pd(II) complexes anchored on different supports, have been the subject of several investigations ^[8–11], relatively few studies have been focused on the use of palladium supported on metal oxides. To the best of our knowledge, Pd-containing perovskites (in particular LaFe_{0.57}Co_{0.38}Pd_{0.05}O₃) ^[19,20], Pd/MgLa mixed oxides ^[21], Pd/MgO ^[22], Pd/Al₂O₃ ^[23,24], Pd/TiO₂ ^[24–26], Pd/SiO₂ ^[25], and Pd-doped mixed oxides ^[27] are the only examples in this field reported in the

literature. Interestingly, Pd on various MO₂ supports (M= Ti, Si, Zr and Ce) has shown to be catalytically active for the homocoupling of phenylboronic acid [28]. Worth of note is also the catalytic efficiency of supported gold (on Y₂O₃ and CeO₂) for the same reaction [29,30]. The authors of these works have also compared isoelectronic Pd(II) and Au(III) supported on ceria finding that the latter selectively promotes homocoupling, while the former catalyzes the cross-coupling reaction with lower activity and selectivity [30]. In some cases palladium leaching during catalysis was evidenced. Although no noble metal leaching was observed using Pd/MgLa mixed oxides, in the first recycling the activity of the catalytic system slightly decreased (after 1 h the yield dropped from 99 to 95%). No information was given by the authors on further recycling of the catalyst [21]. The Pd-containing perovskite catalyst was recycled four times without apparent loss of activity [19], and a further detailed study revealed that the effective catalytic species was present in solution phase [20]. It is noteworthy that the catalytic runs have been performed at 333K [8], 353 K [20,21] and 423 K (under microwaves irradiation) [26]. Only in the case of the Pd/MgO catalyst the SM reaction was carried out at room temperature starting from aryl bromides and iodides [22]. Significantly, no coupling product was formed at 298K using Pd/MgLa mixed oxides [21]. With this scenario in mind, it has been decided to evaluate the catalytic efficacy of Pd/CeO₂ in the SM reaction. To the best of our knowledge, such a catalytic system has been previously employed in two single experiments of Suzuki cross-coupling reaction [24,30]. As a matter of fact, Pd/CeO₂ showed less efficiency with respect to Pd/Al₂O₃ and Pd/TiO₂ systems [24]. On the contrary, the Pd/CeO₂ system has found application in other catalytic processes, for example CO, CO₂, and hydrocarbons hydrogenations and C₂–C₆ hydrogenolysis [31]. Herein are report the results of our investigation which showed that Pd/CeO₂ behaves as a very efficient promoter of the SM reaction in a non-toxic solvent (ethanol/water). Furthermore, this catalyst can be reused several times (at least ten) without apparent loss of activity and such an issue is crucial for scaling up this environmentally friendly catalytic process.

Experimental

1.1 General

All reagents were purchased from Aldrich and used without further purification. Commercial solvents were dried according to standard methods and freshly distilled before use. The high-resolution transmission electron microscopy (HRTEM) was carried out at 200 kV with a JEOL 2010F instrument equipped with a field emission gun. The point-to-point resolution of the microscope was 0.19 nm and the resolution between lines was 0.14 nm. The powder samples were directly deposited on holey-carbon coated Cu grids, whereas a drop of the mother liquor was deposited and evaporated on a grid covered by a thin polymer. The Pd loading of the catalyst was measured on a Spectro Analytical Instruments Spectromass 2000 Type MSDIA10B. Inductively Coupled Plasma Mass Spectrometer. Samples (20 mg) were digested on a microwave apparatus MILESTONE Mega 1200 by use of 1mL of 65% HNO₃, 0.4mL of 30% H₂O₂ and 0.1mL of 40% HF with a mineralization program at 650W for 20 min in Teflon vessels. The mean value for two different samples was 1.85±0.04%. For the Pd determination in solution, four different samples were prepared by filtration and centrifugation of the reaction mixture obtained after a catalytic complete conversion of **1** into **3**. Each sample was digested as described above on a microwave apparatus MILESTONE Mega 1200. The mean concentration value of Pd was 1.4 ppb (instrumental detection limit = 0.5 ppb). Calibration curves were obtained by using a Palladium ICP/DCP standard solution purchased from Aldrich (10,000mg/mL Pd in 6% HCl solution). The GC-MS analyses, run to control the identity of the compounds obtained in the catalytic trials, were carried out with a Fisons TRIO2000 gaschromatograph-mass spectrometer working in the positive ion 70 eV electron impact mode. Injector temperature was kept at 523K and the column (Supelco® SE-54, 30mlong, 0.25mmi.d., coated with a 0.5µm phenyl methyl silicone film) temperature was programmed from 333 to 573K with a ramp rate of 10 K/min. The GC analyses were run on a Fisons GC 8000 Series gaschromatograph equipped with a Supelco® PTA-5 column (30m long, 0.53mm i.d., coated with a 3.0 µmpoly (5% diphenyl–95% dimethylsiloxane) film). Injector and column temperatures as indicated above.

1.2 Catalyst preparation and characterization

The catalyst containing 2% wt Pd was prepared by the incipient wetness impregnation on a commercial CeO₂ support (B.E.T. surface area after

calcination at 1073K=31m² g⁻¹). The Pd precursor was a 10% Pd(NO₃)₂ solution(99.999%), which was added drop by drop to the support to obtain a catalyst with a nominal Pd loading of 2% wt. The powder was impregnated in subsequent steps: after the first impregnation, the catalyst was dried in oven for 1 h at 373 K and then impregnated a second time with the remaining amount of solution. The complete impregnation was achieved in three cycles. The complete impregnation was achieved in three cycles. After complete impregnation the powder was dried overnight at 393K and then calcined at 1073K for 2 h. B.E.T. surface area was 28m² g⁻¹ after calcination. Surface area measurements were carried out on a fraction of sample of about 200 mg in a Micromeritics TriStar surface and porosity analyzer by N₂ adsorption/desorption at 77 K. Before measurement, the samples were degassed at 423 K for 90 minutes. The X-Ray spectra were recorded on a Philips X'Pert diffractometer equipped with Cu K α radiation source. Stepsize was 0.01 $^{\circ}$ with a time-per-step of 80 s. The Temperature Programmed Oxidation (TPO) experiment was carried out on 150mg of Pd/CeO₂. The catalyst was exposed to a flow of 2% of O₂ in N₂, while the temperature was increased from room temperature up to 1273K and then decreased to 373K for two subsequent heating/cooling cycles at 10 K/min. Oxygen release during heating (due to PdO decomposition) and oxygen uptake during cooling (due to Pd reoxidation) were measured. Quantitative analysis of the oxygen release/uptake allowed to evaluate the amount of Pd in oxide form (~75%) present on the catalyst surface.

1.3 Synthesis and NMR characterization of biaryls3–12

In a thermostated bath at 298K, a 25mL Schlenk flask was charged in air with a magnetic stirring bar, Pd/CeO₂ (Pd = 2 wt%) (53.2 mg), the appropriate arylboronic acid (1.2 mmol) and arylbromide (1.0 mmol), K₂CO₃ (1.2 mmol), ethanol (3.0 mL) and H₂O(1.0 mL). The reaction mixture was kept under vigorous stirring until the GC control showed no residual aryl bromide in solution. Water (10 mL) was added to the suspension and the organics were extracted with dichloromethane (3 \times 10 mL). The organic phase was dried over Na₂SO₄ and then filtered through a column filled with silica gel (for samples3–11) or Celite® (for sample 12) to remove eventual traces of metal. Elimination of the solvent under vacuum gave the desired biaryl as white microcrystalline solid.

1.4 Catalytic runs

The following procedure was adopted for the standard reaction catalyzed by Pd/CeO₂ (1 mol% Pd). In a thermostated bath at 298K, a 10mL Schlenk flask was charged in air with a magnetic stirring bar, Pd/CeO₂ (Pd= 2 wt%) (26.6 mg), 4-tolylboronic acid (**2**) (0.6 mmol), diethylene glycol diⁿbutyl ether (GC internal standard, 0.5 mmol), K₂CO₃ (0.6 mmol), ethanol (1.5 mL) and H₂O (0.5 mL). The reaction was then started by addition of bromobenzene (**1**) (0.5 mmol). The mixture was extracted from the flask by means of a syringe (the volume of the sample was ~ 0.1 mL). To the sample 0.5mL of water were added, followed by immediate extraction with dichloromethane (2×1mL). The solution was dried over Na₂SO₄ and analyzed by GC after purification on a microcolumn filled with silica gel. All other catalytic trials were carried out similarly, using Celite® instead of silica gel in the case of product **12** (see Scheme 2 and Table 2 at pag 23-24 for molecules indexes).

1.5 Catalyst recycling

Two different methods for catalyst recycling were employed:

- a) consecutive reuse
- b) parallel reuse.

Method a):

in a thermostated bath at 298 K, a 8mL conical centrifuge test tube was charged in air with a magnetic stirring bar, Pd/CeO₂ (2 wt% Pd) (26.6 mg), 4-tolylboronic acid (**2**) (0.6 mmol), diethylene glycol diⁿbutyl ether (GC internal standard, 0.5 mmol), K₂CO₃ (0.6 mmol), ethanol (1.5 mL) and H₂O (0.5 mL), and the reaction was started upon addition of bromobenzene (**1**) (0.5 mmol). After 9 h, the suspension was centrifuged for 3min at 3500rpm and the supernatant was removed and analyzed by GC. The solid was washed with water and ethanol, dried in air and reused for the second test, which was performed upon addition in sequence of solvents, **2**, GC internal standard, base and **1**, as indicated above. Again, the reaction was stopped after 9 h by centrifugation and the successive workup was analogous to that previously described. Iteration of this procedure was continued for other nine reuses of the catalyst. The yields of **3** from the GC measurements were the following:

First use = **99.9%**
First reuse = **99.9%**
Second reuse = **99.6%**
Third reuse = **98.4%**
Fourth reuse = **98.4%**
Fifth reuse = **97.8%**
Sixth reuse = **97.0%**
Seventh reuse = **98.7%**
Eight reuse = **97.9%**
Ninth reuse = **97.0%**
Tenth reuse = **97.6%**

The *method a* represents the standard recycling test in which the same sample undergoes a series of repetitions of the test. Since the sample has to be recovered and cleaned up from the reaction medium, accidental loss of part of catalyst may occur distorting the results of the test. For this reason it has been decided to perform another recycling test (*method b*) in which, every time, the exact amount of catalyst was taken from a huge batch of catalyst subject to the proper number of recycles.

Method b):

A 50mL Schlenk flask was charged with a magnetic stirring bar, Pd/CeO₂ (2 wt% Pd) (400 mg), 4-tolylboronic acid (**2**)(9 mmol), diethylene glycoldiⁿbutyl ether (GC internal standard, 7.5 mmol), K₂CO₃ (9 mmol), ethanol (22.5 mL) and H₂O (7.5 mL), and the reaction was started upon addition of bromobenzene (**1**)(7.5 mmol). The reaction was stopped when **1** was quantitatively converted into product **3**, as judged by GC. The solid was then recovered by filtration, washed with water and ethanol and dried under vacuum. A sample of 26.6mg was used for the first recycling test (amounts of organic substrates, GC internal standard, base and solvents were as indicated above for method a)), the reaction was stopped after 9 h and the solution was analyzed by GC. The remaining amount of catalyst, after weighting, was used to convert completely **1** into **3** by employing appropriate amounts of organic substrates, base, GC internal

standard and solvents. Again, a sample of 26.6mg was used for the second recycling test which was stopped after 9 h, while all the remaining catalyst was used for the catalytic transformation of **1** and **2** into **3**. This procedure was then iterated for a total of ten reuses of the catalyst. The yields of **3** from the GC measurements were the following:

First use = **99.9%**
First reuse = **99.2%**
Second reuse = **99.4%**
Third reuse = **99.5%**
Fourth reuse = **99.8%**
Fifth reuse = **99.3%**
Sixth reuse = **99.1%**
Seventh reuse = **99.4%**
Eight reuse = **99.2%**
Ninth reuse = **99.0%**
Tenth reuse = **98.6%**.

Results and discussion

1.6 Preparation and characterization of Pd/CeO₂

The catalyst was prepared by the incipient wetness impregnation method. A 10% wt solution of Pd(NO₃)₂ (99,999%) in HNO₃ was added drop by drop to CeO₂ to obtain a Pd/CeO₂ catalyst with a nominal Pd loading of 2% wt. After impregnation, the catalyst was dried at 393 K for 15h and then calcined at 1073 K for 2h as previously described for analogous compounds ^[32]. The loading of the sample was confirmed by elemental analysis.

The B.E.T. surface area was 28m² g⁻¹ after calcination

The X-Ray diffraction analysis showed the presence of reflections belonging to fluorite lattice of ceria but did not show distinct reflections attributable to either PdO and Pd.

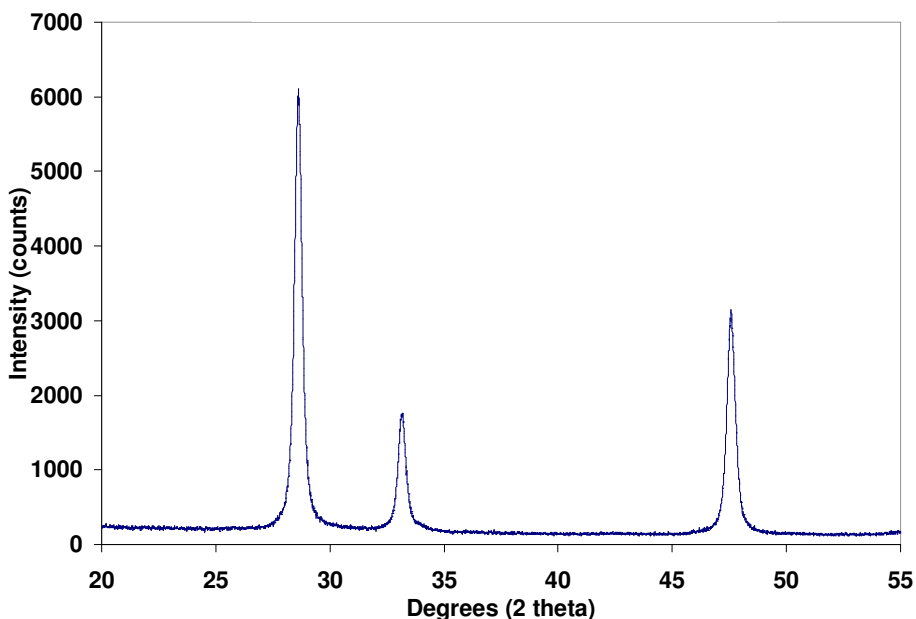


Figure 1: XRD spectrum of 2% Pd/CeO₂

To spread light into this feature, high-resolution transmission electron microscopy (HRTEM) analysis of a freshly prepared sample was undertaken, and a general view is shown in Figure 2.

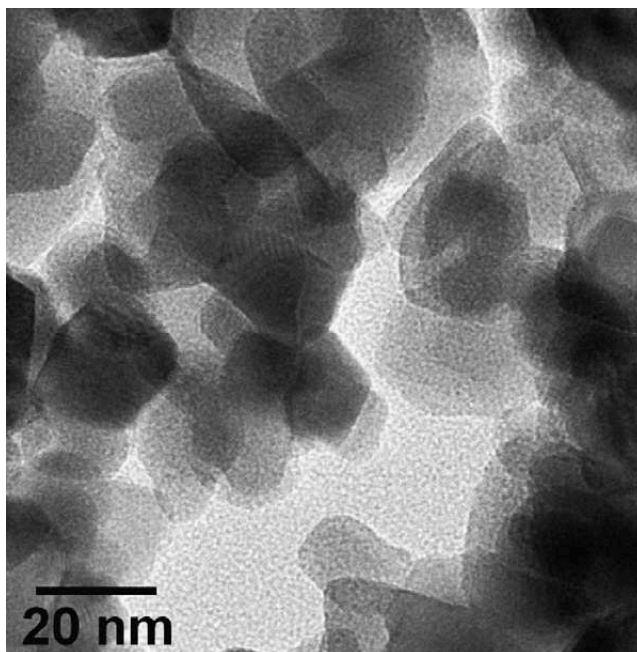


Figure 2: TEM micrograph of Pd/CeO₂.

The sample is dominated by particles of CeO₂ of ca. 20nm in size. Figure 3 (left) shows a representative HRTEM image of the sample along with Fourier transform (FT) images of particles labeled **a** and **b**.

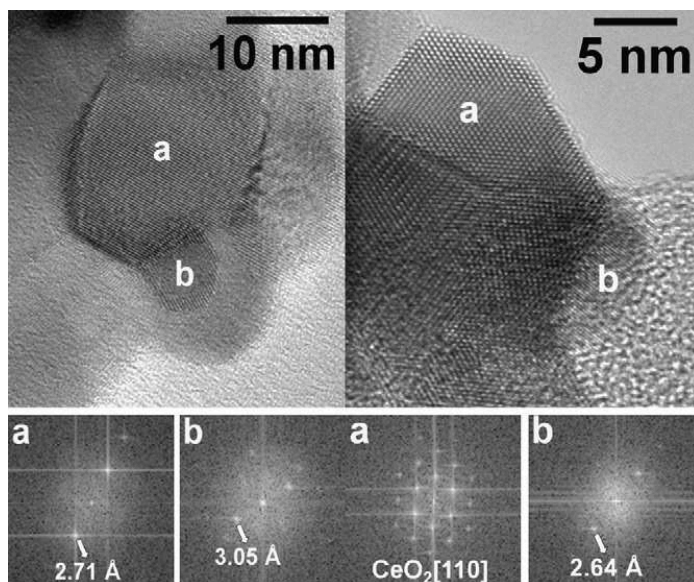


Figure 3: Representative HRTEM image of Pd/CeO₂ along with Fourier transform (FT) images.

Particle **a** exhibits lattice fringes at 2.71 Å, which correspond to [200] crystallographic planes of CeO₂. Particle **b** shows spots in the FT image at 3.05 Å, which are ascribed to the [100] crystallographic planes of PdO. PdO crystallites are well distributed over the CeO₂ support, with a particle size distribution centered at 6.7 nm (the particle size distribution is shown in Figure. 4).

In the sample prepared by Willis and Guzman using a nanocrystalline ceria support, a larger range for the particle size was observed (2–35 nm), which was centered at about 15 nm^[28]. Another representative image of this sample is shown in Figure 2 (right). Again, a PdO particle (labeled **b**) is supported over a CeO₂ crystallite (particle **a**). The image shows an atomically resolved CeO₂ crystal oriented along the [110] crystallographic direction, as deduced from the corresponding FT image. In particle **b**, lattice fringes at 2.64 Å correspond to [101] crystallographic planes of PdO.

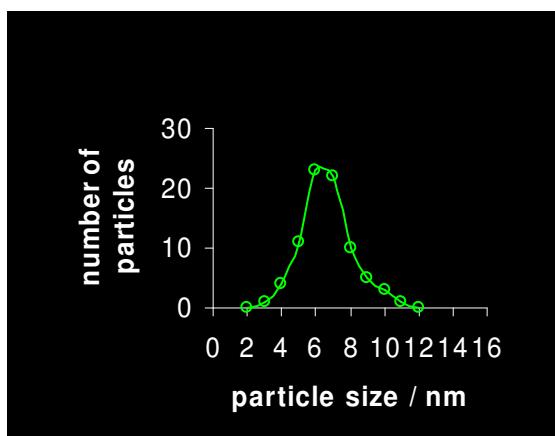


Figure 4: Particle size distribution relative to a fresh sample of Pd/CeO₂.

The HRTEM analysis of the sample did not evidenced the presence of metallic palladium particles on the ceria surface. On the other hand a portion of about 25% of total Pd present in the sample did not cycle if exposed to O₂ under Temperature Programmed Oxidation (TPO) conditions, which could indicate the presence of metallic Pd (Figure 5)

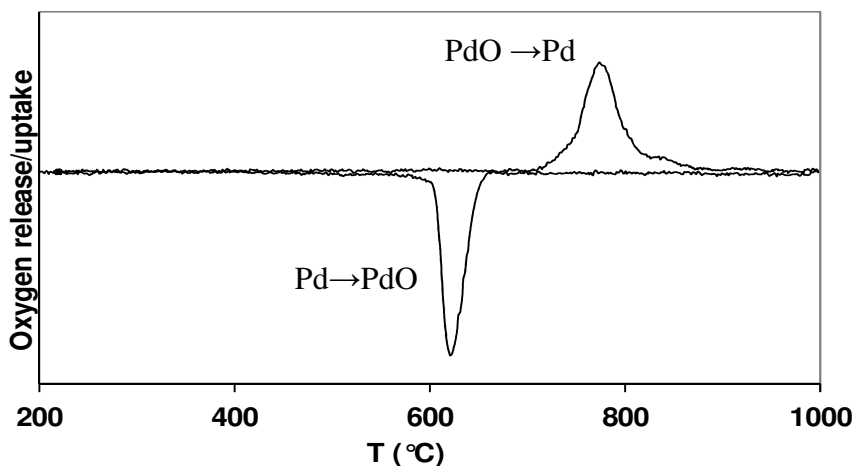


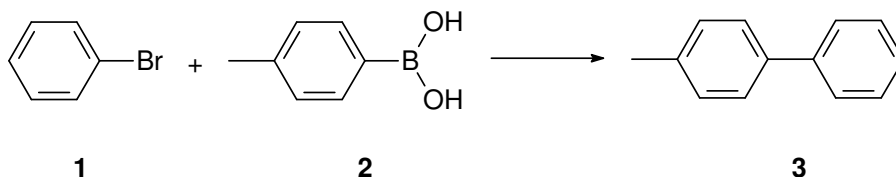
Figure 5: TPO profile of 2% Pd/CeO₂

Undetection of metallic Pd by HRTEM could originate either from its dimensions which fall outside the range of detection of 2–100nm and from the

presence of Pd-PdO core-shell particles when PdO particles are covered by thin Pd metal shells.

1.7 Catalytic activity of Pd/CeO₂ in the Suzuki–Miyaura reaction

Initially, the catalytic trials were run in EGME/H₂O (3:1, v/v) (EGME = ethylene glycol monomethyl ether), according to our previous studies that demonstrated the beneficial effect of this type of solvent on the rate of Pd-catalyzed Heck^[33,34] and Suzuki^[35] reactions. At 298K, a complete conversion of bromobenzene (**1**) and 4-tolylboronic acid (**2**) into 4-methyl-1,1'-biphenyl (**3**) (model reaction, Scheme 2) was achieved in 11 h by using K₂CO₃ as the base and 1mol% amount of Pd with respect to **1** (Table 1, entry1). However, the reaction run in ethanol/H₂O (3÷1, v/v) was faster, as complete formation of **3** was obtained in 8 h (Table 1, entry2). The beneficial role played by ethanol in the SM reaction has been already reported^[36]. It is important to stress that, in the same experimental conditions, no product was formed within 12 h by employing palladium-free CeO₂ (Table 1, entry 3). The use of ethanol/H₂O in 1÷3 (v/v) ratio or water alone, resulted in a neat increase of the reaction time (Table 1, entries 4 and 5). Finally, the reaction rate did not substantially change when ethanol was replaced by methanol (Table 1, entry 6), while a very slow formation of **3** was observed by using 2-propanol/H₂O (3÷1, v/v) (Table 1,entry 7). On the light of these preliminary results, further catalytic tests were run exclusively in ethanol/H₂O3÷1 (v/v). Other inorganic bases have been screened, thus also KF and KO^tBu have shown to be effective. Though the reaction went to completion with both bases, less than 92% of **3** was obtained after 8 h (Table 1, entries 8 and 9). A neat decrease of catalyst amount apparently did not markedly affect the reaction rate. For example, in the presence of 0.1 mol% of Pd the yield of **3** after 8 h was 92%, while the complete conversion of **1** into **3** was achieved in 16 h (Table 1, entry 10). Finally, completion of the model reaction was achieved within 10 min at 353K (Table 1,entry 11).



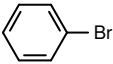
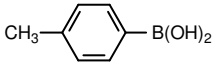
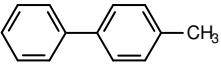
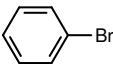
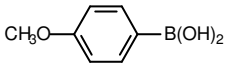
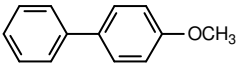
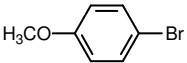
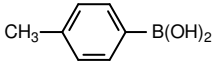
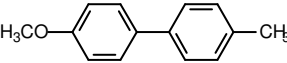
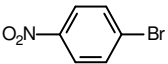
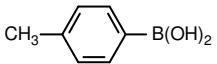
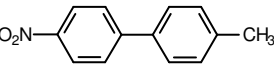
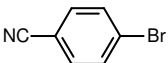
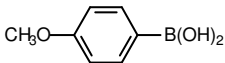
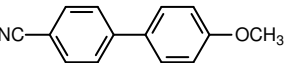
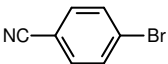
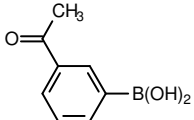
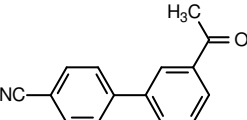
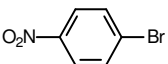
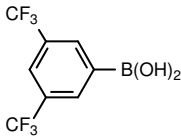
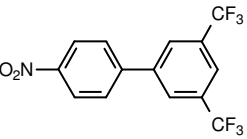

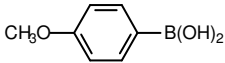
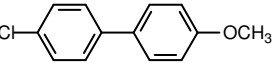
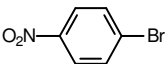
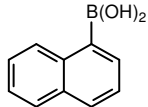
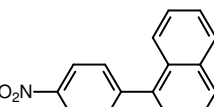
Scheme 2: The model SM reaction between bromobenzene (**1**) and 4-tolylboronic acid (**2**) leading to 4-methyl-1,1'-biphenyl (**3**).

Entry	Catalyst	Solvent (v/v ratio)	Base	Yield (%)	Time (h)
1	Pd/CeO ₂ (2 %wtPd)	EGME/H ₂ O 3 ÷ 1	K ₂ CO ₃	> 99 %	11
2	Pd/CeO ₂ (2 %wtPd)	Ethanol/H ₂ O 3 ÷ 1	K ₂ CO ₃	> 99 %	8
3	CeO ₂	Ethanol/H ₂ O 3 ÷ 1	K ₂ CO ₃	0 %	12
4	Pd/CeO ₂ (2 %wtPd)	Ethanol/H ₂ O 1 ÷ 3	K ₂ CO ₃	> 99 %	40
5	Pd/CeO ₂ (2 %wtPd)	H ₂ O	K ₂ CO ₃	95 %	72
6	Pd/CeO ₂ (2 %wtPd)	Methanol/H ₂ O 3 ÷ 1	K ₂ CO ₃	> 99 %	8
7	Pd/CeO ₂ (2 %wtPd)	2-propanol/H ₂ O 3 ÷ 1	K ₂ CO ₃	> 99 %	30
8	Pd/CeO ₂ (2 %wtPd)	Ethanol/H ₂ O 3 ÷ 1	KF	87 %	8
9	Pd/CeO ₂ (2 %wtPd)	Ethanol/H ₂ O 3 ÷ 1	KO ^t Bu	92 %	8
10	Pd/CeO ₂ (2 %wtPd)	Ethanol/H ₂ O 3 ÷ 1	K ₂ CO ₃	> 99 %	16
11	Pd/CeO ₂ (2 %wtPd) (353 K)	Ethanol/H ₂ O 3 ÷ 1	K ₂ CO ₃	> 99 %	10 min

Table 1: Suzuki–Miyaura reaction of bromobenzene (**1**) with 4-tolylboronic acid (**2**) to give 4-methyl-1,1'-biphenyl (**3**).

The results of a screening of different electron rich and electron poor aryl halides and arylboronic acids to give products **4–12**, which are collected in Table 2, successfully confirmed the efficiency of Pd/CeO₂ as promoter of the SM reaction and scope of the protocol. Compounds **4–11** were formed quantitatively after 1–14 h, while the heterocycle **12** required about 4 days. All the products were isolated in the solid state in excellent yield and high purity

($\geq 97\%$ checked by $^1\text{H-NMR}$). Purity was lower (93%) only in the case of 4-methyl-1,1'-biphenyl (**3**), as it was contaminated by 7% of 4,4'-dimethyl-1,1'-biphenyl (the byproduct arising from homocoupling of **2**), which could not be separated by chromatography or fractioned crystallization.

Aryl halide	Arylboronic acid	Product	Yield (%)	Time (h)
		 3	89	8
		 4	86	14
		 5	87	10
		 6	85	1
		 7	95	1
		 8	83	3
		 9	88	4
		 10	88	7
		 11	91	1.5

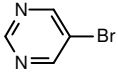
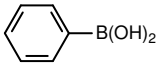
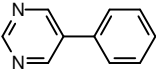
		 12	85	96
-----------------------------------------------------------------------------------	-----------------------------------------------------------------------------------	---------------------------------------------------------------------------------------------	----	----

Table 2: Suzuki-Miyaura reaction between different aryl halides and arylboronic acids catalyzed by Pd/CeO₂

As reported above, the biaryl **3** can be quantitatively formed even by lowering the catalyst amount to 0.1 mol% Pd. In order to test the limits of the catalytic system, also the formation of compounds **5** and **6** starting from an electron rich and an electron poor aryl bromide, respectively, was evaluated by using 0.1 mol% Pd. Successfully, both biaryls were obtained again quantitatively.

1.8 Catalyst reuse

The reusability of the catalyst was examined in the case of the model reaction (Scheme 2). Measurements were carried out using a 1 mol% palladium amount for both consecutive and parallel recycling. The results have been summarized in Figure 6, where yields of **3** relative to the first use and ten successive reuses of the catalyst are reported.

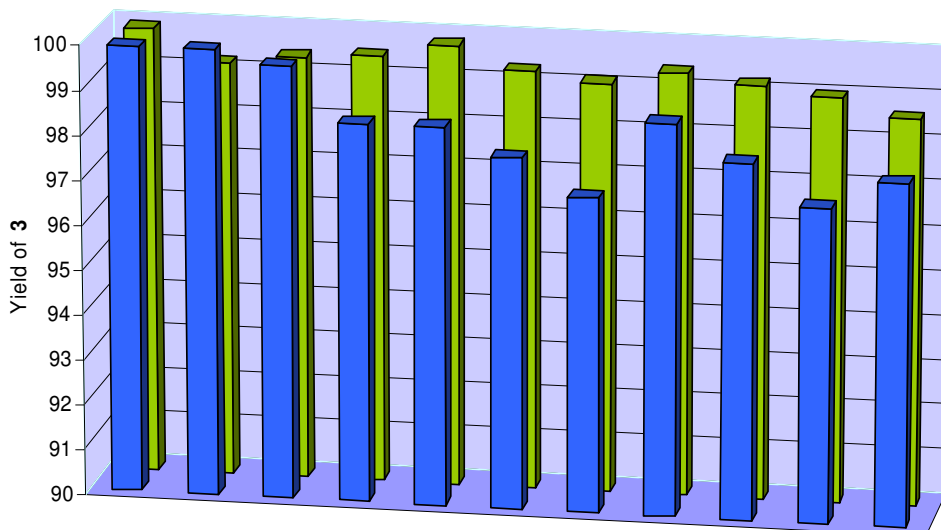


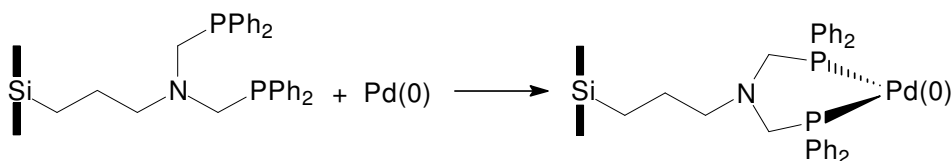
Figure 6: Pd/CeO₂ recycling tests for the standard reaction between **1** and **2** to afford **3**. The GC yields of **3** are relative to the first use and ten consecutive (blue columns) and parallel reuses (green columns).

As clearly evidenced by the histogram, the catalytic performance of Pd/CeO₂ did not appreciably fade after ten reuses. In particular, the GC yield values found for the consecutive recycling were never below 97%. Both sets of experiments were stopped after the tenth reuse, but the lack of a neat decreasing trend may suggest that Pd/CeO₂ effectively behaves as an outstanding long-living catalyst, and such a finding is of particular interest for its possible application in large-scale syntheses of biaryls. As reported above, when the reaction was performed at 353 K, complete formation of **3** was achieved in about 12 min. At this temperature, the yield after the first two consecutive reuses was 98.9% and 99.1%, thus apparently the catalyst seems to maintain its stability even at high temperature.

1.9 Evidences for homogeneous catalysis

To possibly ascertain whether Pd/CeO₂ operates by heterogeneous or homogeneous mechanism at room temperature, the filtration test^[37,38] and the

CS₂ test^[38] were run on the model reaction. The catalyst was filtered off from the reaction mixture after 15 min and the solution was then stirred at 298 K. The GC measurement run immediately after filtration showed 19.8% yield of **3**, which increased to only 23.9% after 8 h, the time necessary for completion of the reaction in the presence of Pd/CeO₂. Thus, a drastic slowing down of the reaction rate was effectively achieved upon elimination of the catalyst, but such a result did not provide a decisive answer about the nature of the true active species. The CS₂ test was accomplished by using three different CS₂/Pd molar ratios, namely, 1÷1, 1÷10 and 1÷50. In the first two cases product **3** was not detected in solution by GC within 24 h. Differently, the C-C coupling occurred when the CS₂/Pd molar ratio was 1÷50 at roughly the same rate as that observed in the absence of carbon sulfide. Such a result is generally considered as proof of occurrence of heterogeneous mechanism, although it should not be viewed as conclusive^[7,20,38]. On the contrary, enlightening was the result of a third test, which was performed by introducing in the reaction mixture a Davisil silica with a 150 Å mean pore size functionalized with a bis(diphenylphosphane) bidentate ligand^[39], (Scheme 3).



Scheme 3: Palladium “trapping” by a diphosphane arm anchored to silica.

Such a kind of poisoning test was first adopted in the Heck C-C coupling by Jones and co-workers^[40] and then applied by Richardson and Jones to both Heck^[41,42] and SM^[42] reactions. Thus, in the presence of a twice molar amount of the -N(CH₂PPh₂)₂ functionality with respect to total palladium present in the reaction vessel, the catalytic activity was nearly suppressed, as only 2.8% of **3** was formed after 8 h. The amount of added silica was based on the loading of organic functionality (0.39mmol·g⁻¹) obtained by combination between elemental analysis (N, P) and TGA measurements^[39]. Therefore, the diphosphane arm is able to extinguish catalysis by chelating a soluble form of palladium, which acts as the effective catalyst. Some authors have suggested that the true catalyst should be a mononuclear Pd(0) species generated by soluble colloidal nanoparticles, which in turn arise from the precatalyst^[12-18,43].

As only traces of noble metal are effectively present in solution at a ppb level, as evidenced below, there is indeed a large excess of supported poisoning bidentate ligand. Notably, Richardson and Jones have found that 35 equivalents of PVPy poison are ineffective, while catalysis was almost stopped in the presence of 350 equivalents of the same polymer^[42]. In line with the hypothesis of formation of an active soluble species from supported palladium, the kinetic plot (Figure 7) shows the typical sigmoidal shape associated with an induction period of the reaction due to formation of the true catalyst in C-C coupling reactions starting from aryl halides^[40-47].

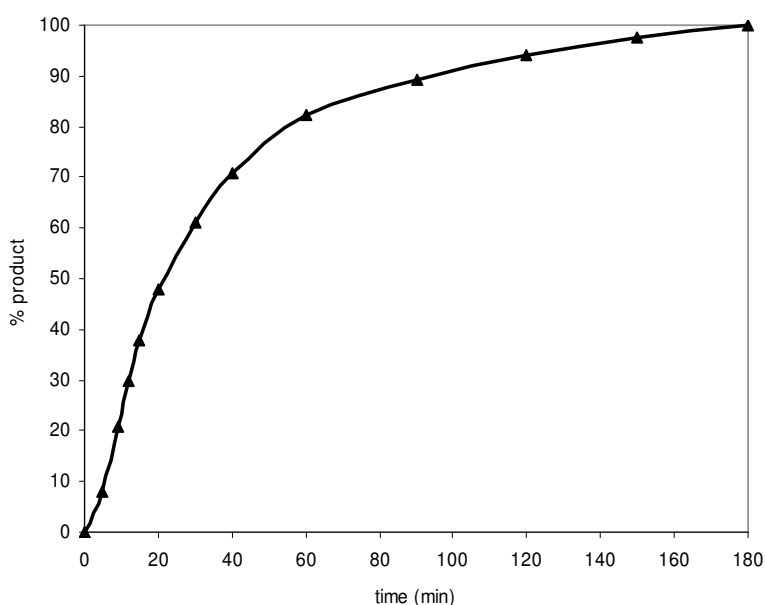


Figure 7: Formation of product **3** as a function of time.

It is quite evident, however, that its generation takes place very rapidly. To check the presence of any nanometric palladium species in solution, after the third reuse of the catalyst, the mother liquor was carefully analyzed by HRTEM, but no evidence for the presence of metal nanoparticles was found. The detection limit of Pd entities under the conditions employed is about 0.8 nm. When directly observed, the size of catalytically active colloidal nanoparticles were 1.7nm (mean value)^[14] or in the range 1.1-2.6 nm^[12]. On the other hand, the ICP-MS analysis showed that 1.4 ppb (instrumental

detection limit = 0.5 ppb) of palladium was present, at the end of the reaction, in the filtered solution after the first use of the catalyst. Thus, though in very low concentration, palladium is effectively present in solution as result of metal leaching from the solid precatalyst. These results seem to suggest that Pd/CeO₂ acts as a reservoir of “homeopathic” amounts [48-50] of catalytically active palladium. Furthermore, the maintenance of catalytic activity upon several reuses could be reasonably explained by a release/re-deposition mechanism [46,51-54], the latter being favoured by the low temperature at which the catalytic process is carried out [54]. This finding is in line with the results reported by Kohler et al. who demonstrated the presence of higher concentration of noble metal during SM catalysis with respect to that measured when the reagents are almost consumed [24]. In our case, the results of the HRTEM analysis of a catalyst sample used four times show that it is virtually indistinguishable from the fresh material. Figure 8 corresponds to a low magnification image of the recycled sample, where the distribution and appearance of CeO₂ support particles are similar to those of the freshly prepared catalyst (Figure 1).

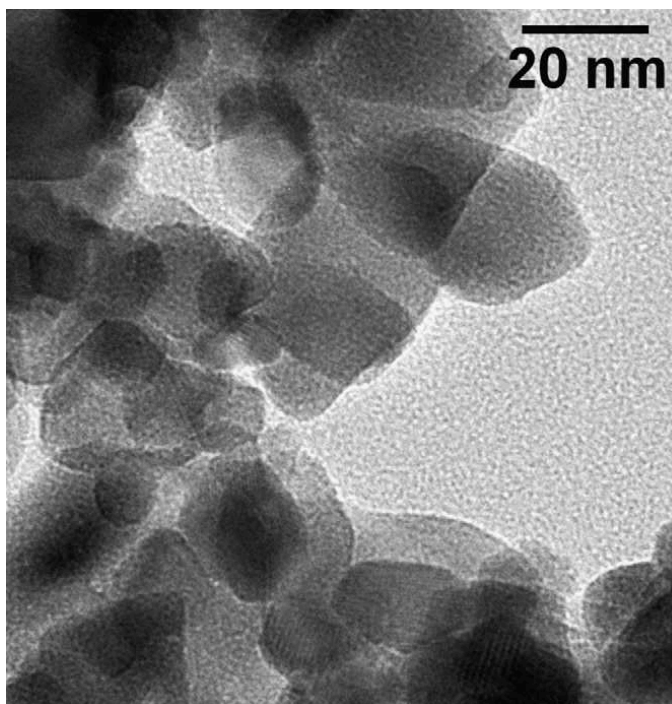


Figure 8: TEM micrograph of a sample of Pd/CeO₂ after four uses in catalytic test.

The HRTEM study of the used sample also denotes the presence of PdO crystallites, and the particle size distribution is only slightly biased towards larger particles (Figure 9).

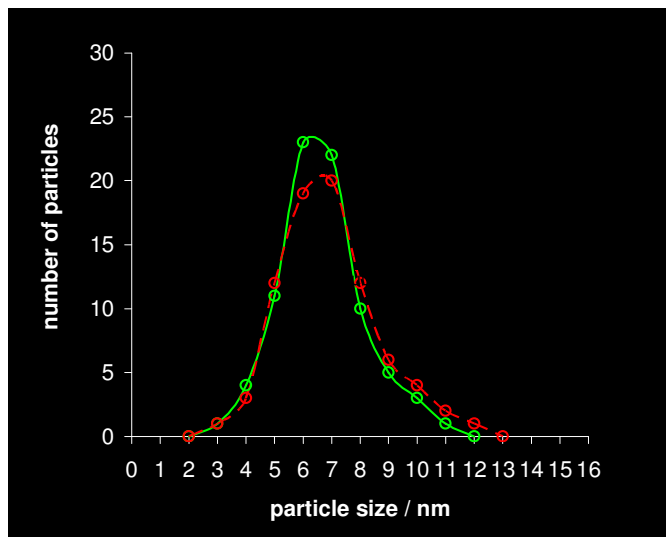


Figure 9: Comparison of particle size distribution between a fresh sample of Pd/CeO₂ (green) and a sample used four times (red) as catalyst of the standard reaction.

The mean particle size has increased only from 6.7 to 6.9 nm. Figure 10 shows a representative HRTEM picture of the used sample, where two PdO particles have been identified. The FT image recorded over the selected area shows spots at 2.64 Å, which are ascribed to the [101] crystallographic planes of PdO. A second representative HRTEM image is depicted in the same figure. Again, spots at 2.64 Å are recognized in the FT image of the area selected, in accordance to PdO [101] crystallographic planes.

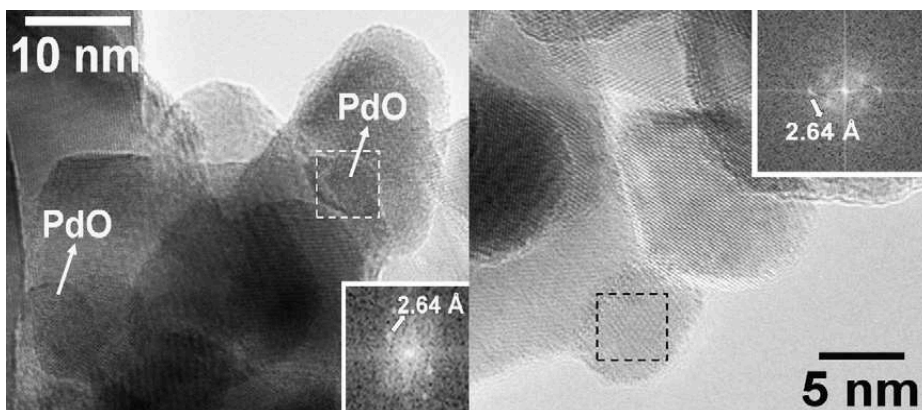


Figure 10: Representative HRTEM image of a sample of Pd/CeO₂ after four uses in catalysis along with Fourier transform (FT) images.

1.10 Conclusions

In this work it has been shown that Pd/CeO₂ behaves as an efficient catalyst in the SM coupling reaction starting from aryl bromides with different electronic substituents. The most remarkable results of the present investigation are the following:

1. the catalyst is active at room temperature, in air, in an environmentally friendly solvent such as 3÷1 ethanol/water mixture;
2. Pd/CeO₂ can be easily prepared, is relatively cheap and is active also in low amount (Pd 0.1 mol%);
3. all couples of substrates employed were quantitatively transformed into the coupling products;
4. the catalyst can be recycled at least ten times without appreciable decrease of activity. For all these reasons, the Pd/CeO₂ system seems to be a good candidate for large-scale applications of the SM reaction.

It has also been demonstrated that a homogeneous mechanism takes place most probably through a release/re-deposition process. At the end of the reaction the amount of palladium in solution was at the ppb level. Thus, if the coupling product showed comparable metal content, it is clear that our procedure meets the requirements of the pharmaceutical industry (<5ppm residual metal in the commercial product).

References

- [1]. N. Miyaura, in: A. de Meijere, F. Diederich (Eds.), *Metal-Catalyzed Cross-Coupling Reactions*, 1, 2nd ed., Wiley–VCH, Weinheim, 2004 (Chap. 2).
- [2]. L.F. Tietze, H. Ila, H.P. Bell, *Chem. Rev.* 104 (2004) 3453.
- [3]. R.B. Bedford, C.S.J. Cazin, D. Holder, *Coord. Chem. Rev.* 248 (2004) 2283.
- [4]. J. Dupont, C.S. Consorti, J. Spencer, *Chem. Rev.* 105 (2005) 2527.
- [5]. L. Bai, J.-X. Wang, *Curr. Org. Chem.* 9 (2005) 535.
- [6]. K.H. Shaughnessy, R.B. DeVasher, *Curr. Org. Chem.* 9 (2005) 585.
- [7]. N.T.S. Phan, M. Van Der Sluys, C.W. Jones, *Adv. Synth. Catal.* 348 (2006) 609.
- [8]. F.-X. Felpin, T. Ayad, S. Mitra, *Eur. J. Org. Chem.* (2006) 2679.
- [9]. M. Seki, *Synthesis* (2006) 2975.
- [10]. L. Yin, J. Liebscher, *Chem. Rev.* 107 (2007) 133.
- [11]. F. Alonso, I.P. Beletskaya, M. Yus, *Tetrahedron* 64 (2008) 3047.
- [12]. M.T. Reetz, E. Westermann, *Angew. Chem. Int. Ed.* 39 (2000) 165.
- [13]. A.H.M. de Vries, J.M.C.A. Mulders, J.H.M. Mommers, H.J.W. Henderickx, J.G. de Vries, *Org. Lett.* 5 (2003) 3285.
- [14]. M.T. Reetz, J.G. de Vries, *Chem. Commun.* (2004) 1559.

- [15]. C.C. Cassol, A.P. Umpierre, G. Machado, S.I. Wolke, J. Dupont, J. Am. Chem. Soc. 127 (2005) 3298.
- [16]. J.G. de Vries, J. Chem. Soc., Dalton Trans. (2006) 421.
- [17]. A.M. Trzeciak, J.J. Ziołkowski, Coord. Chem. Rev. 251 (2007) 1281.
- [18]. D. Astruc, Inorg. Chem. 46 (2007) 1884.
- [19]. M.D. Smith, A.F. Stepan, C. Ramarao, P.E. Brennan, S.V. Ley, Chem. Commun. (2003) 2652.
- [20]. S.P. Andrews, A.F. Stepan, H. Tanaka, S.V. Ley, M.D. Smith, Adv. Synth. Catal. 347 (2005) 647.
- [21]. A. Cwik, Z. Hell, F. Figueras, Org. Biomol. Chem. 3 (2005) 4307.
- [22]. M. Lakshmi Kantam, S. Roy, M. Roy, B. Sreedhar, B.M. Choudary, Adv. Synth. Catal. 347 (2005) 2002.
- [23]. D. Kudo, Y. Masui, M. Onaka, Chem. Lett. 36 (2007) 918.
- [24]. K. Kohler, R.G. Heidenreich, S.S. Soomro, S.S. Prockl, Adv. Synth. Catal. 350 (2008) 2930.
- [25]. N. Kim, M.S. Kwon, C.M. Park, J. Park, Tetrahedron Lett. 45 (2004) 7057.
- [26]. L.-S. Zhong, J.-S. Hu, Z.-M. Cui, L.-J. Wan, W.-G. Song, Chem. Mater. 19 (2007) 4557.
- [27]. U. Kazmaier, S. Hahn, T.D. Weiss, R. Kautenburger, W.F. Maier, Synlett (2007) 2579.
- [28]. N.G. Willis, J. Guzman, Appl. Catal. A: Gen. 339 (2008) 68.

- [29]. S. Carrettin, J. Guzman, A. Corma, *Angew. Chem. Int. Ed.* 44 (2005) 2242.
- [30]. S. Carrettin, A. Corma, M. Iglesias, F. Sanchez, *Appl. Catal. A: Gen.* 291 (2005)247.
- [31]. A. Trovarelli, *Catal. Rev. Sci. Eng.* 38 (1996) 439.
- [32]. S. Colussi, A. Trovarelli, G. Groppi, J. Llorca, *Catal. Commun.* 8 (2007) 1263.
- [33]. A. Del Zotto, E. Zangrando, W. Baratta, A. Felluga, P. Martinuzzi, P. Rigo, *Eur. J. Inorg. Chem.* (2005) 4707.
- [34]. A. Del Zotto, F. IognaPrat, W. Baratta, E. Zangrando, P. Rigo, *Inorg. Chim. Acta*362 (2009) 97.
- [35]. A. Del Zotto, F. Amoroso, W. Baratta, P. Rigo, *Eur. J. Org. Chem.* (2009) 110.
- [36]. O. Diebolt, P. Braunstein, S.P. Nolan, C.S.J. Cazin, *Chem. Commun.* (2008) 3190.
- [37]. R.A. Sheldon, M. Wallau, I.W.C.E. Arends, U. Schuchardt, *Acc. Chem. Res.* 31(1998) 485.
- [38]. J.A. Widgren, R.G. Finke, *J. Mol. Catal. A: Chem.* 198 (2003) 317.
- [39]. A. Del Zotto, C. Greco, W. Baratta, K. Siega, P. Rigo, *Eur. J. Inorg. Chem.* (2007)2909.
- [40]. K. Yu, W. Sommer, M. Weck, C.W. Jones, *J. Catal.* 226 (2004) 101.
- [41]. J.M. Richardson, C.W. Jones, *Adv. Synth. Catal.* 348 (2006) 1207.
- [42]. J.M. Richardson, C.W. Jones, *J. Catal.* 251 (2007) 80.

- [43]. T. Rosner, J. Le Bars, A. Pfaltz, D.C. Blackmond, *J. Am. Chem. Soc.* 123 (2001)1848.
- [44]. C. Rocaboy, J.A. Gladisz, *New J. Chem.* 27 (2003) 39.
- [45]. K. Yu, W. Sommer, J.M. Richardson, M. Weck, C.W. Jones, *Adv. Synth. Catal.* 347(2005) 161.
- [46]. M. Weck, C.W. Jones, *Inorg. Chem.* 46 (2007) 1865.
- [47]. K. Kohler, W. Kleist, S.S. Prockl, *Inorg. Chem.* 46 (2007) 1876.
- [48]. I.P. Beletskaya, A.V. Chepakrov, *Chem. Rev.* 100 (2000) 3009.
- [49]. A. Alimardanov, L. Schmieder-van de Vondervoort, A.H.M. de Vries, J.G. de Vries, *Adv. Synth. Catal.* 346 (2004) 1812.
- [50]. A.K. Diallo, C. Ornelas, L. Salmon, J.R. Aranzaes, D. Astruc, *Angew. Chem. Int. Ed.*46 (2007) 8644.
- [51]. A. Biffis, M. Zecca, M. Basato, *Eur. J. Inorg. Chem.* (2001) 1131.
- [52]. F. Zhao, M. Shirai, Y. Ikushima, M. Arai, *J. Mol. Catal. A: Chem.* 180 (2002) 211.
- [53]. S.S. Prockl, W. Kleist, M.A. Gruber, K. Kohler, *Angew. Chem. Int. Ed.* 43 (2004)1881.
- [54]. MacQuarrie, J.H. Horton, J. Barnes, K. McEleney, H.-P. Looock, C.M. Crudden, *Angew. Chem. Int. Ed.* 47 (2008) 3279.

CHAPTER 2:

Room-temperature Suzuki–Miyaura reaction catalyzed by Pd supported on rare earth oxides: influence of the point of zero charge on the catalytic activity

The metal catalyzed cross-coupling process has been proven to be amongst the most useful and widely applied methods for C(sp²)–C(sp²) and C(sp²)-heteroatom bonds formation^[1–4]. The exponential growth of studies in this field is mainly due to the exceptional relevance of the Ar–Ar moiety present in several fine chemicals, drugs and natural products. Even more than others, the Suzuki–Miyaura (SM) cross-coupling method has found increasing application for the production of asymmetric biphenyls^[3, 5–8]. The development of new palladium-containing heterogeneous catalysts is one of the main goals in this area in view of the recovery and reuse goal^[2, 9]. However, it is now well recognized that Pd-containing heterogeneous systems employed as catalysts in the cross-coupling reaction generally act as precursors of active forms of palladium through a leaching process^[10–17], even if there are few studies suggesting that the catalytic process may occur on the surface of the solid^[18–23]. Emblematic is the case of Pd/C where contrasting interpretations have been put forward concerning the role of Pd leaching on the catalytic activity^[13, 23]. Starting from precatalysts based on palladium supported on metal oxides, it is generally accepted that the released, catalytically active, metal particles originate from amorphous PdO^[24–27]. The same is true also starting from various forms of (PdO contaminated) metallic palladium^[28]. As a matter of fact, in the case of Pd/Al₂O₃ catalyst, a reductive pretreatment using hydrogen that partially converts Pd²⁺ into Pd(0) afforded a much less catalytically active species^[25]. In addition, a neat decrease of catalytic efficiency has been also observed when a high crystalline form of PdO was provided by prolonged thermal treatment in air^[28]. Such a finding is supported by the fact that thermally treated Pd/Al₂O₃ precatalyst showed reduced catalytic activity in the Suzuki coupling^[25]. Efficiency and reusability of different Pd/supported catalysts have been correlated to the occurrence of a leaching/re-deposition mechanism^[25, 27]. Accordingly, at the end of the catalytic organic transformation, Pd(0) is supposed to deposit back on the surface of the support. In our study on the SM reaction catalyzed by Pd/CeO₂^[14], clear evidences for re-adsorption of palladium onto the surface at the end of the catalytic process

were not achieved. The High Resolution Transition Electron Microscopy (HRTEM) analysis of fresh and used (four times) precatalyst as well as particle size distribution did not show any remarkable modification. Despite this, Pd/CeO₂ showed to be reusable at least ten times without evident loss of catalytic activity. In principle, these results can be roughly interpreted in terms of heterogeneous coupling, but experimental results provided clear and unambiguous evidence for the occurrence of a homogeneous catalytic process^[14]. Literature data strongly support this conclusion^[10, 24, 25]. Another intriguing issue is the paramount importance of the nature of the base, absolutely necessary for the reaction to occur. For example, catalytic systems that showed high efficiency in the presence of NaOH, gave poor results using Na₂CO₃^[28]. Analogously, K₂CO₃ was a better choice with respect to KF or KO^tBu^[14]. Notably, not only the nature of the anion is important for obtaining high yields of the coupling product, but also that of the cation. In a preliminary base screening, K₂CO₃ showed to be much more helpful than Na₂CO₃. Finally, very recently, the decisive effect of the (polar or non polar) nature of the solvent on the formation of a well-defined catalytically active species in the SM reaction has been clearly evidenced^[29]. In this contradictory context, the recent finding that palladium particles released by Au@Pd nanoparticles are more active for a second catalytic run than the residual palladium present in the recovered nanoparticles is very interesting^[30]. The authors also found that there is not a close relation between the amount of noble metal present in solution and the catalytic activity; thus, most probably, only a part of the total palladium released by the nanoparticles is present in a catalytically active soluble form. The most striking feature of the study is the demonstration of the exclusive and cooperative role played by the base and the arylboronic acid on the formation of catalytically active soluble Pd(0). A previous investigation based on Pd/C catalyst showed, on the contrary, that both the aryl halide and the arylboronic acid, but not the base, promote palladium leaching^[13]. Stimulated by the need for new investigations that could spread light into this scientific fix, the catalytic studies have been extended on the Pd/CeO₂ system to other Pd/REOs (rare earth oxide), namely, Pd/La₂O₃, Pd/Pr₆O₁₁, Pd/Sm₂O₃, and Pd/Gd₂O₃. On the bases of previous results obtained using Pd/CeO₂^[14], the first goal was to gain insights about the possibility that Pd²⁺ ions are leached from Pd/REO and then reduced to Pd(0). According to such a scenario, all features that favour a weaker palladium surface interaction with consequent dissolution of Pd²⁺ ions

should result eventually in an increase of the reaction rate. In particular, the study was focused on the degree of surface charging as indirectly estimated by measuring the point of zero charge (PZC) [30–32] of each REO, thus correlating the tendency of Pd²⁺ to enter into solution to the degree of positively/negatively charged surface. Pd²⁺ ions in solution should be easily and rapidly reduced to Pd(0), the effective catalyst that undergoes oxidative addition by the aryl halide substrate, as the first step of the catalytic cycle. If this mechanism is true, then it is reasonable that the higher is the amount of leached Pd²⁺ ions, the higher is the rate of formation of the coupling product, unless aggregation into catalytically inactive form causes a decrease of the amount of active metal centres.

Experimental Section

2.1 Materials

The salts La(NO₃)₃·6H₂O, Ce(NO₃)₃·6H₂O, Pr(NO₃)₃·6H₂O, Sm(NO₃)₃·6H₂O, and Ga(NO₃)₃·6H₂O were purchased from Aldrich. The Pd precursor was a Pd(NO₃)₂ solution (10 wt% in 10 wt% nitric acid, Pd 99.999 %) purchased from Aldrich. All solvents were reagent grade and used without further purification.

2.2 Synthesis of Pd/REO 1–5

The Pd/REO catalysts Pd/La₂O₃**1**, Pd/CeO₂**2**, Pd/Pr₆O₁₁**3**, Pd/Sm₂O₃**4**, and Pd/Gd₂O₃**5** were synthesized by a two steps procedure as follows.

First step:

The rare earth oxides were prepared starting from the corresponding nitrate precursor. The lanthanide nitrate (3 g) was dissolved in water (100 mL) and the mixture was heated at 333 K under stirring to facilitate dissolution. Addition of a concentrated solution of NH₃ (5 mL) to the cooled solution resulted in the precipitation of the rare earth hydroxide. The stirring was stopped and the precipitate was allowed to stand for 1 h, then the suspension was filtered off and the solid was washed with water to remove traces of NH₃. The product was dried at 393 K for 15 h and then calcined at 873 K for 4 h with a temperature ramp of 10 K/min to afford the rare earth oxide.

Second step:

The Pd/REO catalysts were prepared according to the incipient wetness technique. The Pd precursor was a solution of 10% Pd(NO₃)₂ (99.999%) that was added drop by drop to the REO support to obtain a Pd/REO catalyst with a nominal 2 wt% palladium loading. After impregnation, the solid was dried at 393 K for 15 h and then calcined at 873 K for 4 h with a temperature ramp of 10 K/min. In the case of Pd/La₂O₃, a sample with a nominal 0.5 wt% palladium has been prepared following the same procedure. A sample of Pd/La₂O₃ has been reduced by treatment for 3 h at 573 K with H₂ (4 % in Ar) in a Carbolite oven. Cooling of the sample was performed at 10 K/min rate in He atmosphere.

2.3 PZC Determinations

The PZC value of each REO was measured according to a published procedure [31]. Water (100 mL) was thermostated under stirring at 298 K and a 0.12 M solution (0.8 mL) of NaNO₃ was added. The pH of the solution was measured and a solution of NaOH 1 M was added drop by drop until the pH reached a basic value. At this point, a crop of REO (about 15–20 mg) was added and the mixture was left under stirring for 2 minutes. After this time, the pH of suspension was measured and another crop of REO was added. After 2 minutes of stirring, the pH was measured again. The addition of REO caused the pH value to change until pH value approached PZC value. At this point, the addition of further amounts of REO did not cause variations in the pH of the solution. The whole procedure was repeated starting from a different initial basic pH. Analogously, the method was applied to two starting solutions whose pH was adjusted to an acidic value by adding, drop by drop, a solution of 1 M HCl. The PZC value was obtained graphically from the four curves pH versus REO total mass as shown in figure 1.

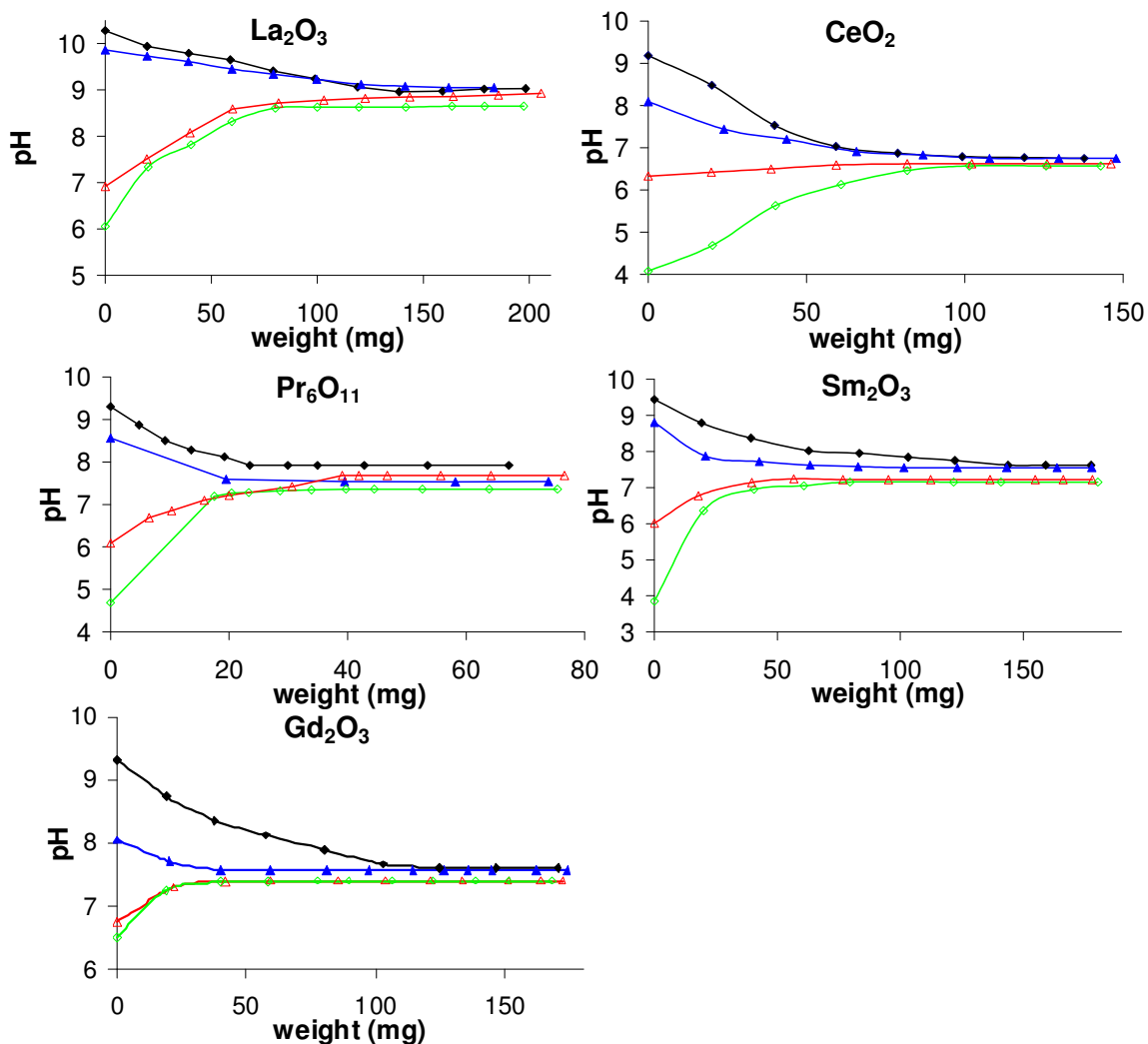


Figure 1: PZC determination of the REOs by adopting the mass titration method [26].

2.4 Catalytic Runs

The following general procedure was adopted for all reactions catalyzed by **1–5**. In a thermostated bath at 298 K, a 10 mL Schlenk flask was charged in air with a magnetic stirring bar, catalyst (1 mol% Pd), arylboronic acid (0.6 mmol),

diethylene glycol diⁿbutyl ether (GC internal standard, 0.5 mmol), K₂CO₃ (0.6 mmol), ethanol (1.5 mL) and H₂O (0.5 mL). The reaction was then started by the addition of aryl bromide (0.5 mmol). For the GC analysis, about 0.1 mL of mixture was extracted from the flask by means of a syringe and 0.5 mL of water was added to the sample to quench the conversion, followed by extraction with dichloromethane (2 x 1 mL). The solution was dried over Na₂SO₄ and analyzed by GC after purification on a microcolumn filled with silica gel. Analogous procedure was adopted when the Pd loading was 0.1 or 0.05 mol%.

2.5 Determination of the Palladium Amount in Solution

Four independent experiments were run with both Pd/La₂O₃ and Pd/CeO₂.

(a) In a thermostated bath at 298 K, a 10 mL Schlenk flask was charged in air with a magnetic stirring bar, Pd/La₂O₃ (1.5 mg, 0.05 mol%), 1-naphthylboronic acid (0.6 mmol), K₂CO₃ (0.6 mmol), ethanol (1.5 mL) and H₂O (0.5 mL), and the reaction was started upon addition of 1-bromo-4-nitrobenzene (0.5 mmol). After 2 minutes, the suspension was poured into a 100 mL round bottom vessel containing ethanol (30 mL) and H₂O (10 mL) to quench the reaction and then filtered immediately to eliminate the solid material. The palladium content of the solution was analyzed by ICP. Pd amount was 13.2 μg.

(b) The reaction was started as in point a) and was allowed to reach completion (20 minutes). The solution was then filtered in order to eliminate the solid and the palladium content of the solution was analyzed by ICP. Pd amount was found to be 9.5 μg.

(c) As in b). The organic product [1-(4-nitrophenyl)naphthalene] was extracted with dichloromethane (2 x 10 mL). After elimination of the solvent, the palladium content of the recovered crude solid (117 mg, 94 % yield) was analyzed by ICP. Pd amount was 8.7 μg.

(d) As in b) but Pd/CeO₂ (1.4 mg, 0.05 mol%) was used instead of Pd/La₂O₃, Pd amount detected by ICP was 1.2 μg.

2.6 Catalyst Recycling

In a thermostated bath at 298 K, a 8 mL conical centrifuge test tube was charged in air with a magnetic stirring bar, Pd/La₂O₃ (30.2 mg), 4-methylphenylboronic acid (0.6 mmol), diethylene glycol diⁿbutyl ether (GC internal standard, 0.5 mmol), K₂CO₃ (0.6 mmol), ethanol (1.5 mL) and H₂O (0.5 mL), and the reaction was started upon addition of 1-bromo-4-nitrobenzene (0.5 mmol). After 1 h, the suspension was centrifuged and the supernatant was removed and analyzed by GC. The solid was washed with water and ethanol, dried on air and reused for the second test, which was performed upon addition in sequence of solvents, 4-methylphenylboronic acid, GC internal standard, base and 1-bromo-4-nitrobenzene, as indicated above. Again, the reaction was stopped after 1 h by centrifugation and the successive workup was analogous to that previously described. Iteration of this procedure was continued for four consecutive reuses of the catalyst. Yields of 4-methyl-4'-nitro-1,10-biphenyl from the GC measurements were the following:

first use: **99.9%**
first reuse: **99.7%**
second reuse: **84.5%**
third reuse: **20.8%**
fourth reuse: **5.4%.**

The same procedure was adopted when Pd/CeO₂ (27.5 mg) was used as the catalyst. In this case the reaction time was prolonged to 6 h. Yields of 4-methyl-4'-nitro-1,1'-biphenyl from the GC measurements were the following:

first use: **99.8%**
first reuse: **99.3%**
second reuse: **99.1%**
third reuse: **98.6%**
fourth reuse: **97.3%**

After the fourth reuse, the residual palladium loading of Pd/La₂O₃ was 0.04 %, while that of Pd/CeO₂ was 0.58 % (measurements by ICP).

2.7 Instruments

The GC–MS analyses, run to control the identity of the compounds obtained in the catalytic trials, were carried out with a Fisons TRIO 2000 gaschromatograph-mass spectrometer working in the positive ion 70 eV electron impact mode. Injector temperature was kept at 523 K and the column (Supelco® SE-54, 30 m long, 0.25 mm i.d., coated with a 0.5 µm phenyl methyl silicone film), temperature was programmed from 333 to 553K with a gradient of 10K/min. The GC analyses were run on a Fisons GC8000 Series gaschromatograph equipped with a Supelco® PTA-5 column (30 m long, 0.53 mm i.d., coated with a 3.0 µm poly(5 % diphenyl-95 % dimethylsiloxane) film). Injector and column temperatures were as indicated above. The X-Ray spectra were recorded on a Philips X'Pert diffractometer equipped with Cu K α radiation source. Stepsize was 0.01° with a time-per-step of 80 s. SEM (Scanning Electron Microscopy) measurements were run on a ZEISS EVO scanning electron microscope. X-Ray Photoelectron Spectroscopy (XPS) was carried out with a SPECS system equipped with an Mg anode XR50 source operating at 200 W and a Phoibos MCD-9 detector. XP spectra were recorded with pass energy of 25 eV at 0.1 eV steps at a pressure below 10⁻⁹ mbar.

Results and Discussion

2.7 Synthesis and Characterization of 1–5

Pd/REO **1–5** used in this work were easily prepared by a two-step synthesis, starting from nitrate salts of the rare earths and Pd(NO₃)₂. Characterization of **1–5** was done by means of BET and XRD measurements and Pd elemental analysis. The data and the PZC values are shown in Table 1.

Compound	%Pd	SA[m ² ·g ⁻¹]	PV[cm ³ ·g ⁻¹]	PZC[pH]
Pd/La ₂ O ₃ 1	1.76	16.6	0.24	8.8
Pd/CeO ₂ 2	1.93	31.5	0.18	6.7
Pd/Pr ₆ O ₁₁ 3	1.93	22.4	0.36	7.8
Pd/Sm ₂ O ₃ 4	1.85	11.9	0.21	7.4
Pd/Gd ₂ O ₃ 5	1.99	10.2	0.09	7.5

Table 1: Physical and PZC data for compounds **1-5**

Furthermore, compounds Pd/La₂O₃ and Pd/CeO₂ were subjected to X-Ray Photoelectron Spectroscopy analysis. The XPS data have been collected in Table 2. The co-presence of both Pd⁰ and Pd²⁺ was clearly evidenced in the two samples, with a neat prevalence of the latter.

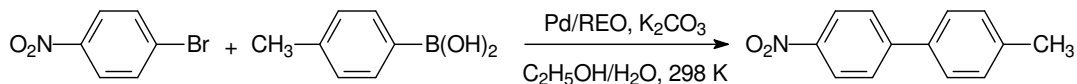
Compound	Binding Energy (eV)				%	
	3d _{5/2} Pd ⁰	3d _{5/2} Pd ²⁺	3d _{3/2} Pd ⁰	3d _{3/2} Pd ²⁺	Pd ⁰	Pd ²⁺
1^a	335.5	336.9	340.7	342.5	36.2	63.8
1^b	335.3	337.0	340.3	342.8	74.6	25.4
2^a	335.7	336.6	341.1	342.6	21.8	78.2
2^b	335.3	336.8	340.4	342.9	61.4	38.6

Table 2; XPS data for compounds **1** and **2**

^a Fresh sample ^b Sample used 4 times

2.8 Catalytic Investigation

Preliminary catalytic tests were carried out according to Scheme 1. The coupling reaction was between 1-bromo-4-nitrobenzene and 4-methylphenylboronic acid in the presence of K₂CO₃, in a 3÷1 ethanol/H₂O mixture, at 298 K in air, according to a well-established protocol [14, 15].



Scheme 1: The Suzuki-Miyaura model reaction

Initially, the reaction was performed using 1 mol% catalyst (with respect to the aryl bromide), then the catalyst amount was decreased to 0.1 mol%, and finally to 0.05 mol%. The results of the last series of catalytic tests are collected in Table 3. Among all precatalysts, Pd/La₂O₃ gave the best catalytic performances. A slightly slower reaction was observed in the case of Pd/Pr₆O₁₁, Pd/Sm₂O₃, and Pd/Gd₂O₃. Noticeably, Pd/CeO₂ showed to be one order of magnitude less effective.

Entry	Catalyst (0.05mol %)	Time (min) ^a	Yield (%) ^b	TOF (h ⁻¹)
1	Pd/La ₂ O ₃ 1	13	68	9130
2	Pd/La ₂ O ₃ ^b	420	0	280
3	Pd/La ₂ O ₃ ^d	360	0	330

4	Pd/CeO ₂ 2	260	2	450
5	Pd/Pr ₆ O ₁₁ 3	17	60	6980
6	Pd/Sm ₂ O ₃ 4	21	52	5650
7	Pd/Gd ₂ O ₃ 5	20	56	5940

Table 3: Comparison of the catalytic activity of **1-5**

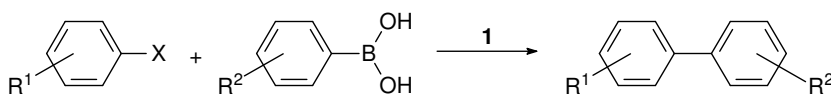
^a Time necessary to achieve > 99 % yield of 4-methyl-4'-nitro-1,1'- biphenyl, determined by GC using diethylene glycol dibutyl ether as internal standard

^b Product yield after 2 min of reaction

^c 0.025 mol% using nominal 0.5 wt% Pd (0.47 wt% Pd from ICP analysis)

^d Catalyst **1** left for 3 h at 573 K under a stream of H₂ (4 % in Ar)

Analogous trend was observed by reacting other substrates. The scope of the catalyzed reaction has been explored. In particular, in the presence of Pd/La₂O₃, about twenty different combinations of aryl bromides and arylboronic acids always resulted in the quantitative formation of the cross-coupling product (isolated yields were in the range 89–97 %). Selected demonstrative results are presented in Table 4. Poor yields of the coupling product were observed starting from aryl chlorides. For example, the reaction between 1-chloro-4-nitrobenzene and 4-methylphenylboronic acid gave only 38 % (GC yield) of 4-methyl-4'-nitro-1,1'-biphenyl at 353K (Table 4, entry 8). On the other hand, only 3-chloro-3'-methoxy-1,1'-biphenyl has been detected in solution by GC–MS when 1-chloro-3-bromobenzene reacted with 3-methoxyphenylboronic acid at 298 K (Table 4, entry 4). This clearly indicates that, in the given experimental conditions, the C–C coupling selectively occurs at the C–Br bond.



Entry	X	R ¹	R ²	Product	Yield
1	Br	4-NO ₂	4-CH ₃		96
2	Br	4-CHO	-		91
3	Br	4-CN	3-COCH ₃		89

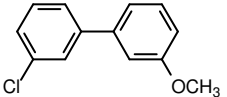
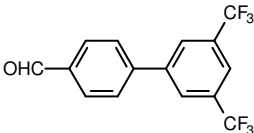
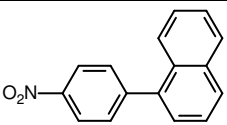
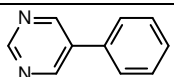
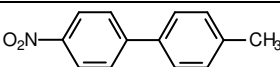
4	Br	3-Cl	3-OCH ₃		91
5	Br	4-CHO	3,5-CF ₃		93
6	Br	4-NO ₂	^a		96
7	Br	^b	-		97
8	Cl	4-NO ₂	4-CH ₃		38

Table 4: Scope of the catalyzed reaction

^a 1-Naphthylboronic acid ^b 5-Bromopyrimidine

2.9 Insights into the Formation of the True Catalyst

It is reasonable to expect that the sequence of activity observed over the REO support (Pd/La₂O₃>Pd/Pr₆O₁₁>Pd/Gd₂O₃>Pd/Sm₂O₃»Pd/CeO₂) have to be related to the tendency of each Pd-REO combination to deliver different amounts of palladium in solution. In a previous investigation based on the application of both Pd/CeO₂^[14] and PdO hydrate^[15] to the SM cross-coupling, we have found that the catalytic activity is completely suppressed in the presence of a diamine arm grafted on silica (“heterogeneous chelation test”). It is likely that the–NHCH₂CH₂NH₂ functionality is able to capture by chelation the Pd²⁺ ions present in solution. However, in principle, the much less probable co-ordination of Pd(0) atoms cannot be excluded^[33, 34]. In literature it is reported that the properties of the support, in particular the surface charging that depends on its PZC, play a major role in the adhesion of metal nanoparticles onto the surface^[35, 36]. For this reason we decided to measure the PZC of each REO under conditions close to that used in the catalytic runs. A reliable determination of PZC, according to the method of Kallay and coworkers^[31, 32], was done in pure water. The PZC values of **1–5** are collected in the last column of Table 1. The values obtained for CeO₂ and La₂O₃, 6.7 and 8.8, respectively, are very close to those previously reported^[37], while no data have been found in

the literature for the other REOs here investigated. It should be noted that the PZC value measured for a given REO is the same obtained for the corresponding Pd/REO, this means that, the presence of ~ 2 wt% of palladium on the surface does not affect appreciably PZC, as expected. The effective relation between the catalytic activity shown by **1–5** and their PZC values is clearly evidenced in Figure 2, that shows a surprisingly good linear correlation between the yield of the coupling product in the early stages of the reaction (after 2 minutes) and the proton molar concentration corresponding to the related PZC ($[\text{H}_3\text{O}^+] = 10^{-\text{PZC}}$). Similar good linear correlation between product yield and $[\text{H}_3\text{O}^+]$ was also obtained at longer reaction times (5 and 10 minutes).

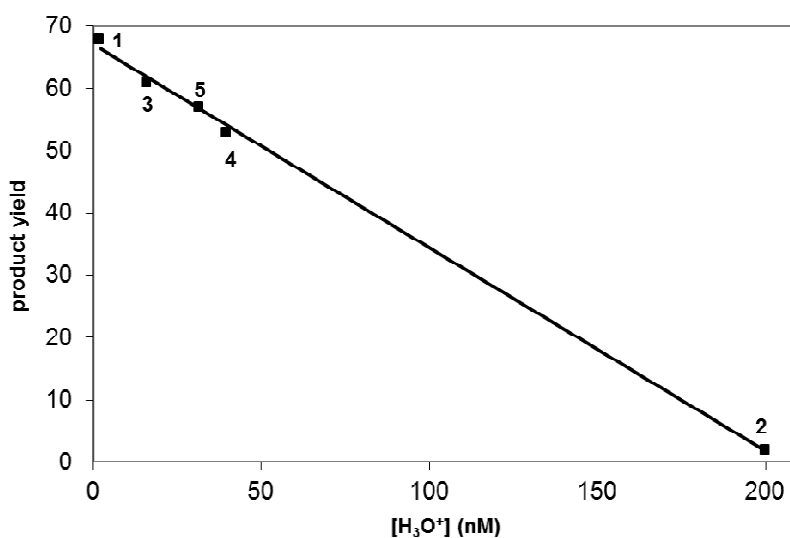


Figure 2: Yield of 4-methyl-4'-nitro-1,1'-biphenyl (after 2 min of reaction) vs. $[\text{H}_3\text{O}^+]$

The higher reactivity of Pd/La₂O₃ is therefore correlated to a marked degree of Pd²⁺ leaching from the surface of La₂O₃, favoured by its less negatively charged surface. According to the observations of Feltes et al. ^[38] in fact, at basic pH such as that of the catalytic reaction (~10.5), high PZC oxides are less negatively charged than low PZC ones. Within the systems under investigation, La₂O₃ shows the higher PZC and thus the lower density of negatively charged sites onto the surface. On the contrary, the lowest activity observed with Pd/CeO₂ is correlated to the higher degree of negatively charged surface which

helps keeping Pd²⁺ ions anchored to the support, as schematically represented in Figure 3.

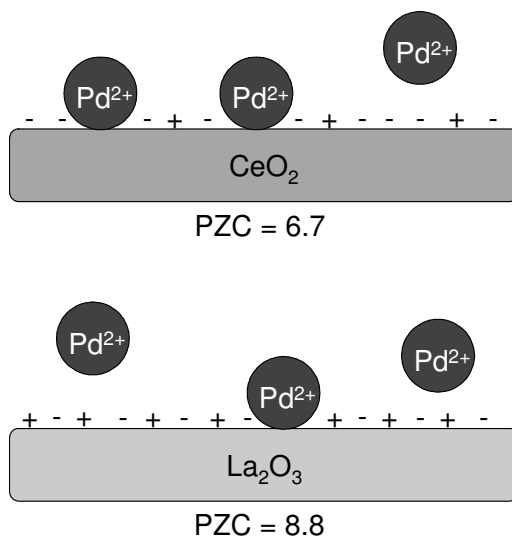


Figure 3: Representation of adhesion and release of Pd²⁺ from the REO surface under catalytic conditions (pH ~ 10.5).

To confirm our hypothesis, two sets of measurements on the model reaction were carried out using modified Pd/La₂O₃ samples. The first one was prepared with a much lower metal loading (nominal 0.5 wt% Pd), the second one was obtained by reducing catalyst **1** at 573 K for 3 h under a stream of H₂. A very slow reaction rate was observed using nominal 0.5 wt% Pd (0.025 mol% Pd with respect to 1-bromo-4-nitrobenzene), (see entry 2 in Table 3). In fact, the reaction was completed (yield > 99 %) only after 7 h. Thus, the lower the noble metal loading on the REO surface, the lower the release of Pd²⁺ ions in solution. Consistently, the H₂-reduced Pd/La₂O₃ sample also showed a very low catalytic activity due to the prevailing presence of Pd(0) on the surface of the support^[25], (see entry 3 in Table 3). The higher tendency of Pd²⁺ to enter in solution in the case of Pd/La₂O₃ is also confirmed by the rapid deactivation of this precatalyst following recycling. Thus, only 5.4 % yield of the coupling product was obtained upon the fourth reuse of **1**. Not surprisingly, the recovered catalyst showed only 0.04 % residual palladium, as checked by ICP elemental analysis. Conversely, catalyst Pd/CeO₂ showed better reusability, as almost quantitative

formation of the coupling product (GC yield 97.3 %) was detected upon the fourth reuse. In this case, the ICP analysis of the recovered catalyst showed that the Pd content was still high (0.58 %). Suitably designed experiments have been carried out in order to assess the Pd content in solution during catalysis, at the end of the reaction, and in the isolated organic product. In the coupling reaction between 1-bromo-4-nitrobenzene and 1-naphthylboronic acid catalyzed by Pd/La₂O₃ (0.05 mol%, 26.4 µgPd), the amount of Pd in solution was 9.5 µg (36 %) at the end of the reaction (20 min) and 13.2 µg (50 %) after 2 minutes, when about 65 % of the total coupling product was already formed. This findings are in line with those previously reported by Köhler and coworkers ^[25] using Pd/Al₂O₃ precatalyst at 333 K, though they found a higher ratio between the two values (~ 5 vs. 1.5). Their conclusion was that at the end of the reaction palladium was almost completely redeposited onto the support. Reasonably, if it is assumed that 13.2 µg may be about the maximum amount of leached palladium in the first use of **1**, then it can be concluded that re-deposition onto the REO support involves less than 30 % of dissolved palladium. Interestingly, when Pd/CeO₂ was used as the precatalyst, the amount of Pd in solution at the end of the reaction (~ 4 h) was only 1.2 µg, in accordance with its much lower catalytic activity due to a reduced palladium leaching. In the case of **1**, we have also measured the amount of Pd on the isolated organic product. It was found that 1-(4-nitrophenyl)naphthalene was contaminated by 8.7 µg of Pd (of the residual 9.5 µg). Thus, more than 90 % of the noble metal detected in solution at the end of the reaction is present in the isolated crude coupling product. The XPS analysis of samples of **1** and **2** recovered after the fourth reuse showed a neat increase of the Pd(0)/Pd²⁺ ratio in the residual noble metal present on the surface of the REO support (Table 2). This may be seen as a further proof that the release of Pd²⁺ ions from Pd/REO is the crucial step for the formation of the actual catalyst. On the other hand, it may be due also to partial re-deposition of palladium on the surface of REO in the form of Pd(0). Furthermore, from the XPS analyses of both fresh and used precatalysts **1** and **2**, Pd/La and Pd/Ce ratios have been obtained. Very interestingly, while in the case of **2**, the Pd/Ce value remained unchanged (fresh: 0.066, used 4 times:0.064), in the case of **1** the Pd/La ratio notably increased (fresh: 0.050, used 4 times: 0.073). Thus, despite the amount of palladium on the La₂O₃ surface strongly decreases during repeated uses of **1**, the residual noble metal on the surface shows higher dispersion. At low temperature this may be ascribed mainly to a re-deposition

process. In a previous work we demonstrated that a sample of Pd/CeO₂ calcined at higher temperature (1027 K instead of 827 K) gave still good performances upon the tenth reuse ^[14]. Thus, the higher the temperature of calcination of Pd/REO, the higher the reusability, but conversely the lower the reaction rate. Reasonably, a thermal treatment of the precatalyst at 1027 K results in an increase of the grade of crystallinity of PdO, thus making more difficult the displacement of Pd²⁺ ions from the surface of the support. Finally, a comparative SEM/EDXS analysis of freshly prepared and used (four times) Pd/La₂O₃ did not show appreciable differences in the morphology of the two samples. However, it should be noted that this result maybe due to limitation of the resolution. On the contrary, the elemental analysis confirmed the extremely low amount of palladium on the exhaust catalyst and revealed the presence of potassium (~ 10 %) on the La₂O₃ surface. This finding can be of importance regarding the potential role, if any, played by the cation of the base (K₂CO₃) on the abstraction of Pd²⁺ ions from the REO support. Studies are in progress to explore such intriguing issue.

Conclusions

In summary, different Pd/REO compounds have been prepared and tested for the first time as catalysts in the SM cross-coupling reaction. All of them have shown to effectively promote the coupling of aryl bromides with arylboronic acids at room temperature. Leaching of Pd²⁺ ions from the surface of Pd/REO seems to be the first step for achieving the true soluble catalyst. We have shown that a close relation does exist between the charge of the surface (measured trough the PZC value) and the extent of palladium leaching at the pH of catalysis. Thus, more positively charged is the surface (this is the case of Pd/La₂O₃), more consistent is the leaching process, and therefore higher is the reaction rate. Consistently, a much slower reaction is observed when Pd/CeO₂ is used as the catalyst, which shows the lowest PZC value within the series of Pd/REO1–5. This is confirmed by the much higher amount of palladium measured in solution for Pd/La₂O₃ with respect to Pd/CeO₂. As a consequence, prolonged recycling is possible in the case of Pd/CeO₂. On the contrary, after four reuses, almost all palladium is disappeared from the surface of more active Pd/La₂O₃. Thus, the use of Pd/CeO₂ as the precatalyst should be preferred for two reasons: (i) it can be recycled several times without decrease of activity, and (ii) the organic product is poorly contaminated by the noble metal. Such

considerations are important in view of potential utilization of these systems in the production of drugs.

References:

- [1]. Miyaura N (2004) In: de Meijere A, Diederich F (eds) Metal catalyzed cross-coupling reactions, vol 1. Wiley-WCH, Weinheim, pp 41–123
- [2]. Yin L, Liebscher J (2007) Chem Rev 107:133
- [3]. Alonso F, Beletskaya IP, Yus M (2008) Tetrahedron 64:3047
- [4]. Slagt VF, de Vries AHM, de Vries JG, Kellogg RM (2010) Org Proc Res & Develop 14:30
- [5]. Miyaura N, Suzuki A (1995) Chem Rev 95:2457
- [6]. Suzuki A (2002) In: Negishi E (ed) Handbook of organopalladium chemistry for organic synthesis, vol 1. Wiley, New York, pp 249–262
- [7]. Kotha S, Lahiri K, Kashinath D (2002) Tetrahedron 58:9633
- [8]. Bai L, Wang J-X (2005) Curr Org Chem 9:535
- [9]. Lamblin M, Nassar-Hardy L, Hierso J-C, Fouquet E, Felpin F-X(2010) Adv Synth Catal 352:33
- [10]. Pröckl SS, Kleist W, Gruber MA, Köhler K (2004) Angew Chem Int Ed 43:1881
- [11]. Phan NTS, Van Der Sluys M, Jones CW (2006) Adv Synth Catal 348:609
- [12]. Richardson JM, Jones CW (2007) J Catal 251:80
- [13]. Chen J-S, Vasiliev AN, Panarello AP, Khinast JG (2007) Appl Catal A: Gen 325:76

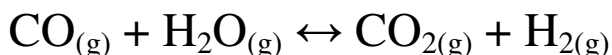
- [14]. Amoroso F, Colussi S, Del Zotto A, Llorca J, Trovarelli A (2010) *J MolCatal A: Chem* 351:197
- [15]. Amoroso F, Colussi S, Del Zotto A, Llorca J, Trovarelli A (2011) *Catal Commun* 12:563
- [16]. Conlon DA, Pipik B, Ferdinand S, Leblond CR, Sowa JR Jr, IzzoB, Collin P, Ho G-J, Williams JM, Shi Y-J, Sun Y (2003) *Adv Synth Catal* 345:931
- [17]. MacQuarrie S, Horton JH, Barnes J, McEleney K, Loock H-P, Crudden CM (2008) *Angew Chem Int Ed* 47:3279
- [18]. Huang Y, Zheng Z, Liu T, Lu J, Lin Z, Li H, Cao R (2011) *Catal Commun* 14:27
- [19]. Ellis PJ, Fairlamb IJ, Hackett SFJ, Wilson K, Lee AF (2010) *Angew Chem Int Ed* 49:1820
- [20]. Kurokhtina AA, Schmidt AF (2009) *ARKIVOC* xi:185
- [21]. Gniewek A, Ziółkowski JJ, Trzeciak AM, Zawadzki M, Grabowska H, Wrzyszczyk J (2008) *J Catal* 254:121
- [22]. Webb JD, MacQuarrie S, McEleney K, Crudden CM (2007) *J Catal* 252:97
- [23]. Maegawa T, Kitamura Y, Sako S, Udzu T, Sakurai A, Tanaka A, Kobayashi Y, Endo K, Bora U, Kurita T, Kozaki A, Monguchi Y, Sajiki H (2007) *Chem Eur J* 13:5937
- [24]. Köhler K, Heidenrich RG, Soomro SS, Pröckl SS (2008) *Adv Synth Catal* 350:2930
- [25]. Soomro SS, Ansari FL, Chatziapostolou K, Köhler K (2010) *J Catal* 273:138
- [26]. Joucla L, Cusati G, Pinel C, Djakovitch L (2010) *Adv Synth Catal* 352:1993

- [27]. Tarabay J, Al-Maksoud W, Jaber F, Pinel C, Prakash S, Djakovitch L (2010) *Appl Catal A* 388:124
- [28]. Amoroso F, Cersosimo U, Del Zotto A (2011) *Inorg Chim Acta* 375:256
- [29]. Proutiere F, Schoenebeck F (2011) *Angew Chem Int Ed* 50:8192
- [30]. Fang P-P, Jutand A, Tian Z-Q, Amatore C (2011) *Angew Chem Int Ed* 50:12184
- [31]. Preočanin T, Kallay N (1998) *Croatica Chem Acta* 71:1117
- [32]. Kallay N, Preočanin T, Ivšič T (2007) *J Colloid Interface Sci* 309:21
- [33]. Trzeciak AM, Mieczysłowska E, Ziółkowski JJ, Bukowski W, Bukowska A, Noworól J, Okal J (2008) *New J Chem* 32:1124
- [34]. Zhao SF, Zhou RX, Zheng XM (2004) *J Mol Catal A: Chem* 211:139
- [35]. D'Souza L, Regalbuto RJ, Miller JT (2011) *J Catal* 254:157
- [36]. Hao X, Barnes S, Regalbuto RJ (2011) *J Catal* 279:48
- [37]. Kosmulski M (2011) *J Colloid Interface Sci* 353:1
- [38]. Feltes TE, Espinosa-Alonso L, de Smit E, D'Souza L, Meyer RJ, Weckhuysen BM, Regalbuto RJ (2010) *J Catal* 270:95

PART 2:

Palladium-based catalysts for fuel processing for fuel cells applications.

The water gas shift reaction is a reversible chemical reaction that takes place between carbon monoxide (CO) and water vapour (H₂O_g) to produce hydrogen (H₂) and carbon dioxide (CO₂):



The WGSR found its first application at the beginning of 20th century in the industrial production of synthesis gas (or water gas, CO + H₂), as a part of the Haber–Bosch process for ammonia manufacture ^[1] and, since Fe-based catalysts employed in this process were deactivated by carbon monoxide, the WGSR played a crucial role in the upgrade of CO to H₂.

Industrial WGS reaction takes place in two stages: a high temperature shift (HTS) between 300 °C and 500 °C, and a low temperature shift (LTS) between 210 °C and 250 °C. Each temperature range requires the use of a specific catalyst.

The Fe-based catalysts are the first heterogeneous catalysts industrially used in the WGS reaction and are commonly called HT (High Temperature) shift catalysts. Many industrial HT shift catalysts contain chromium oxide (Cr₂O₃) as well as iron oxide, and it is being generally believed that Cr₂O₃, possess a retarding effect on the sintering and loss of surface area of the iron oxide, with the consequence of enhancing the activity and stability of Fe catalysts ^[2]. However, its replacement is strongly desirable after considering the health and environmental negative effects associated with hexavalent chromium.

The development and the introduction of Cu-based catalysts, commonly called LT (Low Temperature) shift catalysts, revolutionized the industrial WGS process because the improvements obtained in the performances of the process allowed higher CO conversions and yields in the production of H₂. Since their first usage ^[3], several Cu formulations have been employed in the LT-WGS stage. Improvements in the catalyst activity, stability as well as resistance to

poisoning and sintering were based on such developments. The most used LT-WGS catalyst is a mixture of copper, zinc oxide and aluminum oxide (Cu/ZnO/Al₂O₃). Zinc and aluminum oxides seem to have the function of chemical promoters and structural stabilizers. Many authors evidenced the improvement in catalytic activity of Cu supported on ZnO due to the presence of Cu in different oxidation states inside the metal lattice^[4,5]. The enhancement in WGS activity over binary Cu/ZnO by ternary Cu/ZnO/Al₂O₃ has been highlighted by Apestequia in his work^[6].

With the growing concerns about environmental issues water gas shift reaction is receiving more and more attention due to its application in the field of energy production, as a key step for the purification of hydrogen rich streams coming from a reformer and fed to PEM (Proton Exchange Membrane) fuel cells. Platinum electrodes of a PEM fuel cell can be easily poisoned by a very low amount of CO (~ 2 ppm for on-board vehicle applications – 2007 DOE Guidelines); for this reason WGS coupled with CO preferential oxidation has a fundamental role in lowering CO content to less than few ppm. Within this field, new catalysts are being developed in order to satisfy rigid safety requirements (in addition to fuel cell requirements) such as lower operation temperature, use of non-pyrophoric materials and high attrition resistance, improving at the same time the WGS activity for on-board hydrogen processing.

Noble metal based catalysts supported on reducible oxides seem to be promising candidates for fuel processing, mainly due to their high activity at low temperature and potential stability in oxidizing atmospheres^[7-9]. In particular, Au- and Pt-based materials have been considered for this purpose.

Haruta and coworkers first investigated the potentiality of gold as a catalyst when they observed a high catalytic activity for CO oxidation reaction by using Au-based catalysts containing Au particles smaller than 5 nm deposited on metal oxides like TiO₂, α -Fe₂O₃ and Co₃O₄^[10-12]. The size of Au particles is crucial for the catalytic activity; this means that the preparation method plays a key role for the final application. Since the major requirement for its performances is the contact of the metal structure with the support, it follows that higher the dispersion, better the activity.

Many authors have then carried out studies on highly dispersed Au catalysts over different metal oxides such as Al₂O₃^[13], ThO₂^[14], ZrO₂^[15], CeO₂^[16-18],

TiO₂ [16, 19, 20], mixed oxides of CeO₂-TiO₂ [21], Fe₂O₃-ZnO and Fe₂O₃-ZrO₂ [22], as well as over supports of a different crystalline state [22]. Among all these supports, ceria has received more attention because of its oxygen storage capability. Au-supported ceria has also been reported as a very good catalyst system for CO oxidation [23, 24], alcohol oxidation [25] and NO_x reduction [26].

Platinum group metals (PGM) formulations have been developed by Johnson Matthey with the aim to achieve better catalytic activity, durability and absence of methanation activity over a wide range of temperature (200°C-500°C) [27] with respect to traditional Pt/CeO₂ catalysts. PGM catalysts were employed in a Johnson Matthey fuel processor for stationary applications for WGS in a single stage

Even if Pt- and Au-based systems are very promising for WGS reaction for fuel processing, they also present some drawbacks. First of all, their high price precluded their employment in commercial applications. Pt/TiO₂, one of the most active Pt-based catalysts, requires a high temperature to reduce the support (catalytic activity is proven to increase with the increasing reducibility of TiO₂) [28]. Furthermore it is pyrophoric, deactivates with time on stream runs and, generally speaking, Pt-based catalysts are insufficiently active under 250°C. On the other side, Au-based catalysts are very active only when the size of Au particles is very small (between 1 and 5 nanometres) but they easily deactivate during use.

For all these reasons we have decided to investigate the behavior of palladium-zinc supported on CeO₂, Ce_{0.5}Zr_{0.5}O₂ and ZrO₂ as a promising alternative to platinum-based low temperature WGS catalysts.

References

- [1]. C. Bosch, W. Wild, Canadian Patent 153 379, **1914**
- [2]. H.F. Rase. *Handbook of Commercial Catalysts: Heterogeneous Catalysts*, CRC Press: **2000**; p.520.
- [3]. M.V. Twigg. *Catalyst Handbook* (2nd ed.) Wolfe Publishing Ltd.: London, **1989**.

- [4]. T.M. Yurieva, T.P. Minyukova. *React. Kinet. Catal. Lett.*, **1985**; 29(1), 55–61.
- [5]. Y. Kanai, T. Watanabe, T. Fujitani, M. Saito, J. Nakamura, T. Uchijima. *Catal. Lett.*, **1994**; 27(1–2), 67–78.
- [6]. C.R. Apesteguia, M.J.L. Gines, N. Amadeo, M. Laborde. *Appl. Catal.*, **1995**; 131(1), 283–296.
- [7]. T. Bunluesin, R.J. Gorte, G.W. Graham. *Appl. Catal. B*, **1998**; 15(1–2), 107–114.
- [8]. S.L. Swartz, M.M. Seabaugh, C.T. Holt, W.J. Dawson. *Fuel Cell Bull.*, **2001**; 4(30), 7–10.
- [9]. D. Cameron, R. Holliday, D. Thompson. *J. Power Sources*, **2003**; 118(1–2), 298–303.
- [10]. M. Haruta, N. Yamada, T. Kobayashi, S. Iijima. *J. Catal.*, **1989**; 115(1), 301–309.
- [11]. M. Haruta, S. Tsubota, T. Kobayashi, H. Kageyama, M.J. Genet, B. Delmon. *J. Catal.*, **1993**; 144(1), 175–192.
- [12]. M. Haruta. *CATTECH*, **2002**; 6(2), 102–115.
- [13]. D. Andreeva, V. Idakiev, T. Tabakova, A. Andreev. *J. Catal.*, **1996**; 158(1), 354–355.
- [14]. T. Tabakova, V. Idakiev, K. Tenchev, F. Boccuzzi, M. Manzoli, A. Chiorino. *Appl. Catal. B*, **2006**; 63(1–2), 94–103.
- [15]. V. Idakiev, T. Tabakova, A. Naydenov, Z.Y. Yuan, B.L. Su. *Appl. Catal. B*, **2006**; 63(3–4), 178–186.

- [16]. D. Mendes, H. Garcia, V.B. Silva, A. Mendes, L.M. Madeira. *Ind. Eng. Chem. Res.*, **2009**; 48(1), 430–439.
- [17]. D. Andreeva, V. Idakiev, T. Tabakova, L. Ilieva, P. Falaras, A. Bourlinos, A. Travlos. *Catal. Today*, **2002**; 72(1–2), 51–57.
- [18]. Z.Y. Yuan, V. Idakiev, A. Vantomme, T. Tabakova, T.Z. Ren, B.L. Su. *Catal. Today*, **2008**; 131(1–4), 203–210.
- [19]. M.S. Chen, D.W. Goodman. *Science*, **2004**; 306(5694), 252–255.
- [20]. V. Idakiev, T. Tabakova, Z.Y. Yuan, B.L. Su. *Appl. Catal.*, **2004**; 270(1–2), 135–141.
- [21]. V. Idakiev, T. Tabakova, K. Tenchev, Z.Y. Yuan, T.Z. Ren, B.L. Su. *Catal. Today*, **2007**; 128(3–4), 223–229.
- [22]. T. Tabakova, V. Idakiev, D. Andreeva, I. Mitov. *Appl. Catal.*, **2000**; 202(1), 91–97.
- [23]. W.L. Deng, J. De Jesus, H. Saltsburg, M. Flytzani- Stephanopoulos. *Appl. Catal.*, **2005**; 291(1–2), 126–135.
- [24]. G. Panzera, V. Modafferi, S. Candamano, A. Donato, F. Frusteri, P.L. Antonucci. *J. Power Sources*, **2004**; 135(1–2), 177–183.
- [25]. A. Abad, A. Corma, H. Garcia. *Chem. Eur. J.*, **2008**; 14(1), 212–222.
- [26]. L. Ilieva, G. Pantaleo, I. Ivanov, A.M. Venezia, D. Andreeva. *Appl. Catal. B*, **2006**; 65(1–2), 101–109.
- [27]. C.R.F. Lund. *Ind. Eng. Chem. Res.*, **1996**; 35(9), 3067–3073.
- [28]. Panagiotopoulou, P., Christodoulakis, A., Kondarides, D.I., Boghasian, S. (2006) Particle size effects on the reducibility of titanium oxide and its

relation to the water gas shift activity of Pt-TiO₂ catalysts. J. of Catalysis, 240, 114-125

CHAPTER 3:

Ceria-based palladium-zinc catalysts as promising materials for water gas shift reaction.

Introduction

Hydrogen is the most efficient, cleanest energy source with zero emission of air pollutants. In the last few years the so-called “hydrogen economy” has received increasing attention, in particular in the field of fuel cell technology. Water–gas shift reaction (WGSR), together with CO preferential oxidation, is a key step in fuel processing for fuel cell power systems in order to minimize CO levels in the reformat gas that can poison proton exchange membrane (PEM) fuel cell anodes.

Industrial WGS particulate catalysts (e.g. Cu, Zn, Al) do not have sufficient mechanical stability during startup-shutdown cycles and will rapidly deactivate when exposed to air or liquid water. Pt-based catalysts have low activity at temperatures below 523 K^[1-4]. For these reasons the development of stable, highly active and cost effective materials is still under investigation. Recently palladium-based catalysts have been studied for WGSR^[5] and the formation of alloys between Pd and other metals has been considered as a valid approach for preparing durable and active materials^[6-9]. In particular, within this field, the alloying of Pd with ZnO is a requirement for producing active WGS catalysts as already established for methanol steam reforming^[10]. PdZn has an electronic structure similar to that of copper^[11,12], which is the state-of-the-art catalyst for the low temperature industrial WGSR. Two groups first studied the behavior of alumina-supported PdZn for water gas shift^[13, 14], and the results obtained indicate that these materials are active and stable. In a recent theoretical paper by Wei et al. the authors consider the PdZn alloy as the active site for the WGS reaction and suggest that, on these sites, WGS is likely to proceed through a carboxyl mechanism^[15].

In this work it has been investigated the behavior of PdZn supported on CeO₂ and Ce_{0.5}Zr_{0.5}O₂ recognized as suitable supports for the WGS reaction due to their unique redox properties^[1]. PdZn supported over ZrO₂ is also considered for comparison. Catalytic activity is studied under a typical reformat mixture

and stability is evaluated with time-on-stream and after startup-shut down cycles.

3.1 Experimental

Palladium-zinc based catalysts were prepared by wet impregnation of Pd(NO₃)₂ and Zn(NO₃)₂ solutions on CeO₂, ZrO₂ and Ce_{0.5}Zr_{0.5}O₂. CeO₂ and Ce_{0.5}Zr_{0.5}O₂ supports were synthesized by precipitation/coprecipitation of nitrate precursors at pH 9.5 in the presence of H₂O₂ using ammonia as precipitating agent. The oxides were dried and calcined at 773 K for 4 hours. ZrO₂ was obtained by calcination of Zr(OH)₄ (MEL Chemicals) at 773 K for 4 hours.

After impregnation the catalysts were dried at 348 K for 16 h and calcined in air at 773K for 3 h. The composition of the samples is reported in Table 1.

Sample	Composition (wt%)	Surface area (m ² /g)
PdZnCe	7.5%Pd13%Zn79.5%CeO ₂	41.7
PdZnCZ50	7.5%Pd13%Zn79.5%Ce _{0.5} Zr _{0.5} O ₂	63.7
PdZnZr	7.5%Pd13%Zn79.5%ZrO ₂	46.5

Table 1:Composition and BET surface area of the samples

The materials were characterized by BET surface area measurements (Table 1), X-Ray diffraction (XRD) analysis and Temperature Programmed Reduction experiments. BET surface areas were measured on a fraction of sample of about 200 mg with a Micromeritics Tristar apparatus, by N₂ adsorption/desorption at 77 K. Before measurement, the samples were degassed at 423 K for 90 minutes. X-Ray spectra were collected with a Philips X'Pert diffractometer equipped with an X'Celerator detector using Cu K α radiation, with a step size of 0.02 and a counting time of 80 s per step. Temperature Programmed Reduction Experiments (TPR) were carried out in a Micromeritics AutoChem apparatus. First the samples were treated in air at 673 K for 1 hour, then the temperature was decreased down to 193 K and the gas was switched to a mixture of 4 vol% H₂, followed by a temperature ramp up to 773 K (10 K/min). Catalytic tests were carried out in a typical reformat mixture (38% H₂, 6.5% CO, 9.5% CO₂, 27% H₂O, and 19% N₂) with a GHSV of 10000 h⁻¹ by loading the catalyst powder in a quartz microreactor on a quartz wool bed. Water was fed to the reactor with a Precidor infusion pump through heated lines and was condensed before the analysis of effluent gases. In a catalytic run the sample was heated up

to 773 K at a ramp rate of 2 K/min with a holding time of about 30 min every 50 K. Reactants and products were monitored by an on line Varian CP4900 micro gaschromatograph and catalytic activity was recorded for both fresh and *in situ* reduced samples (indicated as PdZnCe/r, PdZn CZ50/r and PdZnZr/r). Catalyst reduction was carried out at 773 K with 40% H₂ in N₂.

3.2 Results and discussion

Figure 1 presents the powder XRD spectra of fresh, reduced and spent samples. On fresh samples only the reflections of ZnO and the characteristic features of the support are present. Neither Pd nor PdO can be detected. XRD profiles of *in situ* reduced catalysts show clearly the formation of the PdZn alloy that is believed to be the active phase for the WGS. Along with PdZn alloy, also reflections belonging to ZnO are detected while again no traces of Pd or PdO are observed. XRD spectra of spent catalysts (i.e. after a WGS test run) are very similar to those of reduced samples, indicating that alloying of Pd with Zn occurs also during reaction. PdZn particle sizes calculated by Scherrer's formula are similar on all spent and reduced samples and range between 12 and 24 nm.

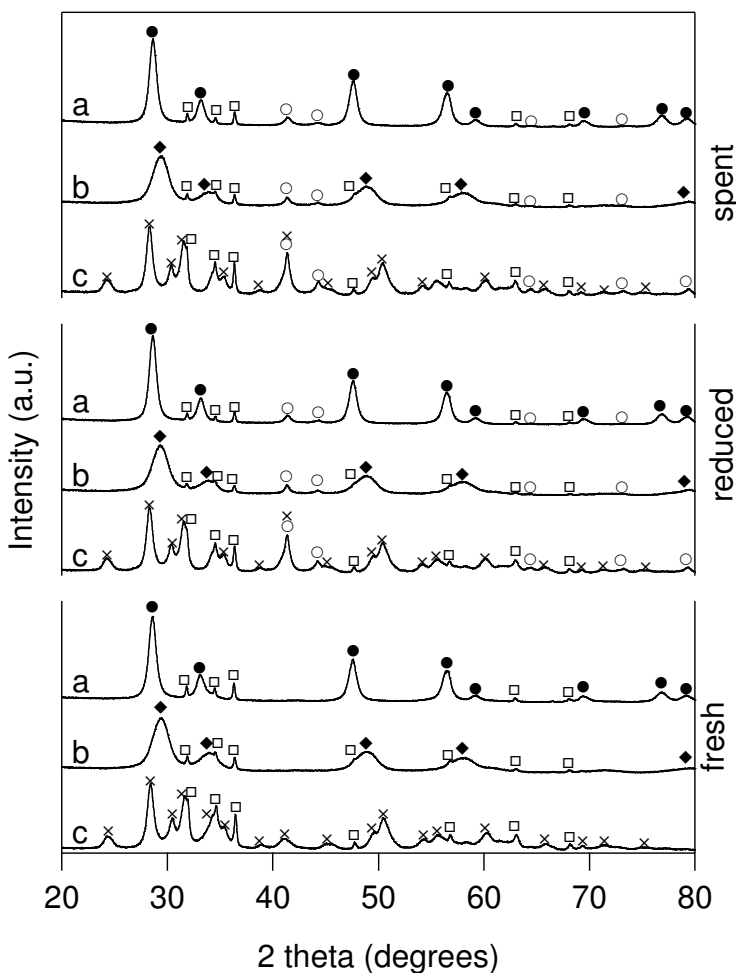


Figure 1: X-Ray diffraction profiles for the samples considered (a: PdZnCe, b: PdZnZr, c: PdZn) ● = CeO₂ (cubic); × = ZrO₂; ◆ = CeZr (tetragonal); □ = ZnO; ○ = PdZn

The effect of the formation of PdZn alloy is evident when comparing the catalytic activity of fresh and reduced catalysts (Figure 2). CO conversion at 523 K increases for all samples, with PdZnCe showing the highest improvement and PdZnZr giving generally poor results.

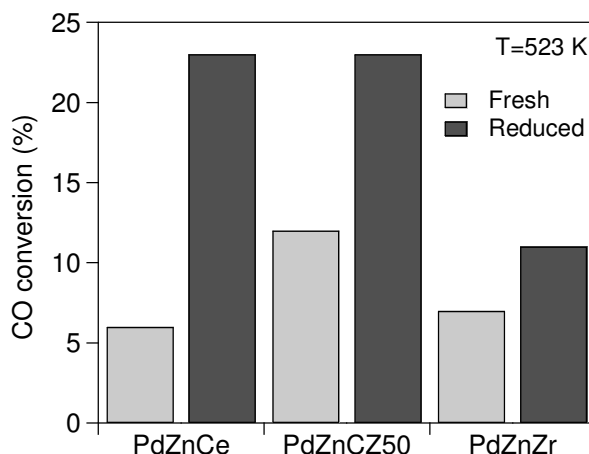


Figure 2: Comparison of CO conversion for fresh and reduced samples at T = 523 K

Figure 3a reports CO conversion curves for all fresh samples, with PdZn CZ50 showing the highest conversion at low temperature. Crossing of the equilibrium curve above 600 K for PdZnCe is due to methane formation. In Figure 3b CO conversion curves for the reduced samples are shown. In this case no methane is detected on PdZnCe/r and its catalytic behavior is almost identical to that of PdZn CZ50/r.

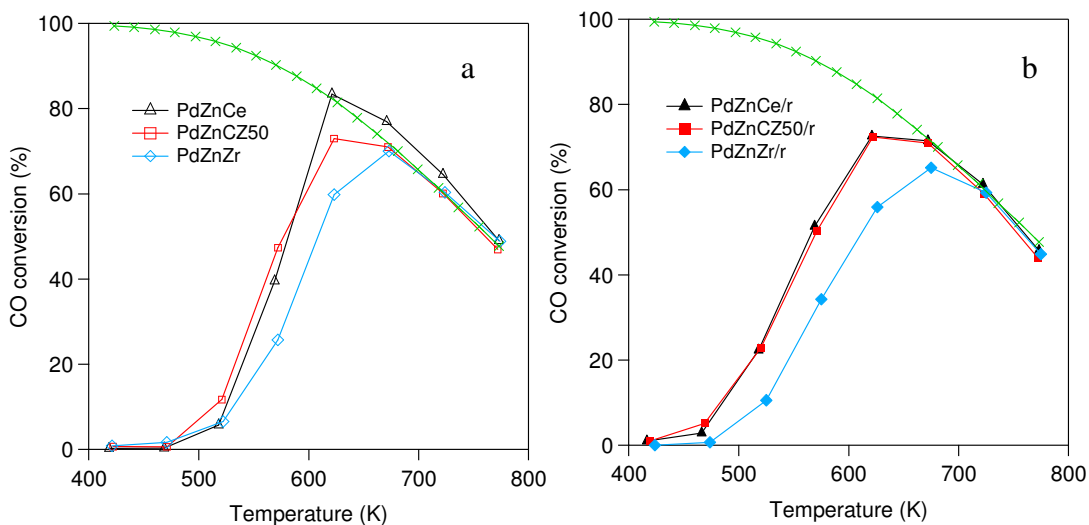


Figure 3: CO conversion curves for a) fresh catalysts and b) reduced catalysts

Since these two reduced catalysts showed the best performances, further investigations were carried out in order to check their stability. Time-on-stream activity tests carried out in the reformat mixture at 523 K for 24 hours did not reveal any significant deactivation for either PdZnCe/r or PdZn CZ50/r (Figure 4), differently from what reported for a Pt/CeO₂-ZrO₂ system under similar conditions^[3].

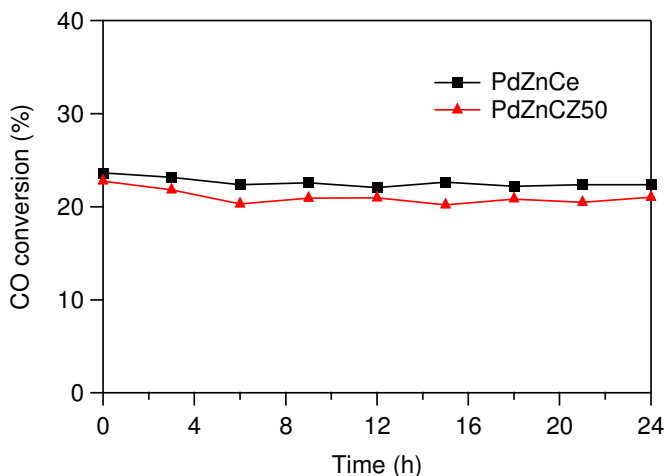


Figure 4: Time-on-stream activity at 523 K for PdZnCe and PdZn CZ50.

The same samples were tested during a series of 8 startup-shutdown cycles in reformat gas. Startup-shut down cycles were carried out as follows. The reduced catalyst was heated up to 573 K in the reformat mixture. The temperature was kept constant for 10 minutes while recording CO conversion. After this period the sample was naturally cooled to 333 K and held at this temperature for 20 minutes before a new heating/cooling cycle started. The results are reported in Figure 5a and 5b for PdZnCe/r and PdZn CZ50/r, respectively.

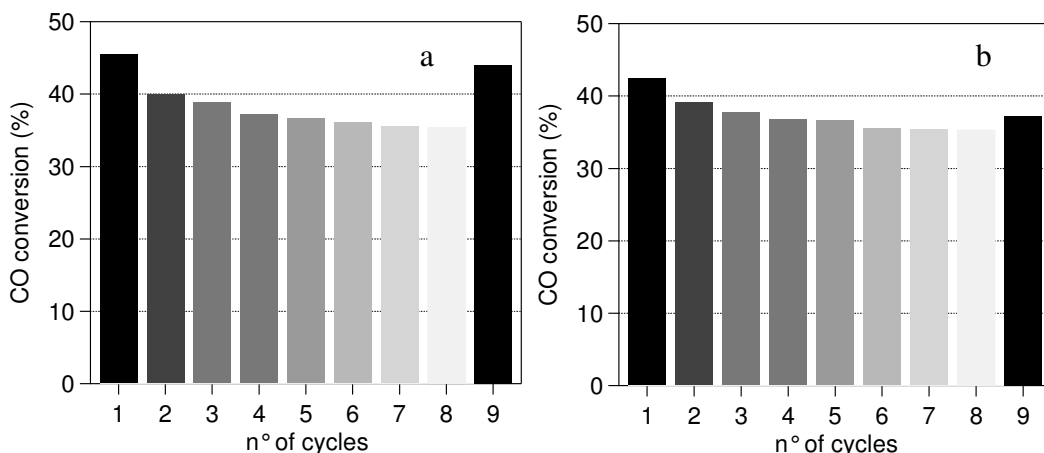


Figure 5: CO conversion during startup-shut down cycles for a) PdZnCe and b) PdZn CZ50

For PdZnCe/r it can be observed that there is a decrease in CO conversion of about 5% after the first shutdown period, while for the following cycles the loss in activity is smaller and becomes almost negligible after cycle 7. The total decrease in CO conversion is only 10%. After cycle 8 the sample was reduced *in situ* and a complete recovery of catalytic activity was observed. For PdZn CZ50, the trend during the 8 startup-shutdown cycles is similar to that of ceria-based sample with a slightly lower decrease in conversion (about 7%) and a stable CO conversion value reached after 5 cycles. On this sample though, only a very small recovery of catalytic activity was recorded after *in situ* reduction (cycle 9). The X-Ray diffraction profiles of the samples subjected to 8 startup-shutdown cycles show the presence of PdZn features comparable to those of the spent catalysts, indicating good structural stability of these materials even if they were exposed to liquid water (water from the feed condensing at 333 K). These results are very encouraging for the further development of PdZn-based catalysts, since it is known that stability under startup-shutdown operation is a key point for fuel processing applications. PdZn catalytic performances during these cycles is promising also in comparison with other noble metal-based catalysts. During a similar series of startup-shutdown cycles on Pt/CeO₂ a loss in conversion of about 70% was reported^[2]. Even if the initial CO conversion for the Pt-based catalyst is almost twice that of PdZnCe, the final value after 8 cycles is much lower (~15% vs ~35%). An analogous treatment carried out on Au/CeO₂ catalyst resulted in an immediate

drop in CO conversion (from ~70% to ~10%) after the first shutdown period [16]. To further investigate the stability of these samples, a second WGS run was performed on both fresh and reduced catalysts. On fresh PdZnCe an increase in CO conversion was observed during the second cycle, in agreement with X-Ray data that show the formation of the active PdZn alloy on the spent catalyst, while similar activity was recorded for the reduced sample during the two catalytic runs. Fresh and reduced PdZnCe presented both an unexpected decrease in CO conversion during the second WGS run, and, to a lesser extent, the same was observed for PdZnZr (Figures 6-8).

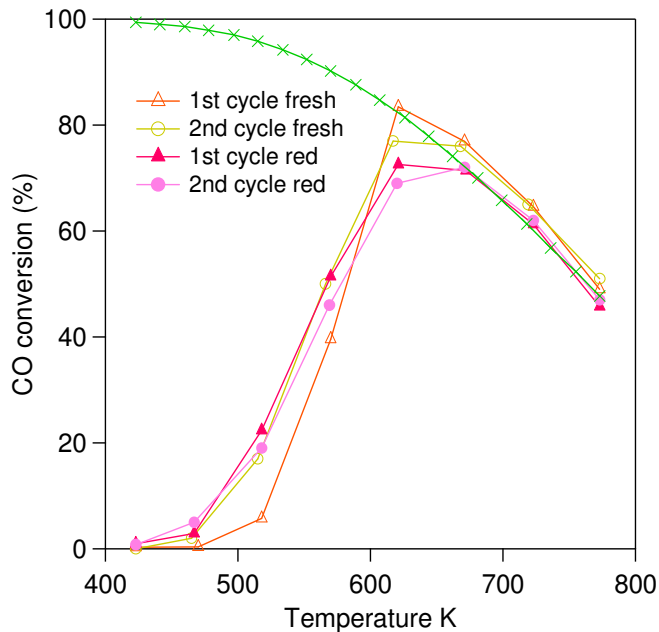


Figure 6: WGS activity for PdZnCe fresh and reduced during two subsequent WGS runs.

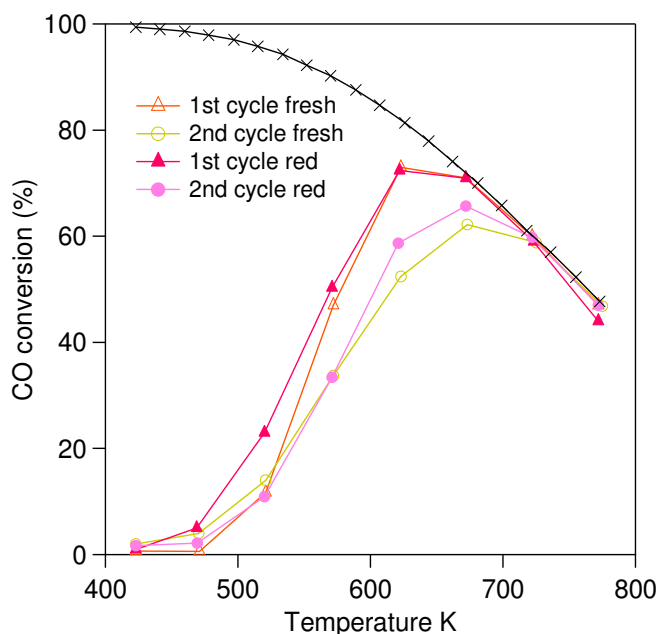


Figure 7: WGS activity for PdZnCZ50 fresh and reduced during two subsequent WGS runs.

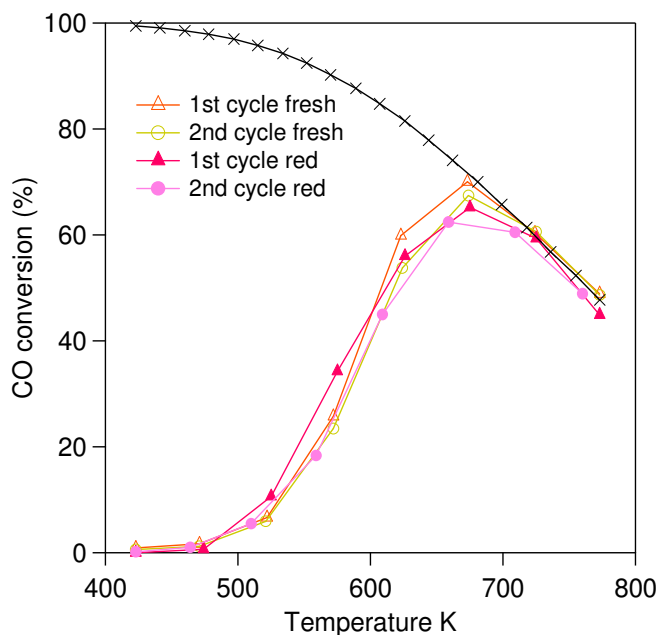


Figure 8: WGS activity for PdZnZr fresh and reduced during two subsequent WGS runs.

The reasons for this behavior are still under investigation, but preliminary studies considered a possible role of carbonaceous species that might block the active sites. To clarify this point, Temperature Programmed Desorption (TPD) experiments were carried out after one WGS test run on reduced catalysts. At 773 K the gas was switched to pure N₂ and the temperature was increased up to 1023 K while monitoring CO and CO₂ evolution by an ABB Uras 14 IR analyzer. TPD profiles are different between the samples, with a slight delay in desorption on zirconia-containing supports (Figures 9a and 9b).

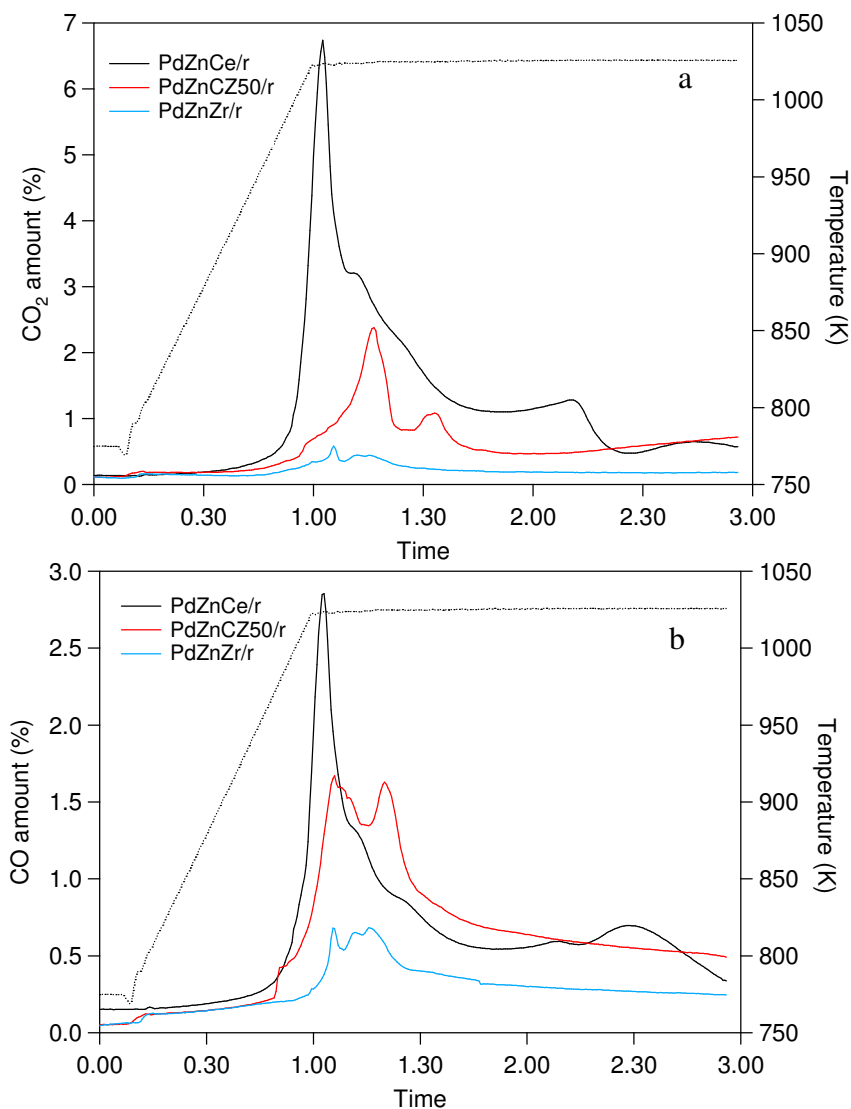


Figure 9: a) CO desorption profiles for all the samples; b) CO₂ desorption profiles for all the samples

Since desorption takes place at constant temperature it seems reasonable to assume that this delay is related to a different bond strength of the species on the catalyst surface. This assumption is supported by the quantitative results reported in Table 2.

Sample	C adsorbed (μmol)	C desorbed (μmol)		ΔC (μmol)
		CO_2	CO	
PdZnCe	3.3×10^3	2.2×10^3	1.0×10^3	0.1×10^3
PdZnCZ50	2.7×10^3	1.0×10^3	1.2×10^3	0.5×10^3
PdZnZr	2.1×10^3	0.3×10^3	0.5×10^3	1.3×10^3

Table 2. Quantitative analysis of carbon species adsorbed/desorbed for each catalyst

It can be observed that PdZn on CeO_2 retains the highest amount of carbonaceous species, and this is in agreement with literature findings that report a higher tendency of carbon build up on pure ceria with respect to ceria-zirconia^[3,17,18]. In contrast, carbonaceous species adsorbed on ceria seem less stable since they are almost completely removed upon heating in inert atmosphere and their desorption starts immediately after reaching the set point temperature (1023 K). This is apparently in conflict with a general report by the same authors stating an easier removal of carbonate-like species from ceria-zirconia mixed oxides. One of the possible interpretations for this behavior is based on the work by Vignatti and coworkers^[19], who observed a higher stability of formate species on Zr-rich surfaces with respect to pure ceria or Ce-rich mixed oxides. The presence of formate-like species on our catalysts cannot be ruled out in principle, since they are generally considered as typical intermediates and/or spectators of WGS^[1]. Investigation of the mechanisms is beyond the scope of this work and will be the object of further studies, nevertheless based on the results we observed blocking of the active sites by strongly bound carbonaceous species cannot be ruled out on PdZnCZ50. The very low activity recovery observed for PdZnCZ50 upon hydrogen treatment carried out after 8 startup-shut down cycles seems to further support this conclusion. These findings would explain the difference between the activation observed under reduction treatment and the loss in activity recorded when the catalyst is exposed to reaction atmosphere (i.e. in presence of C-containing species). For sake of clarity it has to be underlined that the sample presents a marked decrease in activity only after exposure to temperatures up to 773 K and

this might point to some sintering of the active phase, but particle size calculation on the basis of X-Ray analysis seems to minimize this possibility.

Conclusions

In this work the activity of palladium-zinc catalysts supported on CeO_2 , $\text{Ce}_{0.5}\text{Zr}_{0.5}\text{O}_2$ and ZrO_2 was investigated for the water gas shift reaction under realistic process conditions. All samples present an improvement of CO conversion after reduction, due to the formation of the PdZn alloy that is believed to be the active phase. The zirconia-supported catalyst shows the lowest CO conversion in both fresh and reduced form. PdZnCe and PdZnCZ50 retain their catalytic activity with time-on-stream and have greater stability during startup-shutdown cycles compared to similar experiments carried out on Pt-ceria and Au-ceria systems. This lower deactivation rate indicates a good resistance to liquid water, that is one of the main concerns of traditional catalyst formulations (Cu, Zn, Al). After these cycles the activity of PdZnCe can be almost completely recovered by *in situ* reduction, while for PdZnCZ50 only a negligible recovery was detected. PdZnCZ50 shows the highest CO conversion during the first WGS run, but it deactivates after exposure to the reaction atmosphere up to 773 K (even if this temperature is very high for low temperature WGS) and this aspect might be related to carbonaceous species deposited on catalyst surface. These findings open new perspectives for the improvement of PdZn-based materials that appear as a promising alternative to Pt-based catalysts for WGS reaction in fuel processing for fuel cells.

References

- [1]. C. Ratnasamy, J.P. Wagner, *Catal. Rev.* 51 (2009) 325-440
- [2]. X. Liu, W. Ruettinger, X. Xu, R. Farrauto, *Appl. Catal. B* 56 (2005) 69-75
- [3]. W. Ruettinger, X. Liu, R.J. Farrauto, *Appl. Catal. B* 65 (2006) 135-141
- [4]. A. Gayen, M. Boaro, C. de Leitenburg, J. Llorca, A. Trovarelli, *J. Catal.* 270 (2010) 285-298

- [5]. N.L. Wieder, M. Cargnello, K. Bakhmutsky, T. Montini, P. Fornasiero, R.J. Gorte, *J. Phys.Chem. C* 115 (2011) 915-919
- [6]. M.A.H. Juan, C.M.M. Yeung, S.C. Tsang, *Catal. Comm.* 9 (2008) 1551-1557
- [7]. J. Kugai, J.T. Miller, N. Guo, C. Song, *Appl. Catal. B* 105 (2011) 306-316
- [8]. V.M. Shinde, G. Madras, *Appl. Catal. B* 132-133 (2013) 28-38
- [9]. J. Kugai, E.B. Fox, C. Song, *Appl. Catal. A* 456 (2013) 204-214
- [10]. N. Iwasa, S. Masuda, N. Ogawa, N. Takezawa, *Appl. Catal. A* 125 (1995) 145-157
- [11]. Z.X. Chen, K.M. Neyman, A.B. Gordienko, N. Rosch, *Phys. Rev. B* 68 (2003) 075417
- [12]. A. Bayer, K. Fletchner, R. Denecke, H.P Steinruck, K.M Neyman, N. Rosch, *Surf. Sci.* 600 (2006) 78-94
- [13]. R.A. Dagle, A. Platon, D.R. Palo, A.K. Datye, J.M. Vohs, Y. Wang, *Appl. Catal. A* 342 (2008) 63-68
- [14]. L. Bollmann, J.L. Ratts, A.M. Joshi, W.D. Williams, J. Pazmino, Y.V. Joshi, J.T. Miller, A.J. Kropf, W.N. Delgass, F.H. Ribeiro, *J. Catal.* 257 (2008) 43-54
- [15]. H. Wei, C. Gomez, R.J. Meyer, *Top. Catal.* 55 (2012) 313-321
- [16]. X. Liu, P. Guo, B. Wang, Z. Jiang, Y. Pei, K. Fan, M. Quiao, *J. Catal.* 300 (2013) 152-162
- [17]. F. Vindigni, M. Manzoli, T. Tabakova, V. Idakiev, F. Boccuzzi, A. Chiorino, *Appl. Catal. B* 125 (2012) 507-515

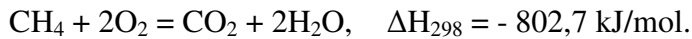
[18]. S. Zeng, X. Zhang, X. Fu, L. Zhang, H. Su, H. Pan, *Appl. Catal. B* 136-137 (2013) 308-316

[19]. C.I. Vignatti, M.S. Avila, C.R. Apesteguía, T.F. Garetto, *Catal. Today* 171 (2011) 297-303

PART 3:

Methane catalytic combustion as a key technology for energy production and emissions abatement

Methane is the main component of natural gas, that nowadays constitutes one of the most exploited energy sources. Furthermore, it has a high H/C ratio and therefore the heat of combustion per mole of CO₂ produced is significantly higher for methane than for other fuels. For example, while the combustion of methane produces 890 KJ per mol of CO₂, the corresponding values for n-decane and coal are 680 and 390 kJ, respectively. The production of energy by the combustion of methane is well known ^[1] and the reaction can be represented by the following equation:



This equation is, however, a simplification of the overall reaction mechanism that involves many radical chain reactions ^[1].

The main drawbacks of traditional flame combustion are that it can occur only within the flammability range between fuel and oxidizer and the fact that the temperatures during the combustion process can reach 1500 °C and higher. At these temperatures, direct combination of nitrogen and oxygen can occur, leading to the formation of noxious nitrogen oxides (NO_x) that are strong atmospheric pollutants.

For this reason, in recent years the catalytic combustion of hydrocarbons has been deeply investigated as a potential alternative to conventional thermal combustion with the aim of minimizing the emission of pollutants (since it takes place at lower temperatures) while optimizing the fuel/oxidizer ratio. Moreover, since one of the concerns about the use of methane as a fuel is that it is a greenhouse gas with a global warming potential much higher than that of CO₂ ^[2, 3], catalytic combustion has been rewarded as a valid secondary emission control technology for the abatement of unburned methane from both stationary and mobile sources.

The general pattern of catalytic combustion of hydrocarbons, commonly known as light-off curve, is shown in figure 1.

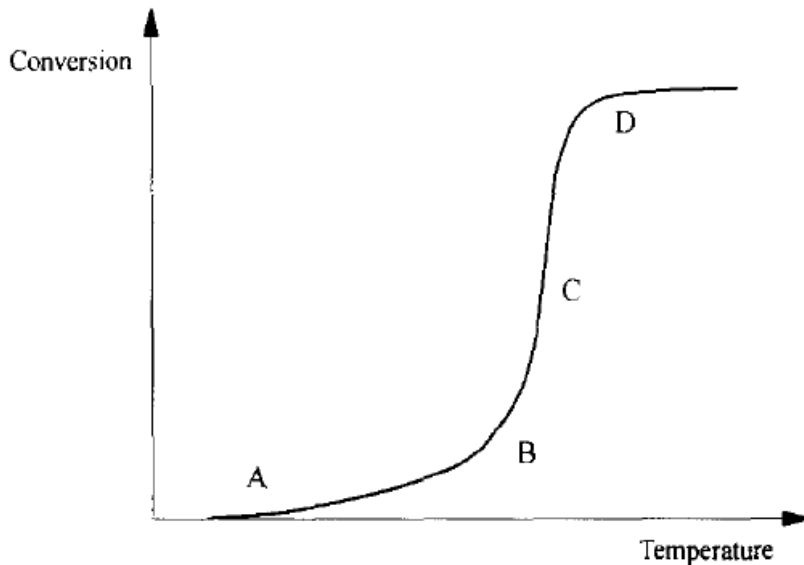


Figure 1: Conversion vs temperature in catalytic combustion

As the temperature increases, the oxidation of the hydrocarbon starts; the value of temperature at which the oxidation begins depends on the hydrocarbon and on the catalyst employed. A further increase in temperature causes an exponential increase in the conversion rate until the point where the heat produced by the reaction is higher than the heat supplied. At this point, the reaction becomes mass transfer controlled until the reactants are depleted.

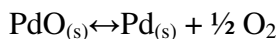
The kinetics of catalytic combustion is relevant only from point A to point B of the curve; then, once light-off takes place (point C), mass and heat transfer are the parameters to consider. At this point, the reaction rapidly approaches complete conversion of the reactants and the heat generated by the combustion of the hydrocarbon causes an increase in the temperature of the catalyst thus, the stability of the catalyst at high temperatures is fundamental.

Both noble metals and metal oxides have been used as catalysts in the catalytic combustion of methane. Noble metals-based materials show better catalytic performances than metal oxides catalysts ^[4, 5]. They are usually used in supported form. A big advantage of supported catalysts is that the metal is dispersed over a greater surface area that helps avoiding sintering at high temperature, moreover the interactions of the metal with the support can improve catalytic activity. Among a large number of formulations investigated, palladium and platinum have shown

superior performances and have been the most widely used catalysts for the catalytic oxidation of methane. The catalytic combustion of methane has been studied also on catalysts based on metal oxides such as Co_3O_4 , $\text{Co}_3\text{O}_4/\text{Al}_2\text{O}_3$, ZnCrO_4 , CuCrO_4 , PbCrO_4 , $\text{Cr}_2\text{O}_3/\text{Al}_2\text{O}_3$, $\text{CuO}/\text{Al}_2\text{O}_3$ and $\text{CeO}_2/\text{Al}_2\text{O}_3$ [4]. Various perovskite-type oxides have also been tested for the catalytic oxidation of methane [5].

The high combustion activity of Pd can be linked to its affinity to oxygen, superior to that of other noble metals such as Pt. For example, the oxygen uptake of a Pd catalyst at 400°C is typically more than 100 times higher than a similar Pt catalyst [6], in good correlation with their relative activities under oxygen lean conditions [7]. The rate and extent of Pd oxidation depends upon the temperature, partial pressure of oxygen, crystallite grain size, and heating rate. There is general agreement in the literature that the active phase of palladium catalysts is palladium oxide, PdO [8-19]. This phase is thermodynamically stable in air only at temperatures below 600°C . Above 600°C PdO decomposes to metallic palladium; since Pd(0) is much less active than palladium oxide in methane combustion, this decomposition implies a loss of catalytic activity. In the last years, intense studies have been addressed to the role of Pd/PdO transformation in CH_4 combustion reaction with the aim of correlating catalytic behaviour with the dynamic of Pd/PdO conversion. It is widely recognized that transformation of PdO to Pd negatively affects catalytic reaction by lowering conversion and that CH_4 combustion activity is reversibly restored upon reoxidation of Pd to PdO [17, 14, 20-24]. In addition to that, a large hysteresis is present between PdO decomposition during heating and Pd reoxidation during cooling making the catalyst less active over a quite large range of temperature [25]. This phenomenon has been widely investigated with different experimental techniques and the effect of many different supports has been tested [20-23]. It has been shown that among the others, cerium oxide is a very effective promoter for Pd reoxidation, resulting in a strong reduction of the Pd–PdO hysteresis [24]. This effect has been tentatively ascribed to the oxygen storage properties of CeO_2 ; lattice oxygen availability in fact seems to be a key factor to initiate PdO reformation.

The dissociation of palladium oxide is expressed as:



Copper oxide is considered as a good replacement for precious metal catalysts due to its comparable catalytic performance and considerably lower cost [26-28]. Supported Cu catalysts exhibit high catalytic performance for methane combustion

due to its high dehydrogenation activity^[29, 30]. However, deactivation due to carbon deposition or to the sintering of the active phase at high temperature has been reported as the major problem for supported Cu catalysts.

There are many papers in literature on the use of copper in CO oxidation, in which Cu is considered both supported^[40, 32-38] and unsupported^[39-46]. Activity of copper in different oxidation states^[41-45], the reaction mechanism in CO oxidation^[44, 45, 47, 48], the effect of the support (related to the presence of oxygen vacancies in the lattice)^[31, 48-52] and the metal loading have been subject of investigation^[34, 38]. In contrast with the CO oxidation reaction, there is only a small amount of papers dealing with the catalytic combustion over Cu catalysts. In most of the studies, alumina is used as support for CuO. Anderson and co-workers investigated the combustion over metal supported catalysts^[31] and reported that the catalytic activity decreased in the order Cr, Mn, Cu, Ce, Co, Fe, Ni, and Ag. Marion et al.^[53] found that the activity per unit mass of catalyst increases for Cu loadings between 2,1% and 4,8%, and then decreases as the metal loading is increased to 9,2%, suggesting the existence of an optimum Cu concentration above which the activity of CuO/Al₂O₃ catalysts decays. Kundakovic and Flytzani-Stephanopoulos^[54] studied the activity of CO and CH₄ oxidation over catalysts prepared with copper oxide and zirconium oxide stabilized with Yttrium. They found that for low Cu loadings (5–15%), the metal is highly dispersed as small clusters or isolated atoms, and when increasing the Cu loading (40%), bulk CuO begins to form. According to these authors, the small Cu clusters are more active than the highly dispersed copper species, and bulk CuO has a little contribution to the catalytic activity. In fact, the catalyst with 15% Cu was the most active for the oxidation of methane.

The information obtained from literature clearly highlight that the nature of the support and the copper loading play an important role on the Cu species present on the catalytic surface. In this study we have investigated the interactions between copper and various supports for potential applications in methane combustion. In particular alumina, ceria, zirconia and ceria-zirconia have been considered as valid materials.

References:

- [1]. Semenov, N.N., **1958**. Some Problems of chemical Kinetics and Reactivity. Pergamon Press, London.

- [2]. B. Hillemann, *Chem. Eng. News*, 1989,67,25.
- [3]. D. Albritton, R. Derwent, I. Isaksen, M. Lal and D. Wuebbles, in *Climate change*
- [4]. Anderson, R.B., Stein, K.C., Feenan, J.J. and Hofer, L.J.E., 1961. Catalytic oxidation of methane. *Ind.Eng. Chem.*, 53: 809-812.
- [5]. Arai, H., Yamada, K., Eguchi, K. and Seiyama, T., 1986. Catalytic combustion of methane over various perovskite-type oxides. *Appl. Catal.*, 26: 265-276.
- [6]. C.F. Cullis and B.M. Willatt, *J. Catal.*, 1983,83,267.
- [7]. K. Muto, N. Katada and M. Niwa, *Appl. Catal., A: General*, 1996, 134,203.
- [8]. J. H. Lee, D. L. Trimm, *Fuel Process Technol.* 42 (1995) 339-359.
- [9]. G. Groppi, C. Cristiani, L. Lietti, C. Ramella, M. Valentini, P. Forzatti, *Catal. Today* 50 (1999) 399-412.
- [10]. J. W. Geus, J. C. Van Giezen, *Catal. Today* 47 (1999) 169-180.
- [11]. G. Centi, *J. Mol. Catal. A-Chem.* 173 (2001) 287-312.
- [12]. T.V. Choudhary, S. Banerjee, V.R. Choudhary, *Appl. Catal. A-Gen.* 234 (2002) 1-23.
- [13]. P. Gélin, M. Primet, *Appl. Catal. B-Environ.* 39 (2002) 1-37.
- [14]. P. Forzatti, *Catal. Today* 83 (2003) 3-18.
- [15]. P. Gélin, L. Urfels, M. Primet, E. Tena, *Catal. Today* 83 (2003) 45-57.
- [16]. A. K. Neyestanaki, F. Klingstedt, T. Salmi, D. Y. Murzin, *Fuel* 83 (2004) 395-408.
- [17]. D. Ciuparu, M. R. Lyubovsky, E. Altman, L. D. Pfefferle, A. Datye, *Catal. Rev.* 44(2002) 593-649.
- [18]. Y. Deng, T. G. Nevell, *Catal. Today* 47 (1999) 279-286.
- [19]. L. M. T. Simplício, S. T. Brandao, E. A. Sales, L. Lietti, F. Bozon-Verduraz, *Appl.*

- [20]. J.G. McCarty, *Catal. Today* 26 (1995) 283.
- [21]. R.J. Farrauto, J.K. Lampert, M.C. Hobson, E.M. Waterman, *Appl.Catal. B* 6 (1995) 263.
- [22]. A.K. Datye, J. Bravo, T.R. Nelson, P. Atanasova, M. Lyubovsky, L.Pfefferle, *Appl. Catal. A* 198 (2000) 179.
- [23]. P.O. Thevenin, E. Pocaroba, L.J. Pettersson, H. Karhu, I.J. Väyrynen, S.G. Järås, *J. Catal.* 207 (2002) 139.
- [24]. P.O. Thevenin, A. Alcalde, L.J. Pettersson, S.G. Järås, J.L.G. Fierro, *J. Catal.* 215 (2003) 78.
- [25]. R.J. Farrauto, M.C. Hobson, T. Kennelly, E.M. Waterman, *Appl. Catal. A* 81 (1992) 227.
- [26]. L.J. Liu, Z.J. Yao, B. Liu, L. Dong, *J. Catal.* 275 (2010) 45–60.
- [27]. H. Zhang, W. Chu, H.Y. Xu, J. Zhou, *Fuel* 89 (2010) 3127–3131.
- [28]. A.C. Furtado, C.G. Alonso, M.P. Cantao, N.R.C. Fernandes-Machado, *Int. J. Hydrogen Energy* 36 (2011) 9653–9662.
- [29]. Aguila G, Gracia F, Cortes J, Araya P. Effect of copper species and the presence of reaction products on the activity of methane oxidation on supported CuO catalysts. *Appl. Catal., B*, 2008, **77**(3-4): 325.
- [30]. Artizzu P, Guilhaume N, Garbowski E, Brullé Y, Primet M. Catalytic combustion of methane on copper-substituted barium hexaaluminates. *Catal. Lett.*, 1998, **51**(1): 69.
- [31]. R. Anderson, K. Stein, J. Feenan, L. Hofer, *Ind. Eng. Chem.* 53 (1961) 809.
- [32]. E. Pierron, J. Rashkin, J. Roth, *J. Catal.* 9 (1967) 38.
- [33]. M. Shelef, K. Otto, H. Ghandi, *J. Catal.* 12 (1968) 361.
- [34]. F. Severino, J. Laine, *Ind. Eng. Chem. Prod. Res. Dev.* 22 (1983) 396.
- [35]. F. Severino, J. Brito, O. Carías, J. Laine, *J. Catal.* 102 (1986) 172.
- [36]. K. Choi, M. Vannice, *J. Catal.* 131 (1991) 22.

- [37]. F. van Neer, B. van der Linden, A. Bliet, *Catal. Today* 38 (1997) 115.
- [38]. P. Park, J. Ledford, *Appl. Catal. B: Environ.* 15 (1998) 221.
- [39]. N. Thomas, L. Caretto, K. Nobe, *Ind. Eng. Proc. Des. Dev.* 8 (1969) 282.
- [40]. Y. Yao, J. Kummer, *J. Catal.* 46 (1977) 388.
- [41]. G. Jernigan, G. Somorjai, *J. Catal.* 147 (1994) 567.
- [42]. W. Crew, R. Madix, *Surf. Sci.* 349 (1996) 275.
- [43]. W. Crew, R. Madix, *Surf. Sci.* 356 (1996) 1.
- [44]. V. Sadykov, S. Tikhov, *J. Catal.* 165 (1997) 279.
- [45]. K. Nagase, Y. Zheng, Y. Kodama, J. Kakuta, *J. Catal.* 187 (1999) 123
- [46]. R. Colen, M. Kolodziejczyk, B. Delmon, J. Block, *Surf. Sci.* 412 (1998) 447.
- [47]. M. Shelef, K. Otto, H. Ghandi, *J. Catal.* 12 (1968) 361.
- [48]. W. Dow, T. Huang, *J. Catal.* 160 (1996) 171.
- [49]. W. Dow, T. Huang, *J. Catal.* 147 (1994) 322.
- [50]. W. Dow, Y. Wang, T. Huang, *J. Catal.* 160 (1996) 155.
- [51]. C. Chien, J. Shi, T. Huang, *Ind. Eng. Chem. Res.* 36 (1997) 1544.
- [52]. T. Huang, K. Lee, H. Yang, W. Dow, *Appl. Catal. A* 174 (1998) 199.
- [53]. M. Marion, E. Garbowski, M. Primet, *J. Chem. Soc. Faraday Trans.* 86 (1990) 3027.
- [54]. L. Kundakovic, M. Flytzani-Stephanopoulos, *Appl. Catal. A* 171 (1998) 13.

CHAPTER 4:

The effect of Ceria on the dynamics of CuO-Cu₂O redox transformation: CuO-Cu₂O hysteresis on Ceria

Introduction

Copper based materials are used in a wide variety of catalytic applications, that range from basic industrial reactions, such as hydrogenation and low temperature water gas shift ^[1], to emissions abatement ^[24] and energy production ^[5, 6]. Recently, copper based catalysts have been considered also for innovative technologies as for example chemical looping combustion (CLC) ^[7-9], chemical looping air separation (CLAS) ^[10, 11] and water splitting ^[12, 13]. The extensive use of these catalysts is mainly due to their chemical stability and low cost, that make them highly attractive for the market. In fact copper has been considered also as a good candidate for the substitution of noble metals in various reactions, such as preferential CO oxidation ^[14, 15], methanol steam reforming ^[16, 17], emissions cleanup from gasoline or diesel engines ^[18, 19] and catalytic combustion of methane ^[20-24]. The choice of support and/or promoters plays a key role in the enhancement of the catalytic performances of any catalyst formulation, and in the case of copper the use of ceria as a support has been regarded as a valid approach to improve the catalytic activity. Cerium oxide is well known for the peculiar oxygen storage capacity of the redox couple Ce⁴⁺/Ce³⁺ that is exploited in several redox reactions ^[25]. Many literature findings clearly indicate that these exceptional redox properties can be tuned by an appropriate combination with other elements, in particular Zr ^[26] and other rare earths ^[27-29]. Various studies evidenced also a beneficial effect on oxygen mobility of ceria by doping it with transition metals such as Co ^[30, 31], Mn ^[32] and Ni ^[33]. Within this field, a synergistic effect of the couple CuO/CeO₂ on catalytic performances has been reported for many applications. For example Flytzani-Stephanopoulos and coworkers investigated copper-ceria catalysts for CO and methane oxidation ^[20, 34]. Their study evidenced a strong interaction at the interface between the two catalyst components: this synergism is explained in terms of stabilization of Cu⁺ species by CeO₂ and increased active oxygen on ceria surface induced by the presence of copper, resulting in higher catalytic activity. Wang and coworkers observed that the presence of Cu facilitates the formation of oxygen vacancies on ceria during water gas shift reaction, thus increasing the number of active sites ^[35]. Martínez-Arias et al. reported a

simultaneous reduction of CuO and ceria during exposure to CO already at room temperature, followed by an easy reoxidation upon contact with O₂ of both materials and attributed to this redox synergy the high catalytic activity of the system for CO oxidation^[36]. A few years later, the same group individuated the interface between Cu and CeO₂ as the preferential site for the onset of Cu²⁺↔Cu⁺ transformation and observed again that copper reduction is accompanied by a slight reduction of the support^[37]. Caputo et al. also studied the behavior of a CuO/CeO₂ catalyst for preferential CO oxidation, demonstrating the participation of surface ceria on the redox reactions favored by Cu-Ce interaction that leads to the formation of very active species^[38]. A strong synergism between copper and ceria was observed by Liu et al.^[39] and Chen et al.^[40] for NO reduction by CO and more recently Nagai and coworkers described a peculiar synchronization of Cu and Ce valence change under periodic rich-lean operation that improves the catalytic activity for NO reduction^[18]. All these evidences point to a very interesting cooperative effect that is worth of further investigation in order to try to better understand the mechanism and the species involved. In the last few years in our group it has been studying in depth the synergy between ceria and palladium oxide, observing a key role of the mutual contact between the two materials on Pd-PdO redox behavior^[41, 42]. In the case of Pd, ceria operates a stabilization effect on palladium oxide and promotes its re-oxidation with respect to an alumina support, reducing the characteristic hysteresis reported for Pd-PdO transformation^[43]. Given the peculiar relationship between copper and ceria evidenced in the literature, it seems worth to investigate it in light of the results obtained for the system palladium-ceria. For this reason in the present work we analyze CuO redox behavior on CeO₂ and Al₂O₃ following a path similar to that used in the previous works, by coupling different analytical techniques such as Temperature Programmed Oxidation (TPO) experiments, X-Ray Photoelectron Spectroscopy (XPS) and X-Ray diffraction analysis (XRD).

Experimental

4.1 Catalyst preparation

Catalysts containing 4% wt of CuO were prepared by incipient wetness impregnation starting from a Cu(NO₃)₂ solution on different supports. The

solution of the precursor was obtained by dissolving the desired amount of copper nitrate salt in a suitable amount of water. Al_2O_3 (Grace Davison MI386) was used as a support after being calcined at 1173K for 4 h, while CeO_2 was prepared by precipitating the nitrate precursor with ammonia solution in presence of H_2O_2 , dried overnight and calcined at 773K for 4 h. After impregnation, the catalysts were dried overnight and calcined at 723K for 4 hours. To check the effect of the support, copper was impregnated also on ZrO_2 obtained by calcination of $\text{Zr}(\text{OH})_4$ (MEL Chemicals) and on $\text{Ce}_{0.3}\text{Zr}_{0.7}\text{O}_2$ obtained by co-precipitation of nitrate precursors at pH 9.5 in the presence of H_2O_2 using ammonia as precipitating agent calcined at 773 K.

4.2 Catalyst characterization

Structural and morphological characterization of the samples was carried out by BET surface area measurements, X-Ray diffraction (XRD) analysis and X-Ray photoelectron spectroscopy (XPS). Surface area measurements were carried out on a fraction of sample of about 200 mg in a Micromeritics TriStar surface area and porosity analyzer, while for X-ray diffraction analysis a Philips X'Pert diffractometer equipped with an X'Celerator detector with $\text{Cu K}\alpha$ radiation was used. X-Ray photoelectron spectroscopy (XPS) was performed with a SPECS system equipped with an Al anode XR50 source operating at 150 W and a Phoibos 150 MCD-9 detector. Spectra were recorded with pass energy of 25 eV at 0.1 eV steps at a pressure below $5 \cdot 10^{-12}$ bar. Binding energies were referred to the adventitious C 1s signal.

Redox properties of the samples were investigated by Temperature Programmed Oxidation (TPO) experiments. For TPO, 100 mg of catalyst were loaded into a quartz microreactor on a quartz wool bed and exposed to 60 mL/min of flowing gas containing 2 vol% O_2 in N_2 . The reactor was placed in a tubular furnace where three heating/cooling cycles were performed with a maximum temperature of 1273 K for each cycle and a ramp rate of 10 K/min. Oxygen uptake/release was monitored with an ABB Magnos 106 paramagnetic analyzer. During a specifically designed TPO experiment, samples were removed from the reactor at 1273K and immediately dipped in liquid nitrogen in order to quench the crystal structure and oxidation state at that temperature^[42]. These samples in the following will be referred to as stop@1273K.

4.3 Results and discussion

In Table 1 composition and surface areas of the samples considered in this work are reported.

Sample	Composition	Surface area (m ² /g)
CuCe	4%CuO-CeO ₂	67.0
CuCZ	4%CuO-Ce _{0.3} Zr _{0.7} O ₂	46.3
CuZr	4%CuO-ZrO ₂	50.1
CuAl	4%CuO-Al ₂ O ₃	176.0

Table 1: Composition and BET surface area of samples.

As expected the values of surface areas reflect the composition of the supports, with the alumina-supported sample showing the highest surface area and the other catalysts having quite similar values between 46 and 67 m²/g.

X-Ray diffraction analysis was carried out on fresh samples, stop@1273K and after 3 complete TPO cycles. In Figure 1, X-Ray patterns of fresh samples are reported. Alumina shows the characteristic features of amorphous γ -Al₂O₃, while cerium oxide presents the typical cubic form with Fm-3m symmetry and on zirconia the reflections of monoclinic ZrO₂ can be observed. Ceria-zirconia diffraction pattern shows the formation of a tetragonal solid solution. It can be observed that on alumina and zirconia-supported catalysts no features belonging to copper metal, CuO or Cu₂O can be detected. This can be ascribed to the overlapping of support reflections in the range between $2\theta=35^\circ$ and $2\theta=43^\circ$ where copper characteristic features are identified and also to the low copper content (~ 3.2 wt% of metallic Cu). For a similar copper-alumina system Águila and coworkers detected CuO reflections on Al₂O₃ only in samples with 12 wt% Cu [23]. For ceria and ceria-zirconia supported samples the characteristic reflections of CuO are observed at $2\theta=35.5^\circ$ and $2\theta=38.7^\circ$, while no Cu nor Cu₂O are detected. This is in agreement with thermodynamic calculations for bulk CuO: for example Cao et al. [44] calculated the phase diagram for CuO, Cu₂O and O₂ by thermogravimetric analysis and observed that in air the transition between CuO and Cu₂O occurs at about 1273 K, far above the calcination temperature used to prepare these samples. Several other literature

works report CuO as being the only phase present also on supported copper systems (see among the others Águila et al. for alumina ^[23] and Luo et al. for zirconia ^[24]). All these observations allow us to consider CuO as the predominant phase also on the other supports.

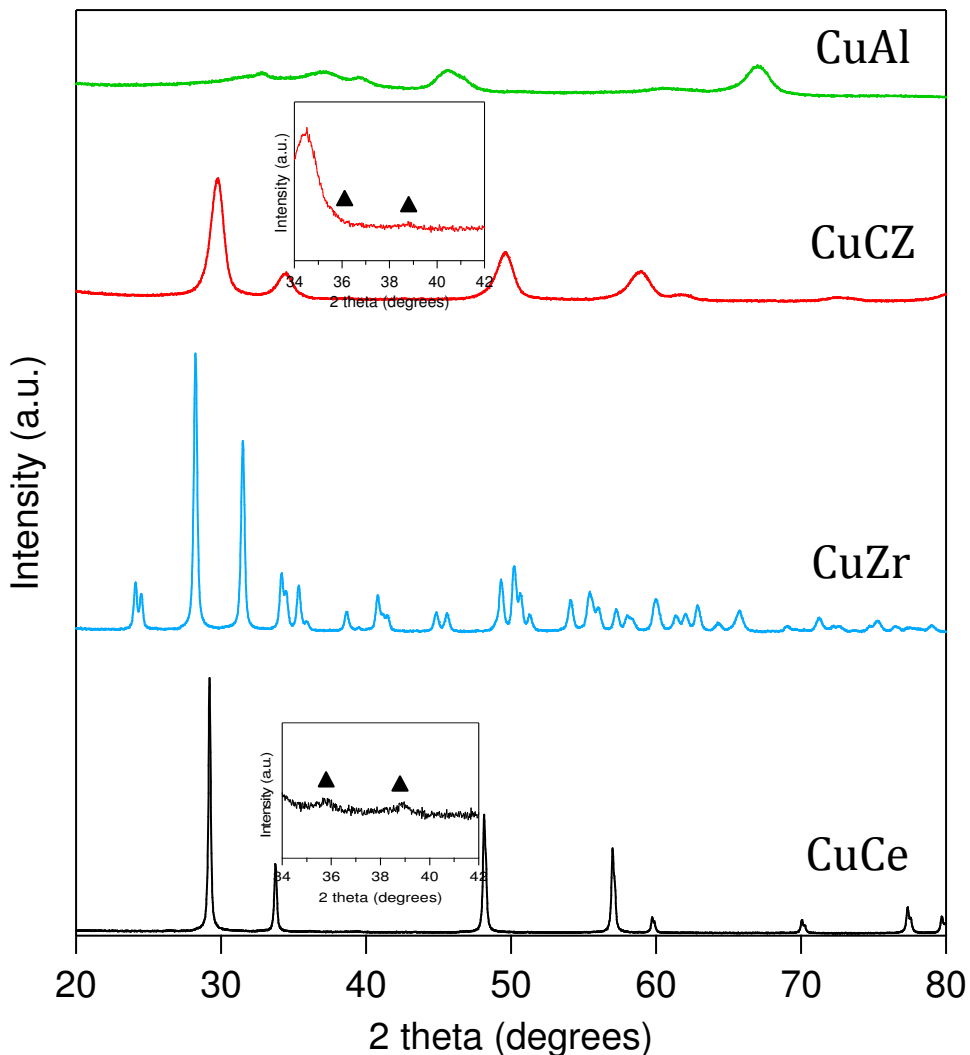


Figure 1: X-Ray spectra of fresh samples (insets: enlargement showing CuO reflections▲)

The presence of copper oxide on fresh samples is confirmed by XPS spectra reported in Figure 2. On CuCe the Cu 2p region exhibits a broad 2p_{3/2} band at 934.0-934.1 eV and strong shake up peaks; these characteristics match well with the XPS spectrum of CuO (all Cu(II) in octahedral sites). On fresh CuAl

again Cu(II) is detected ($2p_{3/2}$ band at 934.7-934.8 eV), but in this case in addition to the main $2p_{3/2}$ and $2p_{1/2}$ photolines small shake up bands are present. Taking into account that Cu(II) in octahedral environment exhibits strong satellite lines (as observed on CuCe), the 2p shape exhibited by the CuAl catalyst may correspond well to copper aluminate spinel, where Cu(II) occurs in both octahedral and tetrahedral environments. Concerning Cu $L_3M_{4,5}M_{4,5}$ Auger lines, on the two fresh samples the bands centered at about 918.0 eV are characteristic of Cu(II).

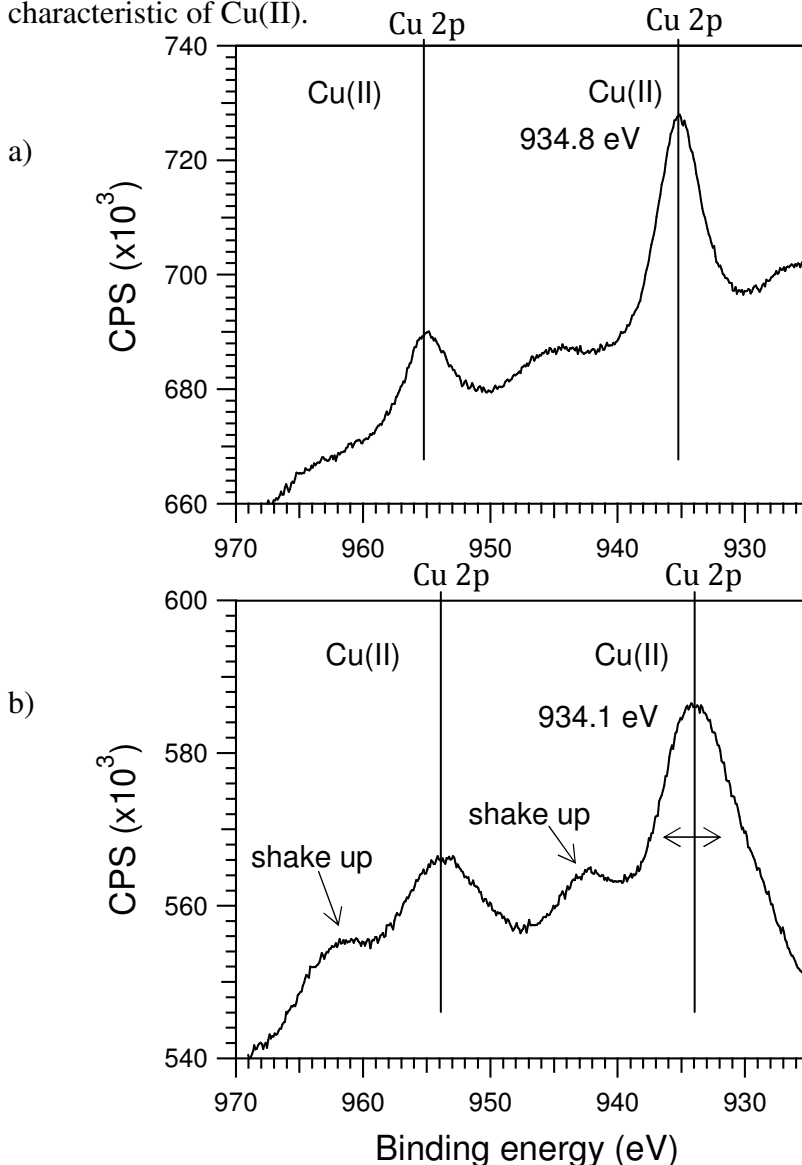


Figure 2: XPS spectra of fresh a) CuAl and b) CuCe samples

TPO experiments were carried out in order to investigate the redox properties of these catalysts. Figure 3 shows three subsequent TPO cycles for CuCe sample.

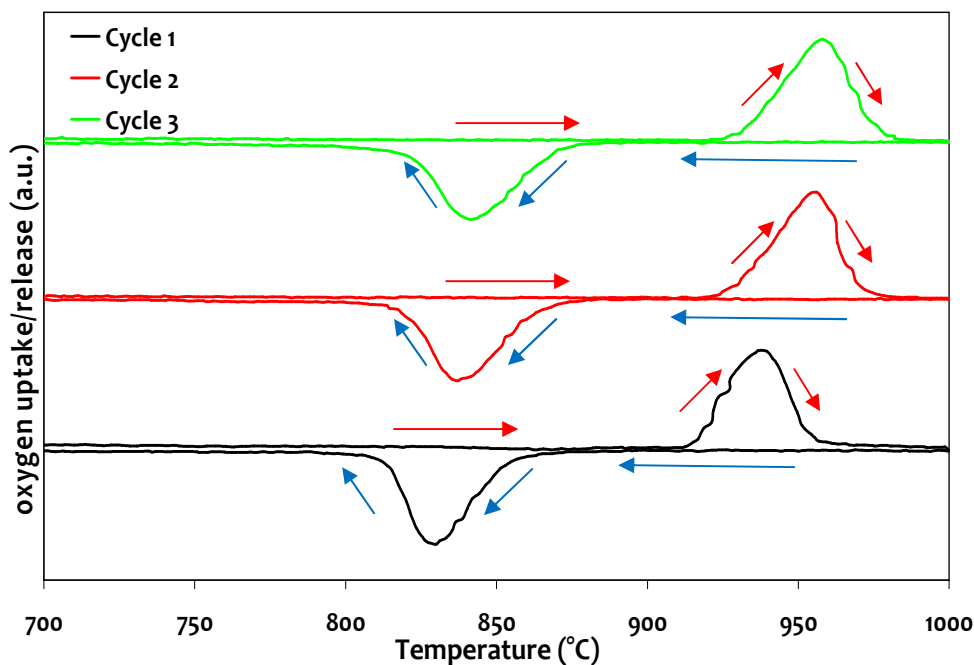


Figure 3: TPO profiles recorded on CuCe sample

→ = warming up

← = cooling down

It can be observed that from the second cycle onwards no significant differences are observed, while between the first and second TPO cycle a shift in the oxygen release peak is recorded. This is likely due to the temperature reached during TPO (1273 K) that is significantly higher than the temperature of calcination (623 K). Based on the observation of this experiment, the third cycle was chosen as representative for all catalysts considered in this work. For CuAl no oxygen uptake or release was detected during all cycles, indicating that on this sample copper did not exchange oxygen during heating/cooling ramps. According to XPS analysis on this catalyst the formation of CuAl_2O_4 is likely to occur already on fresh sample, and this might explain its “inert” behavior towards oxygen. For the other samples, peaks corresponding to oxygen release during heating and uptake during cooling are recorded with intensity and

position varying between the supports, as it is reported in Figure 4. The common aspect of all profiles is the presence of a hysteresis (i.e. a significant temperature gap) between oxygen release and uptake, similar to that well known for Pd-PdO transformation that has been deeply investigated initially by Farrauto and coworkers^[43] and then by several others^[41, 45-47]. The phenomenon is an inherent property of a non-ideal three phase system (gas-metal-metal oxide), as evidenced by Salomonsson et al.^[48], nevertheless its dynamics and the influence of the support on its evolution are complex and difficult to elucidate.

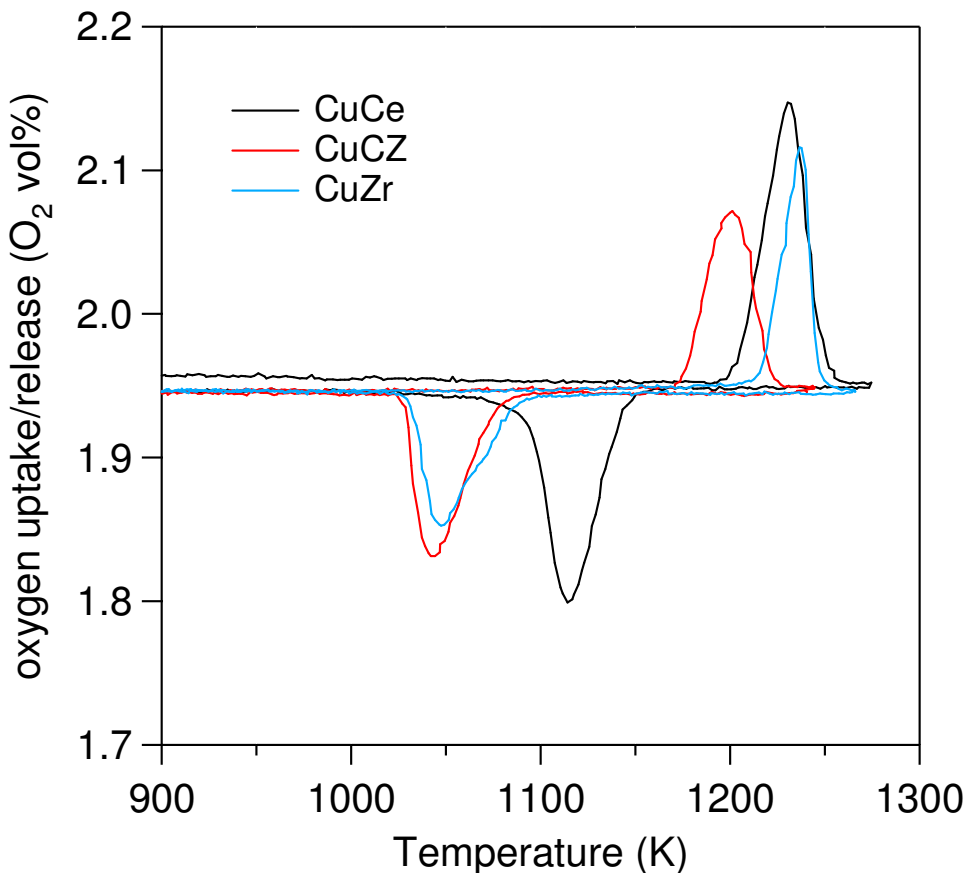


Figure 4: TPO profiles recorded during the third heating/cooling cycle

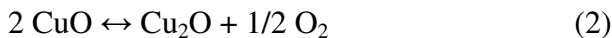
From Figure 4 it is possible to observe that the onset temperature for the peak of oxygen release increases in the order $\text{CuCZ} < \text{CuCe} < \text{CuZr}$, while a different trend is recorded for the onset of the oxygen uptake: $\text{CuCe} > \text{CuZr} \geq \text{CuCZ}$. The

temperature gap between the two peaks is shifted according to the nature of the support and the values range from 40 K for CuCe to 70 K for CuCZ up to 100 K for CuZr. This is in line with what observed for supported PdO where the onset temperatures for PdO decomposition vary with the support together with the amplitude of the hysteresis, with Pd-ceria showing the smallest temperature gap also in this case ^[49-51]. The promotion of metal re-oxidation operated by ceria is a common feature between PdO and CuO, since for both systems the oxygen uptake peak takes place at significantly higher temperatures with respect to other supports ^[49], pointing to a general characteristic of ceria that might be related to its redox properties.

In the case of PdO the reaction taking place is the following:



and it was reported that this redox reaction proceeds via the formation of a surface or interfacial PdO_x^[41]. Copper has a double valence that gives rise to two different oxides: copper oxide (CuO) and cuprous oxide (Cu₂O). According to thermodynamic calculations, the redox reaction for copper during TPO cycles is the following:



XRD and XPS characterization of samples collected at the end of the heating ramp (stop@1273) confirm this point. XRD spectra revealed the presence of Cu₂O on both CuCe and CuZr, as shown in Figures 5a and 5b respectively. On CuCe also some residual CuO was detected. Regarding XPS profiles (Figure 6a and 6b), for CuAl stop@1273 the spectrum is similar to that of the fresh

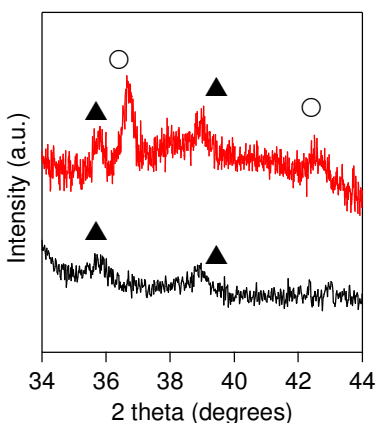


Figure 5a:X-Ray spectra of CuCe sample **fresh** and **stop@1273K** (▲= CuO, ○=Cu₂O)

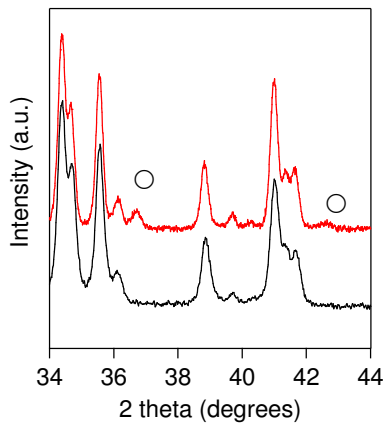


Figure 5b:X-Ray spectra of CuZr sample **fresh** and **stop@1273K** (○=Cu₂O)

sample, indicating the stability of CuAl_2O_4 .

On CuCe stop@1273 the 2p bands are narrower and the satellite lines are less intense than on fresh catalyst, as reported in Figure 6a.

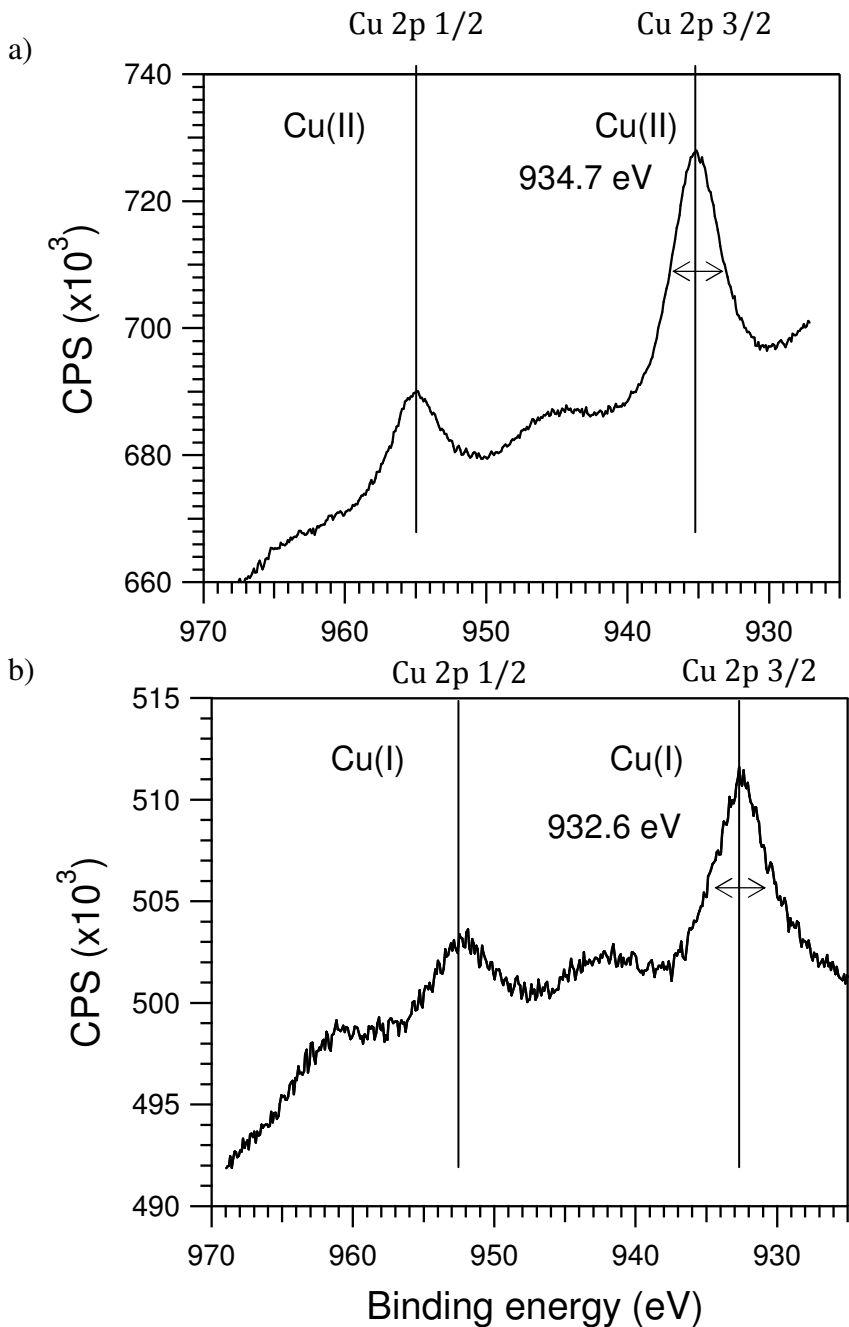


Figure 6: XPS spectra of a) CuAl stop@1273 K and b) CuCe stop@1273 K

The $2p_{3/2}$ band is centered at 932.6 eV, which is characteristic of reduced Cu species, likely Cu(I). The Auger profile is centered at about 917.0 eV, which again can be ascribed to Cu(I). These results are in agreement with what observed by X-Ray analysis that on this sample reveals the presence of Cu_2O together with CuO . The study of the catalysts at the end of the third TPO cycle indicates that copper is completely re-oxidized upon cooling on ceria and zirconia supports. For both samples no reflections belonging to Cu_2O were detected by X-Ray analysis, moreover XPS spectrum of CuCe after 3 TPO cycles is very close to that of the fresh sample, with 2p bands characteristics of Cu(II) (Figure 7).

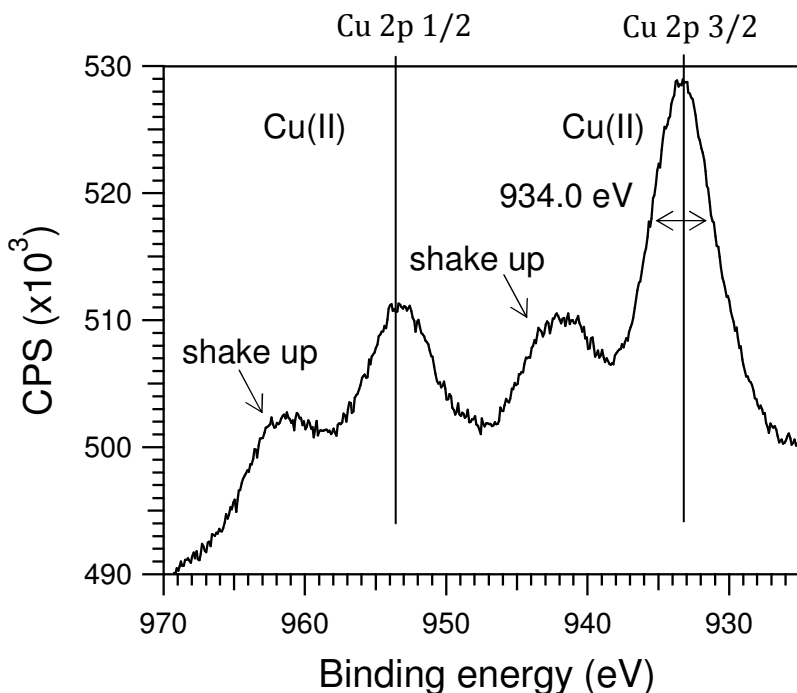


Figure 7: XPS spectrum of CuCe after 3 TPO cycles

Trying to better understand the dynamics of $\text{CuO-Cu}_2\text{O}$ transformation, quantitative analysis on the oxygen uptake/release was carried out during TPO experiments and the results are reported in Table 2.

Sample	$\mu\text{mol O}_2$		$\text{CuO} \leftrightarrow \text{Cu}_2\text{O}$	
	Release	Uptake	Decomposition	Oxidation
CuCe	11.5	11.8	90%	93%
CuCZ	8.4	8.0	68%	66%
CuZr	8.2	7.8	64%	64%

Table 2: Quantitative analysis for the third TPO cycle.

It is interesting to observe that for ceria-supported copper the amount of oxygen exchanged by the catalyst is 20-30% higher than copper on zirconia and ceria zirconia; this is similar to what detected for palladium-based materials in which alumina doping with ceria resulted in an increase of oxygen uptake and release [41]. The total balance between decomposition and oxidation does not change significantly from cycle to cycle, with the oxygen release always being slightly higher than that uptaken.

The reasons for this higher oxygen exchange on ceria appear difficult to elucidate, provided that all the catalysts considered in this work have similar surface areas and consequently it is likely that they have also similar metal dispersion. Since this phenomenon has been observed also for palladium, it can be related to a general tendency of ceria to promote oxygen exchange on metal surfaces. Nevertheless, the several literature reports that describe a sort of redox synergy between CeO_2 and CuO allow to formulate also different hypothesis. One is that the exceeding oxygen release might be due to a partial reduction of ceria support, suggesting a sort of “spillover” mechanism in which CeO_2 transfers some oxygen to CuO during the decomposition of the latter; this would account for the CuO still present on sample stopped at 1273 K. An alternative or coexisting explanation would consider a promotion of ceria reduction operated by CuO , similarly to what reported in some works where this effect was observed in presence of CO and/or NO [18, 36, 37, 40]. In particular, the group of Martínez-Arias first described a redox synergy between CuO and CeO_2 that get reduced and reoxidized simultaneously under CO and O_2 respectively [36], while Nagai and coworkers recently reported a synchronization of the valence change for both Cu and Ce during cycling rich-lean switches [18]. These results were obtained under very different conditions (i.e. alternation of

reducing and oxidizing atmosphere, lower temperatures), nevertheless these evidences of a peculiar redox synchronization suggest the possibility of a similar interaction also in the experimental conditions of this work (i.e. oxidative environment and $T > 1173$ K). Moreover, the significant difference in the amount of CuO and Cu₂O cycling on ceria with respect to the other supports clearly indicate a strongest interaction of the metal with cerium oxide that supports the hypothesis of a cooperative effect in which copper and ceria both promote the mutual reduction.

Conclusions

In this work the redox behavior of CuO supported on Al₂O₃, CeO₂, ZrO₂ and Ce_{0.7}Zr_{0.3}O₂ was investigated by means of XRD, XPS and TPO experiments. The results indicate the presence of copper in the form of CuO on ceria and ceria-zirconia, while on alumina CuAl₂O₄ is formed. Due to the formation of this compound, the sample CuAl does not show any oxygen uptake/release during TPO experiments. On CuCe, CuZr and CuCZ TPO profiles belonging to CuO ↔ Cu₂O transformation are observed and the temperature for the onset of O₂ release and uptake is strongly dependent on the support. On all these samples CuO decomposition and reoxidation take place with a hysteresis similar to that widely described in literature for Pd-PdO transformation. On CuCe and CuZr stopped at 1273 K during a TPO cycle Cu₂O is detected; on CuCe also some residual CuO is observed. Quantitative analysis indicates that on CuCe the amount of oxygen released/uptaken exceeds by far the amount of oxygen exchanged over the other supports. This has been tentatively ascribed to a stronger interaction between Cu and CeO₂.

The tests and the measurements reported in this work are not strictly related to the methane catalytic combustion reaction. Their extension to other reactions run under different reaction conditions could represent an application of relevant importance

References:

- [1]. Bartholomew CH, Farrauto RJ. Fundamentals of industrial catalytic processes. 2nd ed. Hoboken, N.J.: Wiley; 2006.

- [2]. Skarman B, Nakayama T, Grandjean D, Benfield RE, Olsson E, Niihara K, et al. Morphology and structure of CuO_x/CeO₂nanocomposite catalysts produced by inert gas condensation: An HREM, EFTEM, XPS, and high-energy diffraction study. *Chem Mater*. 2002;14:3686-99.
- [3]. Hu CQ, Zhu QS, Jiang Z, Chen L, Wu RF. Catalytic combustion of dilute acetone over Cu-doped ceria catalysts. *ChemEng J*. 2009;152:583-90.
- [4]. Cao HY, Li XS, Chen YQ, Gong MC, Wang JL. Effect of loading content of copper oxides on performance of Mn-Cu mixed oxide catalysts for catalytic combustion of benzene. *J Rare Earths*. 2012;30:871-7.
- [5]. Iamarino M, Chirone R, Lisi L, Pirone R, Salatino P, Russo G. Cu/gamma-Al₂O₃ catalyst for the combustion of methane in a fluidized bed reactor. *Catal Today*. 2002;75:317-24.
- [6]. Kaddouri A, Dupont N, Gelin P, Delichere P. Methane Combustion Over Copper Chromites Catalysts Prepared by the Sol-Gel Process. *CatalLett*. 2011;141:1581-9.
- [7]. Adanez J, de Diego LF, Garcia-Labiano F, Gayan P, Abad A, Palacios JM. Selection of oxygen carriers for chemical-looping combustion. *Energy Fuels*. 2004;18:371-7.
- [8]. Arjmand M, Azad AM, Leion H, Mattisson T, Lyngfelt A. Evaluation of CuAl₂O₄ as an Oxygen Carrier in Chemical-Looping Combustion. *IndEngChem Res*. 2012;51:13924-34.
- [9]. Zhao HY, Cao Y, Kang ZZ, Wang YB, Pan WP. Thermal characteristics of Cu-based oxygen carriers. *J Therm Anal Calorim*. 2012;109:1105-9.
- [10]. Shah K, Moghtaderi B, Wall T. Selection of Suitable Oxygen Carriers for Chemical Looping Air Separation: A Thermodynamic Approach. *Energy Fuels*. 2012;26:2038-45.
- [11]. Shah K, Moghtaderi B, Zanganeh J, Wall T. Integration options for novel chemical looping air separation (ICLAS) process for oxygen production in oxy-fuel coal fired power plants. *Fuel*. 2013;107:356-70.

- [12]. Chen ZF, Meyer TJ. Copper(II) Catalysis of Water Oxidation. *AngewChem-Int Edit.* 2013;52:700-3.
- [13]. Chen ZF, Kang P, Zhang MT, Stoner BR, Meyer TJ. Cu(II)/Cu(0) electrocatalyzed CO₂ and H₂O splitting. *Energy Environ Sci.* 2013;6:813-7.
- [14]. Caputo T, Pirone R, Russo G. Supported CuO/Ce_{1-x}Zr_xO₂ catalysts for the preferential oxidation of CO in H₂-rich gases. *KinetCatal.* 2006;47:756-64.
- [15]. Gamarra D, Camara AL, Monte M, Rasmussen SB, Chinchilla LE, Hungria AB, et al. Preferential oxidation of CO in excess H₂ over CuO/CeO₂ catalysts: Characterization and performance as a function of the exposed face present in the CeO₂ support. *ApplCatal B-Environ.* 2013;130:224-38.
- [16]. Zhang L, Pan LW, Ni CJ, Sun TJ, Zhao SS, Wang SD, et al. CeO₂-ZrO₂-promoted CuO/ZnO catalyst for methanol steam reforming. *Int J Hydrogen Energ.* 2013;38:4397-406.
- [17]. Tong WY, West A, Cheung K, Yu KM, Tsang SCE. Dramatic Effects of Gallium Promotion on Methanol Steam Reforming Cu-ZnO Catalyst for Hydrogen Production: Formation of 5 angstrom Copper Clusters from Cu-ZnGaO_x. *ACS Catal.* 2013;3:1231-44.
- [18]. Nagai Y, Dohmae K, Nishimura YF, Kato H, Hirata H, Takahashi N. Operando XAFS study of catalytic NO reduction over Cu/CeO₂: the effect of copper-ceria interaction under periodic operation. *PhysChemChem Phys.* 2013;15:8461-5.
- [19]. Radlik M, Adamowska M, Laamacz A, Krzton A, Da Costa P, Turek W. Study of the surface evolution of nitrogen species on CuO/CeZrO₂ catalysts. *React KinetMech Cat.* 2013;109:43-56.
- [20]. Kundakovic L, Flytzani-Stephanopoulos M. Cu- and Ag-modified cerium oxide catalysts for methane oxidation. *J Catal.* 1998;179:203-21.

- [21]. Artizzu P, Garbowski E, Primet M, Brulle Y, Saint-Just J. Catalytic combustion of methane on aluminate-supported copper oxide. *Catal Today*. 1999;47:83-93.
- [22]. Qu FF, Chu W, Shi LM, Chen MH, Hu JY. Catalytic combustion of methane over nano ZrO₂-supported copper-based catalysts. *Chin ChemLett*. 2007;18:993-6.
- [23]. Aguila G, Gracia F, Cortes J, Araya P. Effect of copper species and the presence of reaction products on the activity of methane oxidation on supported CuO catalysts. *ApplCatal B-Environ*. 2008;77:325-38.
- [24]. Luo JJ, Xu HY, Liu YF, Chu W, Jiang CF, Zhao XS. A facile approach for the preparation of biomorphic CuO-ZrO₂ catalyst for catalytic combustion of methane. *ApplCatal A-Gen*. 2012;423:121-9.
- [25]. Trovarelli A., Fornasiero P. *Catalysis by ceria and related materials*, 2nd ed. London: Imperial College Press; 2013.
- [26]. Fornasiero P, Balducci G, DiMonte R, Kaspar J, Sergio V, Gubitosa G, et al. Modification of the redox behaviour of CeO₂ induced by structural doping with ZrO₂. *J Catal*. 1996;164:173-83.
- [27]. Si R, Zhang YW, Wang LM, Li SJ, Lin BX, Chu WS, et al. Enhanced thermal stability and oxygen storage capacity for Ce_xZr_{1-x}O₂ ((x)=0.4-0.6) solid solutions by hydrothermally homogenous doping of trivalent rare earths. *J PhysChem C*. 2007;111:787-94.
- [28]. Wang QY, Zhao B, Li GF, Zhou RX. Application of Rare Earth Modified Zr-based Ceria-Zirconia Solid Solution in Three-Way Catalyst for Automotive Emission Control. *Environ Sci Technol*. 2010;44:3870-5.
- [29]. Ran R, Weng D, Wu XD, Fan J, Wang L. Structure and oxygen storage capacity of Pr-doped Ce_{0.26}Zr_{0.74}O₂ mixed oxides. *J Rare Earths*. 2011;29:1053-9.
- [30]. Wang JQ, Shen MQ, Wang J, Gao JD, Ma J, Liu SX. Effect of cobalt doping on ceria-zirconia mixed oxide: Structural characteristics, oxygen storage/release capacity and three-way catalytic performance. *J Rare Earths*. 2012;30:878-83.

- [31]. Li GF, Wang QY, Zhao B, Zhou RX. Modification of $\text{Ce}_{0.67}\text{Zr}_{0.33}\text{O}_2$ mixed oxides by coprecipitated/impregnated Co: Effect on the surface and catalytic behavior of Pd only three-way catalyst. *J MolCatal A-Chem.* 2010;326:69-74.
- [32]. Jia LW, Shen MQ, Wang J, Chu X, Wang JM, Hu ZC. Redox behaviors and structural characteristics of $\text{Mn}_{0.1}\text{Ce}_{0.90}\text{O}_x$ and $\text{Mn}_{0.1}\text{Ce}_{0.6}\text{Zr}_{0.3}\text{O}_x$. *J Rare Earths.* 2008;26:523-7.
- [33]. Kim DK, Stowe K, Muller F, Maier WF. Mechanistic study of the unusual catalytic properties of a new Ni-Ce mixed oxide for the CO_2 reforming of methane. *J Catal.* 2007;247:101-11.
- [34]. Liu W, Flytzani-Stephanopoulos M. Transition metal-promoted oxidation catalysis by fluorite oxides: A study of CO oxidation over Cu-CeO₂. *ChemEng J.* 1996;64:283-94.
- [35]. Wang XQ, Rodriguez JA, Hanson JC, Gamarra D, Martinez-Arias A, Fernandez-Garcia M. In situ studies of the active sites for the water gas shift reaction over Cu-CeO₂ catalysts: Complex interaction between metallic copper and oxygen vacancies of ceria. *J PhysChem B.* 2006;110:428-34.
- [36]. Martinez-Arias A, Fernandez-Garcia M, Soria J, Conesa JC. Spectroscopic study of a Cu/CeO₂ catalyst subjected to redox treatments in carbon monoxide and oxygen. *J Catal.* 1999;182:367-77.
- [37]. Martinez-Arias A, Hungria AB, Fernandez-Garcia M, Conesa JC, Munuera G. Interfacial redox processes under CO/O₂ in a nanoceria-supported copper oxide catalyst. *J PhysChem B.* 2004;108:17983-91.
- [38]. Caputo T, Lisi L, Pirone R, Russo G. On the role of redox properties of CuO/CeO₂ catalysts in the preferential oxidation of CO in H₂-rich gases. *ApplCatal A-Gen.* 2008;348:42-53.
- [39]. Liu LJ, Yao ZJ, Liu B, Dong L. Correlation of structural characteristics with catalytic performance of CuO/Ce_xZr_{1-x}O₂ catalysts for NO reduction by CO. *J Catal.* 2010;275:45-60.

- [40]. Chen JF, Zhan YY, Zhu JJ, Chen CQ, Lin XY, Zheng Q. The synergetic mechanism between copper species and ceria in NO abatement over Cu/CeO₂ catalysts. *ApplCatal A-Gen.* 2010;377:121-7.
- [41]. Colussi S, Trovarelli A, Vesselli E, Baraldi A, Comelli G, Groppi G, et al. Structure and morphology of Pd/Al₂O₃ and Pd/CeO₂/Al₂O₃ combustion catalysts in Pd-PdO transformation hysteresis. *ApplCatal A-Gen.* 2010;390:1-10.
- [42]. Colussi S, Trovarelli A, Groppi G, Llorca J. The effect of CeO₂ on the dynamics of Pd-PdO transformation over Pd/Al₂O₃ combustion catalysts. *CatalCommun.* 2007;8:1263-6.
- [43]. Farrauto RJ, Hobson MC, Kennelly T, Waterman EM. Catalytic Chemistry of Supported Palladium for Combustion of Methane. *Appl Catal A-Gen.* 1992;81:227-37.
- [44]. Cao Y, Casenas B, Pan WP. Investigation of chemical looping combustion by solid fuels. 2. Redox reaction kinetics and product characterization with coal, biomass, and solid waste as solid fuels and CuO as an oxygen carrier. *Energy Fuels.* 2006;20:1845-54.
- [45]. Rodriguez NM, Oh SG, DallaBetta RA, Baker RTK. In situ electron microscopy studies of palladium supported on Al₂O₃, SiO₂, and ZrO₂ in oxygen. *J Catal.* 1995;157:676-86.
- [46]. Lyubovskiy M, Pfefferle L, Datye A, Bravo J, Nelson T. TEM study of the microstructural modifications of an alumina-supported palladium combustion catalyst. *J Catal.* 1999;187:275-84.
- [47]. Wolf MM, Zhu HY, Green WH, Jackson GS. Kinetic model for polycrystalline Pd/PdO_x in oxidation/reduction cycles. *ApplCatal A-Gen.* 2003;244:323-40.
- [48]. Salomonsson P, Johansson S, Kasemo B. Methane Oxidation over PdO_x on the Mechanism for the Hysteresis in Activity and Oxygen-Content. *CatalLett.* 1995;33:1-13.

- [49]. Farrauto RJ, Lampert JK, Hobson MC, Waterman EM. Thermal-
Decomposition and Reformation of PdO Catalysts - Support Effects.
ApplCatal B-Environ. 1995;6:263-70.
- [50]. Thevenin PO, Alcalde A, Pettersson LJ, Jaras SG, Fierro JLG. Catalytic
combustion of methane over cerium-doped palladium catalysts. J Catal.
2003;215:78-86.
- [51]. Colussi S, Trovarelli A, Cristiani C, Lietti L, Groppi G. The influence of
ceria and other rare earth promoters on palladium-based methane
combustion catalysts. Catal Today. 2012;180:124-30.